Politecnico di Milano

SCHOOL OF INDUSTRIAL AND INFORMATION ENGINEERING
Master of Science – Energy Engineering

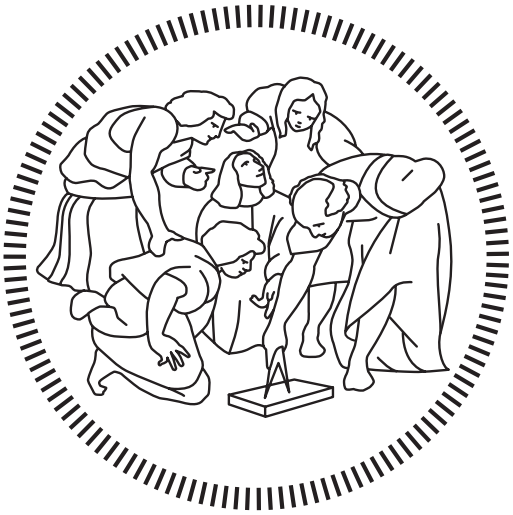

Development of electric vehicles load profiles for sector coupling in European energy system models

in collaboration with the University of Liège and KU Leuven

Supervisor
Prof. Emanuela COLOMBO

Co-Supervisors
Prof. Sylvain QUOILIN
Ing. Francesco LOMBARDI
Ing. Matija PAVIČEVIĆ

Candidate
Andrea MANGIPINTO – 894462

Academic Year 2019 – 2020

Acknowledgements

First, I would like to thank the people who allowed the realisation of this thesis. My gratitude goes to professor Emanuela Colombo, for giving me the opportunity to work on this stimulating topic. To professor Sylvain Quoilin and Matija Pavičević, for the hospitality during the period in Liège, and for giving me the possibility to collaborate to the Dispa-SET project. To Francesco Lombardi, for his constant support and helpfulness during the whole thesis period. To Francesco Sanvito, for assisting me with his experience in the transport sector. Finally, I would like to acknowledge Agnese Beltramo, for kindly sharing the ElaadNL data used in the validation phase.

Ci sono poi tante persone che vorrei ringraziare, per avermi supportato e aver reso questo lungo percorso al Politecnico di Milano unico. Innanzitutto, un grazie particolare va ai miei genitori e a mia sorella, per avermi sempre supportato, anche quando mi sono trovato lontano da casa, per la loro grande fiducia in me e per l'affetto che mi dimostrano quotidianamente. Un grazie a tutta la mia famiglia, benché lontana, mi sostiene sempre. In particolare, grazie ai miei zii e cugini olandesi, che mi hanno fatto sentire a casa durante l'anno e mezzo trascorso all'estero, grazie alla loro ospitalità durante le mie visite a casa loro.

Un grazie agli amici, sia quelli che conosco da sempre che quelli nuovi. Sono sicuro che senza il supporto reciproco del gruppo di amici in università, la mia esperienza sarebbe stata molto diversa e, sospetto, peggiore. I pranzi trascorsi insieme, le innumerevoli pause tra le lezioni e il sostegno durante la preparazione degli esami sono ricordi che porterò con me. Grazie anche ai due Claudio e a Carter, per le regolari uscite del sabato sera, che mi hanno permesso di svagarmi anche quando gli impegni universitari si facevano pressanti. Un ringraziamento va anche a tutti gli amici conosciuti a Delft, Colonia e Liegi, anche se solo per pochi mesi, è stato bello condividere l'esperienza in un paese nuovo insieme.

Un grazie speciale va a Giuliana, che è entrata nella mia vita come un piccolo tornado, e da allora ha reso migliore ogni giorno. Grazie di supportarmi sempre, anche quando io stesso non mi supporterei. Grazie di darmi la forza di affrontare ogni sfida.

Andrea

Contents

Sommario

Tra le diverse strategie per decarbonizzare il sistema energetico, l'accoppiamento tra settori è sempre più riconosciuto come una soluzione efficiente per garantire la flessibilità necessaria a un sistema dominato da fonti di energia rinnovabile intermittenti. Per simulare il settore del riscaldamento e dei trasporti all'interno di modelli del sistema energetico, è fondamentale avere a disposizione i profili di domanda oraria nei diversi paesi. Viene quindi proposto un modello stocastico con l'obiettivo di simulare con elevato dettaglio temporale i profili di carico dei veicoli elettrici in 28 paesi Europei, al fine di colmare questo vuoto nella letteratura. Il modello è chiamato RAMP-Mobility, ed è pubblicato come software open-source. Successivamente, i profili generati dal modello sono usati come input per valutare le potenzialità dell'accoppiamento tra settori nel fornire flessibilità in un sistema energetico Europeo fortemente decarbonizzato. Questa valutazione avviene tramite l'accoppiamento tra i modelli di dispacciamento ottimale Dispa-SET e di pianificazione energetica a lungo termine JRC-EU-TIMES. Gli scenari analizzati sono quattro, un caso base senza integrazione tra settori, seguito dall'introduzione graduale delle tecnologie di accumulo termico e di Vehicle-to-grid (V2G).

RAMP-Mobility viene poi validato usando due serie di dati misurati, per testare l'affidabilità degli algoritmi di calcolo della domanda di mobilità e di ricarica. Entrambe le validazioni mostrano un grado di accuratezza soddisfacente. Successivamente, il database di profili di ricarica per l'Europa viene presentato, discutendo le principali differenze tra paesi. La domanda di mobilità media per veicolo risulta essere il parametro che influenza maggiormente il profilo finale. In aggiunta, anche la composizione della popolazione risulta essere una variabile rilevante, specie nel determinare la sporgenza dei picchi di domanda. Successivamente, tramite i risultati delle simulazioni con Dispa-SET, vengono dimostrati i benefici dell'integrazione tra settori in termini di emissioni di gas serra, costi operativi totali e adeguatezza del sistema. Ciò nonostante, la mancanza di linee di connessione più potenti tra i paesi si configura come un fattore chiave nel limitare la possibilità di usufruire a pieno la capacità di accumulo disponibile. Infine, un'attenta analisi circa le tecnologie di accumulo mostra come il caso base soddisfi quasi completamente la flessibilità richiesta dal sistema, ottenendo l'80% di riduzione delle emissioni rispetto al 1990. Tuttavia, nonostante non risulti essere una condizione necessaria per la fattibilità del sistema, l'accoppiamento tra settori gioca un ruolo importante nel fornire soluzioni di accumulo più economiche ed efficienti, riducendo il costo della transizione energetica.

Parole chiave: Veicoli elettrici, Profilo di carico, Modellazione del sistema energetico, Accoppiamento tra settori, Sistemi energetici intelligenti

Abstract

In the context of energy system decarbonization strategies, sector coupling is increasingly recognised as a cost-effective solution to provide the necessary flexibility in a system characterised by high shares of Variable renewable energy sources (VRES). To accurately account for the heating and transport sector in energy system models, the availability of hourly demand profiles for different countries is crucial. Therefore, a stochastic model to simulate the Electric Vehicles (EVs) load profiles with high temporal detail in 28 European countries is proposed, with the goal of filling this gap in the literature. This is called RAMP-Mobility, and is released as open-source software. Furthermore, the resulting profiles are used as inputs to assess the flexibility potential provided by sector coupling in a future, highly decarbonized, European energy system. This is performed via the soft-linking between the Dispa-SET optimal dispatch and the long-term JRC-EU-TIMES energy planning models. Four scenarios are analysed, starting from a base case without sector integration, and gradually introducing the Thermal energy storage (TES) and Vehicle-to-grid (V2G) technologies.

RAMP-Mobility is validated against two sets of measured data, testing the reliability of both the algorithms computing mobility and charging demand. A satisfying degree of accuracy is registered in the results of both validations. Then, the database of Europe-wide EVs load profiles is presented, and the main differences among countries are discussed. Results show that the average mobility demand per car is the main parameter affecting the final profile. Moreover, also the population composition proves to be a relevant variable, especially in determining the difference between the base load and the height of the demand peaks. Subsequently, the results of the Dispa-SET simulations demonstrate the benefits of sector integration in terms of greenhouse gases emissions, total operational costs and system adequacy. Nevertheless, it is highlighted how the lack of stronger interconnection lines between countries is a key factor hindering the possibility to fully exploit the storage capacity available. Finally, a deeper analysis on the storage technologies shows that the base case already almost meets the flexibility required by the system, obtaining 80% emission reduction with respect to 1990 levels. Nevertheless, even if not strictly necessary for the technical feasibility of the system, sector coupling proves to play an important role in providing cheaper and more efficient storage solutions, reducing the cost of the energy transition.

Keywords: Electric vehicles, Load profile, Energy system modelling, Sector coupling, Smart energy systems

Extended Abstract

Introduction

In December 2019 the European Commission presented the European Green Deal for the European Union (EU), defining a strategy aiming at zero net greenhouse gases emissions in 2050. To reach this ambitious goal, the importance of expanding energy system analyses from the power sector only, to a smart energy system, where all the sector (electricity, transport and heating) are integrated, is analysed by numerous studies [1]–[3]. In particular, when considering a carbon neutral power system, the coupling of the electricity and transport sectors poses some challenges to the electric grid, while at the same time offering a crucial contribution towards decarbonization. For this reason, it is important to represent accurately the transport sector in energy system models, to assess the impact that its electrification can have on the power system. This can be done only using accurate load curves describing Electric Vehicles (EVs)' charging demand. Therefore, the aim of this thesis is to develop an open-source model to simulate EVs load profiles with high temporal detail for 28 European countries. The resulting profiles are then used as one of the inputs for the Dispa-SET optimal dispatch model, by which we assess the impact of sector coupling on the flexibility needs of an energy system with high shares of Variable renewable energy sources (VRES).

Review of large-scale Electric vehicles modelling

Two main types of models simulating EVs load profiles can be identified. Some studies use data related to conventional mobility as inputs. These have the advantage of being able to represent the dynamics of the whole population. For instance, in 2013 the Joint Research Centre (JRC) modelled the charging curves in six large European countries starting from a survey on mobility behaviours [4]. Both uncontrolled and night charging is simulated. The result is a typical weekly profile, with morning and afternoon peaks in the weekdays. However, the results are strongly affected by the limited number of users considered. Fischer in 2018 developed a stochastic model, using Markov-chain, starting from the data collected by the German survey Mobilität in Deutschland (MID) [5]. In this model, the possibility to simulate different charging scenarios is implemented. The results show clearly the two peaks connected to the commuting for working purposes. Nevertheless, the limits of the study lie in the use of the Markov-chain approach, which makes the model highly dependant on the specific input data, and in the lack of an open-source software release.

On the other hand, there are studies using electric mobility data as inputs. These have the advantage of not relying on any assumption regarding the charging process. In 2016, Brady [6] developed a stochastic model starting from an EV demonstration project carried out in Ireland. The schedule of daily travels and charging events is modelled with a Monte Carlo simulation. This model manages to simulate effectively the travel patterns of the original database. Nevertheless, it shows some limits due to issues linked to limitations in the inputs database, and in the modelling techniques. The work from Schäuble [7] starts from data measured in Germany during three field trials. The characteristics of the EV fleet are sampled from this database, along with the number of charges happening each day. Analysing the results, the model manages to simulate a charging profile close to the input data. However, it does not reproduce the typical passenger mobility trend composed by two peaks. This is caused by the type of users that compose the inputs database.

Methodology

In this section, the methodology used to develop the original RAMP-Mobility model is described. Then, the application of the EV load profiles to the soft-linking of Dispa-SET and JRC-EU-TIMES models is presented.

Electric Vehicles charging profiles

RAMP-mobility builds on previous work by the SESAM group on methods for stochastic load simulation [8], and expands it with the development of two original algorithms. First, starting from traditional mobility data, the power consumption requested to the EV battery is computed, called mobility demand. Then, for each travel event, the energy used to charge the EV is derived, called charging demand. To capture the whole spectrum of possible evolutions of the system, different customizable parameters are introduced, such as the charging strategies or the Electric Vehicle Charging Points (CPs) availability. Figure 1 presents an overview of the interaction between the different model components.

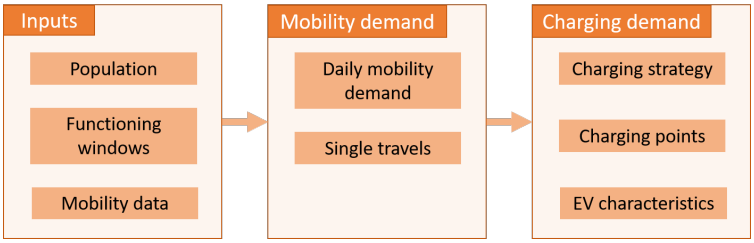

Figure 1. Conceptual scheme of the main components of the RAMP-Mobility model. The input data are first used to compute the mobility demand. Starting from that, the charging power requested to the grid can be computed under different assumptions.

Modelling mobility demand

A conceptual representation of the input data used in the mobility demand calculation and of the algorithm outputs is presented in Figure 2. Traditional mobility data are used in the evaluation of the travel patterns. This is preferred over the alternative of using electric mobility data, which fails at reproducing the whole population dynamics. Overall, the simulated country is subdivided in 9 *Users type*, each composed by a number of independent *Users*, with a uniquely simulated car usage profile. A single EV is associated to each user. The population composition is derived from Eurostat data [9], [10].

In the model we implement the possibility to simulate any year, differentiating between weekdays, Saturdays and Sundays. During the weekdays, different time behaviours are defined for *Student/ Working* users with respect to the *Inactive*; on the weekend, instead, the whole population behaves according to the *Inactive* user daily patterns. Each appliance has a predefined number of functioning windows, defining the time frames in which it can randomly start a travel. The most common trend observed in travelling behaviours is the presence of two peaks of car usage, one in the morning and one in the afternoon, corresponding to the commuting from home to the workplace. For this reason, the *Working* and *Student* users type are characterised by 5 functioning windows, 2 defining the peak hours, and 3 identifying the car usage for non-work related purposes. The *Inactive* user's functioning windows, instead, are identified by one single *Main* functioning window and two complementary *Free time* windows, for the early morning and early evening. For this purpose, data coming from the Harmonised European Time Use Surveys (HETUS) are used [11].

The total distance driven on average each day is modelled through the variable d_{tot}, that combined with the average velocity v_{av}, provides the total usage time that the mobility appliance has to run each day, t_{tot}. The stochastic algorithm randomly switches on the appliance in the allowed functioning window, as many times as needed to satisfy the t_{tot}. The main source for the input data needed to characterise mobility behaviours is the direct survey conducted in 2012 by the JRC. This provides data on daily driven distance and time, on the average trip distance and time and

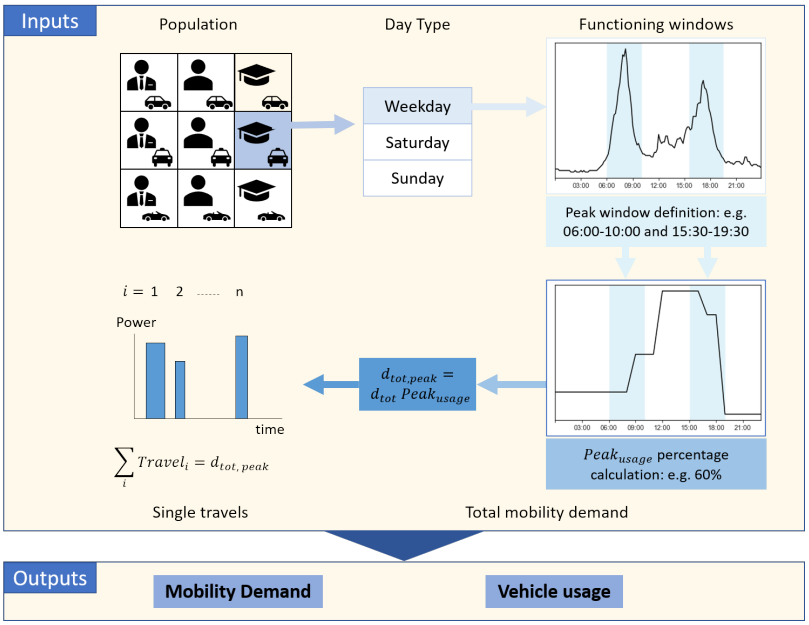

Figure 2. Conceptual scheme of the input data, their relations, and of the main outputs of the mobility demand algorithm. Each user belongs to a certain User type category. For each day type the peak and off-peak functioning windows are defined and the total daily mobility demand is subdivided accordingly. Then, the single travels are simulated until the total transport demand is satisfied. The result of the algorithm are two time series: the power demand to the vehicle battery and the percentage of vehicles travelling in each time step.

other travel-related parameters in 6 EU countries, namely France, Germany, Italy, Poland, Spain and United Kingdom [12].

Afterwards, the definition of the average trip is fundamental to simulate as many switch-on events as needed to cover the total mobility demand. The average travel is implemented in the model through the variables d_{min} and t_{func}, which define the average distance and time of each travel performed by the EV. From these two variables, the average trip velocity v_{av} is calculated. Again, the values of the variables d_{min} and t_{func} are drawn from the 2012 JRC survey. During the simulation of each travel, the model calculates the vehicle power consumption based on the travel average velocity. The relation used to link the two variables is a simplified model developed by the JRC in 2013, consisting of a quadratic function [4].

All the variables presented above are subject to a random variability, whose extent is defined by the user. The variables involved are the average travel data $d_{min,\,rand}$ and $v_{av,\,rand}$ and the power consumption of the EV during the travel, $P_{EV,\,rand}$. Also the functioning windows have a random variability parameter, $window_{rand}$, shifting their length. Another relevant parameter in the model is the *occasional use*, which determines the probability that the appliance will be used in the simulated day. Each of these parameters can be freely modified by the model user.

Modelling charging demand

After a reliable mobility profile is calculated, it is possible to analyse the charging power demand. Few parameters of the charging process function cannot escape from having a certain degree of arbitrariness. Thus, they are made easy to change for the model user. Four charging strategies are implemented in the model, in order to simulate the future evolution of the EV demand profile in different ways, and therefore study the dynamics of interactions with the power grid. Figure 3 shows a flow diagram presenting an overview of the whole charging algorithm:

1. *Uncontrolled*: this is the base case, where no control over the user behaviour is applied. If the CP is available, the battery is charged immediately at the nominal power, until a user-defined value of SOC_{max}.
2. *Perfect Foresight*: this strategy aims at quantifying the possibility to implement a Vehicle-to-grid (V2G) solution. If the CP is available, the car is charged right before the end

of the parking, at the nominal power, until the *SOC* satisfies the needs of the following journey. This allows to compute the part of EV battery available to the Transmission System Operator (TSO), without affecting the user driving range [13].

3. *Night Charge*: it is the first smart charging strategy. It aims at shifting the charging events to the night period. The car is charged only if the CP is available and the parking happens during nighttime.

4. *Renewable energy sources (RES) Integration*: the second smart charging method has the goal of coupling the RES power generation with the transport sector. The car is charged only if the CP is available and the parking happens during periods when there is excess of RES power production. This condition is evaluated through the residual load curve.

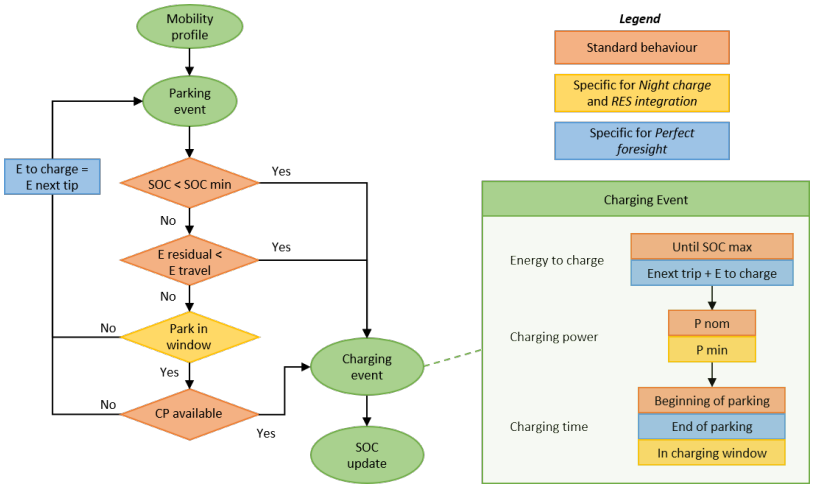

Figure 3. Flow diagram representing the charging process algorithm. The boxes represent different charging strategies: the common standard algorithm is in red, the specificities of the night charge and RES integration in yellow and the peculiarities of the perfect foresight are in blue.

The charging process is characterised by several arbitrary parameters. The first of these is the battery capacity of the different types of EVs, $C_{battery}$. Another important parameter is the definition of the CPs, characterised by a nominal power and relative distribution. Then, two modelling techniques are proposed for the CP_{prob} function, suited for different scenarios. The first assumes constant probability of finding the infrastructure at each parking, and is advised when considering a future scenario where EVs become the main transport mean. The second considers a stepwise probability function, accounting for an higher probability in the morning and in the evening. This is the advised approach when simulating conditions similar to the current ones.

Dispa-SET linking with JRC-EU-TIMES

Dispa-SET is a multi-sector energy system model which allows to define the flexibility requirements of an energy system characterised by high penetration of VRES. The model is defined as a mixed-integer linear programming (MILP) problem. As a detailed explanation of the Dispa-SET model is out of the scope of this thesis, all the relevant information can be found in the model official documentation[1]. The objective function of the model consists of the minimisation of the overall system operational costs. The main costs considered are: shut-down and start-up and, variable, fixed, ramping and load shedding costs. The balance between supply and demand is the main imposed constraint. This is satisfied in the day-ahead market for each time step and zone.

A scenario in 2050 is used to analyse the role of sector coupling technologies in a future energy system. With this aim, the PRORes scenario generated by the JRC-EU-TIMES model provides the overall figures used in the Dispa-SET simulations [14]. This is an energy planning model developed by the JRC of the European Commission. Its main goal is to study energy technologies potential

[1] Dispa-SET documentation: http://www.dispaset.eu

and provide recommendations on European energy policies, simulating capacity expansion and the related costs. The connection between the two models is a uni-directional soft-linking. Therefore, one key feature is related to the input files pre-processing. This is done thanks to a transition model with the aim of converting the JRC-EU-TIMES outputs into Dispa-SET readable format[2]. Outputs from JRC-EU-TIMES include descriptions and characteristics of commodities, zones, generation capacities, prices and available technologies. They also provide yearly energy flows, from which time series are generated.

The analysis is performed on four scenarios: starting from one scenario with no sector coupling (NOFLEX), each one focuses on one sectors at a time (THFLEX for the thermal and EVFLEX for the transport), while the ALLFLEX studies the benefits of a smart energy system. An overview of the difference between the simulated scenarios, along with the main storage capacity assumptions, is presented in Table 1.

	Unit	NOFLEX	THFLEX	EVFLEX	ALLFLEX
Demand					
Electricity		✓	✓	✓	✓
Heating		✓	✓	✓	✓
Transport		✓	✓	✓	✓
Supply					
Hydrogen with storage		✓	✓	✓	✓
HPHS storage	[h]	6	6	6	6
Li-ion BATS storage	[h]	1	1	1	1
Lead acid BATS storage	[h]	4	4	4	4
SCSP TES	[h]	15	15	15	15
CHP TES	[h]	-	12	-	12
P2HT TES	[h]	-	5	-	5
V2G capacity	[kWh]	-	-	60	60
V2G share	[%]	-	-	50	50

Table 1. Summary of the characteristics of each simulated scenario. The main storage capacity assumptions are also reported.

The core of the model inputs is composed by hourly time series. These are total demands for each sector, hydro power reservoirs levels and VRES Availability factors (AF). For the sake of conciseness, only the main inputs are presented in this section. However, both the model source code[3] and the input data[4] can be consulted for further information.

The available power plants are grouped with a "Per-typical technology" approach [15]. It consists of grouping similar plants into a single cluster of N units, characterised by the same parameters. In addition to this, the time series for the wind [16] and solar [17] AF are obtained from the *Renewables.ninja* and EMHIRES datasets. The hydro power inflow times series are obtained from the RESTORE 2050 project [18] for the year 2016. All fuel prices and carbon emission allowances are obtained from the JRC-EU-TIMES model.

To derive the hourly power demand used in Dispa-SET from the yearly electricity demand provided by JRC-EU-TIMES, the European Network of Transmission System Operators for Electricity (ENTSO-E) 2016 data are scaled up to the 2050 levels. However, the transport and heating sector are not expected to have the same load profile as the one of the 2016 electricity demand. Therefore, both sectors are not considered in the scaling up coefficient, and are treated separately in the model.

The transport charging demand is calculated with RAMP-Mobility. In addition to this, the V2G configuration is here implemented as an additional storage technology, with a variable nominal capacity. For each hour, the total energy available to the system is computed based on the minimum energy to be guaranteed to the user for mobility purposes. In the analysed region the total V2G

[2] DispaSET-SideTools: https://github.com/MPavicevic/DispaSET-SideTools

[3] Model source code: https://github.com/energy-modelling-toolkit/Dispa-SET/tree/PowerToGas

[4] Input data: https://github.com/MPavicevic/DispaSET-SideTools/tree/JRC_EU_TIMES

storage capacity is around 7000 GWh, calculated from the total EVs number, with an average car battery capacity of 60 kWh and only 50% of the fleet participating to the V2G program.

The Power-to-Heat (P2HT) technology is included, referring to technologies converting electricity into domestic hot water and space heating. These P2HT are assumed to be subject to Direct load control (DLC) [19], meaning that can be operated flexibly, to minimise system costs. The input for hourly heating profiles is the "When2Heat" dataset [20]. This provides the adimensional time series, which are then scaled to meet the total amount of heat demand for each country.

The commercial Net Transfer Capacities (NTCs) are the maximum amount of energy that each country can exchange with the neighbouring countries. Projection for the network development in 2050 are derived from a combination of the 2014 Ten-Year Network Development Plan (TYNDP) (providing results until 2030) and the e-Highway2050 project evaluating the additional grid reinforcements from 2030 to 2050.

Results

RAMP-Mobility validation

First, RAMP-Mobility results are validated against historical values collected in 2015 in the Netherlands from the public charging points managed by EVnetNL. The database covers around 1750 charging points, that represent approximately 16% of the whole public charging infrastructure available. The data are processed according to the methodology described in Beltramo et al. [13], to filter only the transactions representing frequent EV users.

To simulate in RAMP-Mobility conditions close to the experimental ones, both the input data and the optional parameters are carefully analysed. From the transaction data registered for each car, it is possible to obtain an approximation of the car fleet composition, composed by 60% of small cars and 40% of large ones. Similarly, the CPs' nominal power relative distribution is derived from the transactions data, showing a majority of 3.7 kW plugs. The piecewise CP_{prob} function is selected, as it is likely that charging point availability is higher in residential areas, even if the database consists only of public charging points.

Due to the high degree of uncertainty linked to the piecewise CP_{prob} function, a sensitivity analysis is performed on the curve. As shown in Table 2, 8 cases are identified, varying the 4 parameters identifying the curve shape, namely the higher and lower probability, and the hour of the day at which this changes. Then, an additional parameter is defined, specific for this validation, called *scale factor*. This is necessary as the model accounts for all the charging transactions performed by the users, while the ElaadNL database only records charging events in 16% of the public CPs. The scale factor varies along the year. Hence, a sensitivity analysis will be performed around its median value, equal to 0.4.

	Case 1	Case 2	Case 3	Case 4	Case 5	Case 6	Case 7	Case 8
p_{max}	0.9	1	0.8	0.9	0.9	0.9	0.9	0.9
p_{min}	0.4	0.4	0.4	0.3	0.5	0.4	0.4	0.4
t_1	06:00	06:00	06:00	06:00	06:00	05:00	07:00	06:00
t_2	19:00	19:00	19:00	19:00	19:00	19:00	19:00	20:00

Table 2. Overview of the eight cases analysed in the sensitivity analysis on the piecewise probability function.

The comparison is performed on the load duration curve, as shown in Figure 4. A satisfying match can be noticed, except for the lower loads, that are overestimated by the model. This is due to the decrease in mobility demand during summer vacation, which are intentionally not simulated in RAMP-Mobility. The 0.4 scale factor is the value showing better agreement with the data. Thus, it is analysed through some quantitative parameters, to understand the impact of the 8 different cases. The rate of accuracy of the model is computed with the Normalised Root-Mean-Squared Error (NRMSE), defined as follows:

$$NRMSE = \frac{\sqrt{\frac{\sum_x^{N_t}(P_{model}(x) - P_{measured}(x))^2}{N_t}}}{P_{measured,max} - P_{measured,min}} \quad [\%] \tag{1}$$

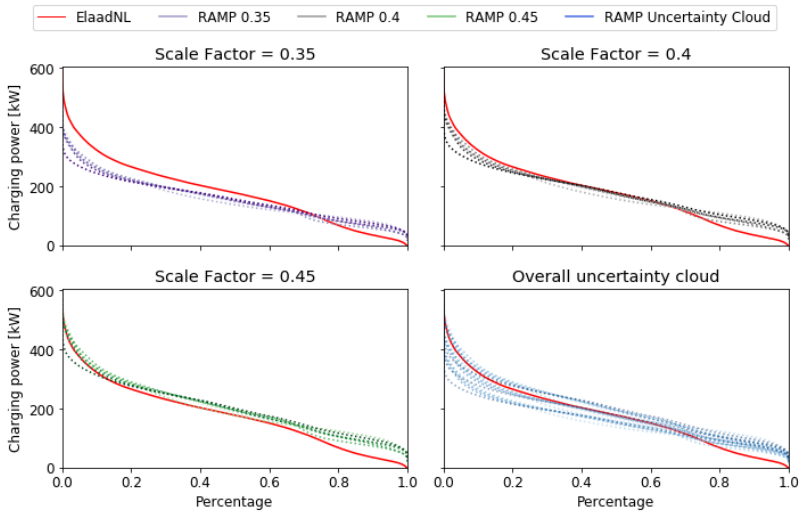

Figure 4. Comparison of load duration curves for different values of scale factor. To each scale factor value correspond eight cases linked to the sensitivity analysis performed on the piecewise probability function.

Where $P_{model}(x)$ and $P_{measured}(x)$ are the power calculated by the model and the measure from the ElaadNL database, N_t is the total number of observations. The denominator is the difference between the maximum and minimum measured values. Another important parameter is the Load Factor (LF), to evaluate if there is wide variability in the charging demand [21]. It is computed as ratio between average demand $P_{average}$, and peak demand P_{peak}:

$$LF = \frac{P_{average}}{P_{peak}} \tag{2}$$

In Table 3 the quantitative parameters calculated are presented for all the 8 cases. Analysing the LF error, it can be seen that Case 3, 7 and 8 are quite far from the ElaadNL data, while the other 5 values are quite similar, around 10%. Then, the NRMSE is computed on the load duration curve. The curve with the lowest NRMSE is the Case 5. This case has the highest CP_{prob} during the central window. This results in a more frequent coincidence of car connections, bringing to a lower frequency of low power values. Therefore, it better follows the trend of the data in the region that the model has more challenges in reproducing.

	ElaadNL	Case 1	Case 2	Case 3	Case 4	Case 5	Case 6	Case 7	Case 8
LF [–]	0.302	0.345	0.334	0.365	0.336	0.336	0.336	0.357	0.421
LF Error [%]	-	12.54	9.54	17.39	10.28	10.26	10.18	15.39	28.32
NRMSE LDC [%]	-	3.86	3.79	3.98	5.00	2.70	3.39	4.17	5.98

Table 3. Summary of the load factor, the load factor error with respect to the data and the NRMSE calculated on the load duration curve. The NRMSE values refer to a 0.4 scale factor, while the load factor is constant for each scale factor.

RAMP-Mobility results

In this section, the complete European database of EV charging demand is presented. As this is used to represent the transport demand in the Dispa-SET power system simulation, some of the parameters are adapted to the models requirements. The *Perfect Foresight* charging strategy is used, to then model the V2G option. The CP_{prob} is constant and set to 80%. Charging stations are distributed as in the default version of the model. As a trade-off between accuracy and computational tractability, 2500 users are simulated for each country, for a total of 70000 users in total. In order to present a clearer comparison of the results, the 28 countries are grouped in 8 macro-regions. For each region, only the results from one country are reported. The comparison is performed on the

load duration curve, to capture the overall yearly trend. The eight resulting curves are presented in Figure 5. Several trends can be highlighted.

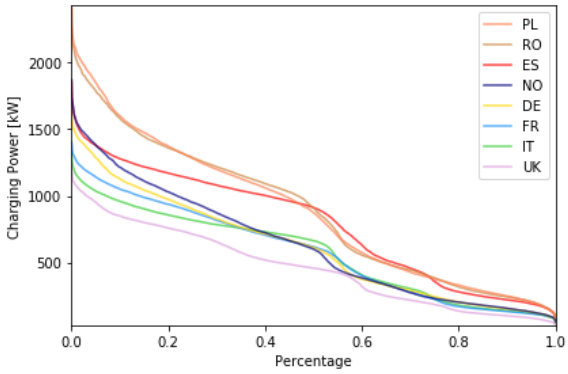

Figure 5. Comparison between the charging demand load duration curve in the 8 selected countries.

First, Poland and Romania present the highest power demand, in particular in the peak region. This is due to the fact that the total daily travel distance per car, d_{tot}, reaches the highest values for Poland, while the mobility data collected in Poland are used also for Romania. Subsequently, Spain shows a similar trend to the one of Romania for the low power values, whereas a lower one for the peak zone of the curve. The reason for this lies in the user type distribution. Indeed, Spain is the country with the highest share of inactive people. As the peaks are mainly determined by the travels made by *Working* and *Student* users, this brings to low peak values. Moving to the lower curves, Norway, Germany, France and Italy have roughly the same curve shape for medium and low power values. The reason is that these three countries all have very similar d_{tot} values. Nevertheless, a declining trend can be noticed in the peak region, moving from Norway to Italy. The explanation can be twofold. On the one hand, going from Scandinavian countries to Italy there is a continuous trend towards warmer climates, that brings to lower consumption. On the other hand, there is also a downward trend in the *Working* and *Students* users, indeed Norway shows the highest share, while Italy the lowest. This, as already seen for Spain, contributes to soften the charging profile peaks. Lastly, the United Kingdom is the country with the lowest values of charging power. This is clearly due to being the nation with the lowest daily mobility demand per vehicle.

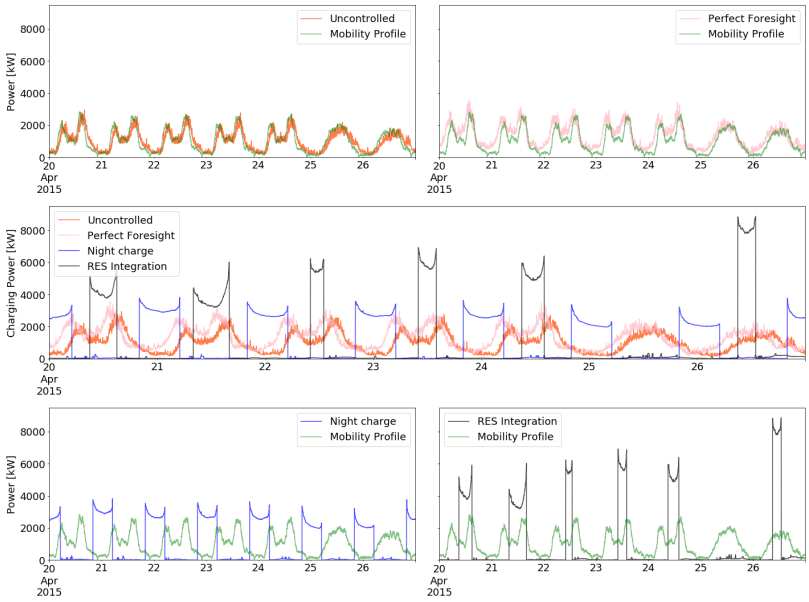

Figure 6. Comparison between the different charging strategies. The plots in the corners show each single strategy along with the mobility demand. In the centre the 4 strategies are compared against each other.

Figure 6 shows the comparison between the four different charging strategies. All the simulations refer to 5000 users in Germany. The mobility stochastic parameters are set to the default values. The *Uncontrolled* case shows the expected slight delay in the charging profile with respect to the transport demand. The opposite trend is visible in the *Perfect Foresight*, where the power demand to the grid is shifted earlier with respect to the mobility profile. Moving to the smart charging strategies, the *Night Charge* shows the load shifting potential offered by postponing the charging events in the night window. The *RES Integration* charging strategy is strongly dependent on the combination of load demand, weather conditions and VRES total installed capacity. In this section the base year 2015 weather was simulated, while the power demand and the installed renewable capacity refer to the 2050 ProRES scenario from the JRC-EU-TIMES model. Usually, as visible in the week presented, the charging happens in the central part of the day, when the solar energy production peaks. However, on Saturday the residual load is never lower than zero. This causes almost no charging events to start. The consequence is that the peak demand on Sunday is higher than the weekly average.

In addition to this, a wide sensitivity analysis is conducted on both the mobility-related arbitrary parameters and on the customizable features available in the charging process function. Overall, the results are more sensible to the charging process customizable features rather than to the mobility arbitrary parameters. This is a relevant result, as it means that the goal of allowing each model user to define its own scenarios and assumptions was successfully achieved.

Dispa-SET simulations results

The final results of the Dispa-SET simulations are here presented and discussed. A detailed costs breakdown of power plants operational costs, divided by technology and fuel, is presented in Figure 7a. First, it is clear how the system cost decreases when integrating additional sector coupling option. Indeed, the ALLFLEX scenario proves to be the most cost-effective solution among the four considered conditions. Additionally, the introduction of extraction Combined heat and power (CHP) plants, coupled with Thermal energy storage (TES) results in a significant increase in the usage of cogeneration technologies. This can be explained by the much higher operational flexibility provided by this kind of plant configuration. The operational carbon emissions from thermal units, both CHP and non-CHP, are shown in Figure 7b. Gas units are the major source of carbon emissions, followed by lignite units. The flexibility provided by the TES reduces the necessity of backup heaters, thus reducing the related CO_2 emissions. Overall, increasing the flexibility potential proves to be beneficial, as can be seen by the reduction of total carbon emissions.

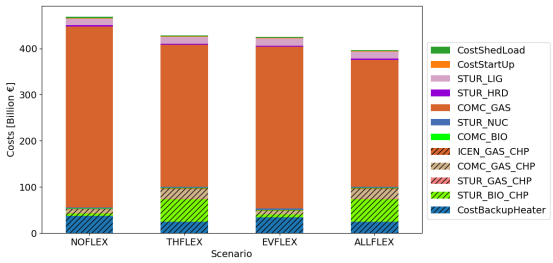

(a) Costs breakdown in all scenarios. Variable fuel costs are presented per fuel and per technology type, the backup heaters cost is represented in blue.

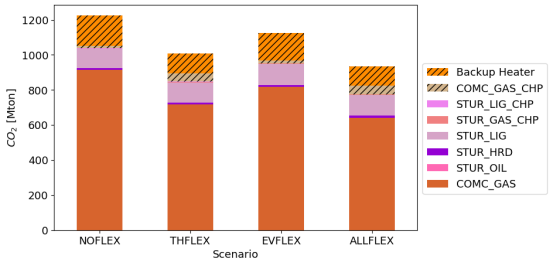

(b) Summary of CO_2 emissions grouped per fuel and per technology type in all scenarios.

Figure 7. Overview of costs breakdown and CO_2 emissions in all scenarios.

The shifted load is presented in Figure 8a, it indicates the extent of exploitation of the available storage technologies. It can be analysed that, with respect to the NOFLEX scenario, the introduction of Battery-powered electric vehicles (BEVS) in the EVFLEX and ALLFLEX scenarios causes a reduction in the usage of competing technologies such as Stationary batteries (BATS), Pumped hydro storage (HPHS) and Power-to-gas storage (P2GS). This could be explained by the fact that the transport sector coupling provides a cheaper and more efficient storage technology than the other competitors. In addition to this, the fact that the storage contribution does not simply sum up might suggest two considerations. On the one hand, the storage available in the base case is already enough to guarantee the necessary flexibility for the analysed system. On the other hand,

the limited NTCs values hinder the possibility to completely exploit the flexibility potential. The situation is different when analysing the introduction of TES. Indeed, here the contribution of the competing technology is almost constant. This can be explained by the fact that the thermal storage acts mainly on the thermal demand, for which there are no competing technologies. The total and the maximum curtailed power is presented in Figure 8b, as a percentage of the total and peak VRES power production, respectively. Overall, the amount of electricity curtailed is quite low across the four scenarios. Anyway, looking at the total curtailment, there is a clear downward trend when activating the TES and the V2G technologies, with the latter providing the biggest contribution. However, in the ALLFLEX scenario the total reduction is lower than the sum of the individual contributions. This is due to limitations in the storage exploitation caused by limits in the European power grid. Instead, when looking at the maximum curtailed power, the heating sector does not contribute significantly, while the transport sector has a more relevant role. When analysing the ALLFLEX scenario, the maximum curtailment decreases more than the sum of the individual contributions. This is due to the exploitation of synergies generated by the availability of the maximum number of storage technologies possible.

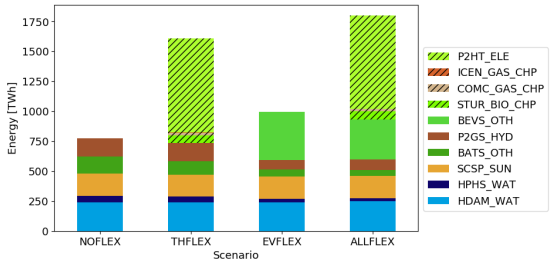

(a) Shifted load per fuel and technology type in all scenarios. Hatched labels indicate TES storage from CHP and P2HT units.

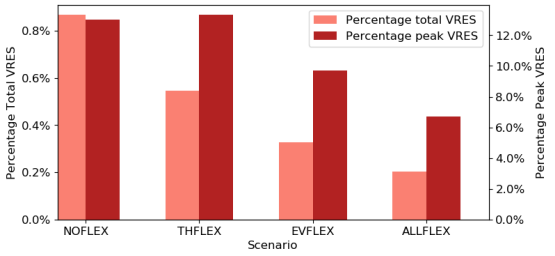

(b) Total annual and maximum aggregated hourly curtailment as percentage of total and peak generation from VRES in all scenarios.

Figure 8. Overview of shifted load and total and maximum curtailment in all scenarios.

Conclusions and future work

In this thesis work, the RAMP-Mobility original, open-source, stochastic model to simulate the EVs load profiles for 28 European countries was successfully developed and validated with a satisfying degree of accuracy. The result is relevant as it leads to the conclusion that the model can be applied to different scenarios describing the evolution of the transport sector. Then, an analysis on the simulated database of European EVs load profiles was performed, highlighting that the different average mobility demand per car and the population composition are the main factors differentiating the charging profiles. The different charging strategies implemented have been compared, proving to provide consistent results.

Moving to the results of the Dispa-SET simulations, four scenarios have been simulated, starting from a base case with no sector coupling option, and then gradually introducing the TES and V2G technologies. The first conclusion is that, as expected, the integration of heating and transport sector plays an important role in improving the performances of the energy system. Nevertheless, the results also indicate that some of the available storage capacity is not fully exploited. This is mainly due to the limited values of NTC. In addition to this, the storage capacity available in the base case is already almost enough to provide the necessary flexibility for the simulated scenario. This is a peculiar result, which suggests that, even if not strictly necessary for the technical feasibility of the system, the additional flexibility provided by sector coupling proves to play an important role in providing cheaper and more efficient storage solutions, reducing the cost of the energy transition.

There are different possible improvements that can be proposed as future development of this work. First, the possibility to rely on accurate mobility data for each of the simulated countries could potentially improve the results of the model. Second, the introduction of an accurate model to obtain a more precise vehicle power consumption calculation, is an aspect that should be considered. Lastly, RAMP-Mobility could be easily adapted to other countries not initially included in this study. The only limit lies in the input data availability. In case several countries are simulated, the data should be collected with comparable methodology across the different countries.

List of Figures

List of Tables

Introduction

Aims of the thesis

The aim of this thesis is to develop an open-source model to simulate Electric Vehicles (EVs) load profiles with high temporal detail for 28 European countries. The necessary inputs are aggregate data regarding mobility, time-related people behaviour, population composition and vehicle fleet characteristics. The output consists of two main time series. First, the mobility demand of the whole country is simulated, in terms of power supplied by the battery to the EV. Then, the charging demand to the grid is computed, based on user-defined assumptions concerning the charging process. Calculations are based on traditional mobility data, as these are more representative of the whole population behaviours with respect to the electric mobility data. Indeed, these cover only the small part of the country already adopting this relatively new technology. Therefore, the work relies on the arguable assumption that the electric mobility users' behaviours are similar to the current ones.

The availability of accurate load curves describing EVs' charging demand is a crucial component for energy system models to assess the impact of coupling the power and transport sector. The integration of this sector is important to allow its decarbonization, as it accounts for 31% of the European final energy consumption and for 25% of greenhouse gases emissions [22]. Furthermore, it can provide additional flexibility to the power system. This can be obtained thanks to two main contributions. First, the possibility to shift the EVs' charging demand when more convenient to the system, thanks to smart charging mechanisms. Then, it can provide a large amount of storage to the system, using the Vehicle-to-grid (V2G) technology. No measured European-wide database exists on EV mobility demand, as it is a technology still in the early adoption phase. For this reason, the few available data on electric mobility are not representative of the whole country behaviours. Furthermore, to the best of the author's knowledge, no model has been developed in the past to simulate the electric mobility charging demand at the European level. Indeed, previous works have focused on modelling mobility behaviours of a single country only. The profiles resulting from this thesis are then used as one of the inputs for the Dispa-SET optimal dispatch model, with which the impact of sector coupling on the flexibility needs of an energy system characterised by high shares of Variable renewable energy sources (VRES) is assessed. This analysis is performed in the context of the soft-linking with the long-term energy planning model JRC-EU-TIMES, which provides the overall outlook of the scenario simulated, called PROREs.

In addition to this, the scientific community is gradually acknowledging the importance of developing models with an open-source mindset when dealing with high degrees of unpredictability and arbitrariness. This is fundamental to guarantee

transparent and reproducible research methodologies and results, and also to enhance productivity and reduce duplicated efforts [23]. For these reasons, this work is fully developed in Python and is released as open-source software. This choice is also made with the purpose of facilitating the possibility for each model user to define personalised assumptions and scenarios. The model is called "RAMP-Mobility", and is available for free on the GitHub repository: https://github.com/RAMP-project/RAMP-mobility.

Outline of the thesis

The structure of this thesis is the following:

- Chapter 1 introduces the role of the integration between electricity and transport sector in the creation of a smart energy system. The importance of sector coupling in the decarbonization of the energy sector is discussed.
- Chapter 2 provides a review of the literature on EV load profiles modelling, along with how past works have dealt with transport sector coupling in energy system models with high temporal detail.
- Chapter 3 presents the methodology used to develop the original model to simulate EVs load profiles on European scale. This includes both the mathematical modelling and the input data collection. Then, the methodology used in the soft-linking between the Dispa-SET and JRC-EU-TIMES models is reported. Here, the simulated EVs load profiles are used as input for the transport sector modelling.
- Chapter 4 is dedicated to results presentation. First, a validation is performed on RAMP-Mobility, to test its accuracy and reliability. Then, the European database of EVs charging demand is presented, discussing the differences among countries. A sensitivity analysis is performed on the main arbitrary parameters and on the customizable features available, to highlight their impact on the results. Finally, the results of the Dispa-SET model are analysed, to study the influence of sector coupling on the flexibility needs of an energy system with high share of VRES.
- Chapter 5 concludes the work, drawing the main outcomes and discussing the possibilities for future developments of the research.

Chapter 1

The context

1.1 The importance of sector coupling

In December 2019 the European Commission presented the European Green Deal for the European Union (EU) and its citizens. This is the response to the challenges that climate change and other environmental problems are posing to the current generation. It defines a strategy with the aim of reaching zero net greenhouse gases emissions in 2050, while ensuring a competitive economy [24]. To this end, the importance of expanding energy system analyses from the power sector only, to a smart energy system, where all the sector (electricity, transport and heating) are integrated, is analysed by numerous studies [1]–[3]. A Smart Energy System can be defined as follows:

> *«An approach in which smart electricity, thermal and gas grids are combined with storage technologies and coordinated to identify synergies between them in order to achieve an optimal solution for each individual sector as well as for the overall energy system»* [1].

In this context, the transport sector plays a pivotal role, as it accounts for 25% of EU's greenhouse gases emissions, and has a growing trend. To achieve the goal of the Green Deal, a 90% reduction in emissions from this sector is needed by 2050. The carbon intensity in the transport sector is high, with only around 5% of transport final consumption satisfied by non-fossil fuel based technologies, most of which through biofuels [22]. When considering a carbon-neutral power system, the coupling of the electricity and transport sectors through electric mobility offers a crucial contribution towards decarbonization. The massive deployment of EVs poses some challenges to the electric grid due to the additional electricity demand, but can also be beneficial for a system with high penetration of VRES. First, the additional electric load caused by the EVs' charging demand can be shifted to the most favourable time for the system, with a smart charging mechanism. This time might be either when the demand is low, or when there is excess electricity production, that would otherwise be curtailed. Second, the introduction of V2G technology can provide a large amount of storage to the power system, that can be used to satisfy the system flexibility requirements.

1.2 Transport sector integration

1.2.1 Technical aspects

The necessary condition for a correct power system operation is the constant balance between supply and demand. Currently, the uncertainty, which is mainly laying in the demand side, is managed through the availability of power plants with fast response time. However, considering a system mainly relying on VRES introduces a high degree of uncertainty also on the supply side. Therefore, the power grid flexibility requirements have to be increased. The V2G technology, consisting of using the battery capacity available in an EV as storage, is characterised by two aspects that make this strategy a candidate to provide substantial flexibility to the power system [25]. Vehicles are parked most of its time, and have an average charging window of about 10 h compared to a much shorter actual charging time of approximately 90 min. This solution is able to provide power quality support, regulation and load balancing. Additionally, it can be important in contributing with ancillary services like frequency and voltage control and spinning reserve.

To contribute significantly to the grid operation, a large number of cars should provide flexibility services in the same time. For this reason, it is important the presence of an entity, called aggregator, placed between the EV owner, the electricity market and the Transmission System Operator (TSO). This subject collects the data from the individual cars, and communicates with the TSO to manage the charging and discharging in the most cost-effective way. Furthermore, considering the cumulative storage capacity provided by the aggregator allows also to predict its behaviour with a higher precision [26]. There are also some challenges related to the large scale integration of electric mobility. Impacts on the distribution network should be carefully taken into account, as the system was designed for unidirectional power flow only. Additionally, issues related to battery degradation can hamper the economic advantage of adopting this solution. Frequent charging and discharging cycles are likely to reduce battery lifetime, negatively impacting the user's economic balance. Finally, another possible limitation might lie in the development of secure communications protocols among the actors involved, namely the vehicle owner, the aggregator and the system operator.

1.2.2 Modelling aspects

In spite of the high expectations surrounding it, electric mobility is still a technology in the early adoption phase. For this reason, a precise representation of the transport sector coupling in energy system models is crucial to assess the impact that its electrification can have on the power system. In addition to this, it can provide useful insights to the industrial players and regulating authorities about how to shape most effectively the technology implementation trajectories. In this regard, the main challenges are linked to difficulties in describing millions of EVs with high operational accuracy, while ensuring computational tractability. To cope with this, studies usually either limit the geographical scope or the technological detail of the analysis. In particular, when considering the V2G technology from the system operator perspective, the most convenient option is to cluster a high number of vehicles together, in the

aggregator perspective described in the previous section. Nevertheless, considering of a single variable storage capacity raises the question of how to handle the individual vehicle's contribution. Indeed, there is a strong linkage between the single user operation, and the possibility from the TSO to exploit the EV battery for flexibility purposes. These two aspects should not enter in conflict, meaning that the system should be able to exploit the services offered by the vehicle without interfering with the user travel patterns.

Chapter 2

Review of large-scale electric vehicles modelling

Before presenting the model developed in this thesis, it is important to study the context of EVs representation in the literature. Two types of analyses are performed. First, models to simulate the load profile caused by electric mobility are reported, to understand the benchmark in this field. At the time of writing there is no open dataset, neither simulated nor measured, of EVs load profiles on the European scale. Therefore, the second part of the review studies how large-scale energy system models have dealt with electric mobility modelling in the past.

2.1 Electric vehicles load profile models

Several models have been developed in the literature, to study the impact that electric transportation can have on the grid, in terms of additional power demand. Two main types of models can be identified, based on the input data used to analyse the driving behaviours. On the one hand, some studies use data related to conventional mobility as inputs. On the other hand, other works use electric cars data as a source, which are usually collected during small trial projects, or from real world data.

2.1.1 Models based on conventional mobility data source

Models using conventional mobility data to simulate driving behaviours have the advantage of being able to represent the whole population, both in terms of driven distance and of time-related habits. Nevertheless, transposing those information to the realm of electric vehicles requires assumptions regarding the charging process, such as availability of charging infrastructure, nominal power or attitudes of the users towards range anxiety. It is important also to point out that studies using regular mobility data rely on the arguable assumption that the electric mobility users' behaviours are similar to the current ones.

One of the first studies in this context was performed in 2013 by the Joint Research Centre (JRC), with the goal of creating a database of EVs load curve starting from conventional mobility data, collected by means of a survey [4]. It should be noticed that this was the first study presenting a methodology to calculate EVs load profiles

starting from quite accurate mobility data, and exploring different charging scenarios for a wide geographical scope, namely six large European countries (France, Germany, Italy, Poland, Spain and United Kingdom).

First, the travel patterns are derived from the survey, creating a time series, with 5 minutes temporal detail, of the car status – driving or parked. Then, the vehicle consumption during the trip is estimated, depending mainly on the type of car and on its average speed. A quadratic function is used to model the data resulting from empirical data measuring the consumption of EVs at various constant driving speed; in addition, the consumption is incremented by 30% to account for the fact that in a urban context the car is hardly ever travelling at constant speed. Once the mobility consumption is defined, the electricity demand to recharge the battery is computed. To model this, the study assumes that home charging is always possible, and that work related trips have higher probability of finding the charging infrastructure when parking. In addition, the user plugs-in the EV only if the parking time is higher than 30 minutes. The charging process has an 80% efficiency, and can be normal (3.6 kW) or fast charging (16.7 kW). Also, the study considers that when the battery is almost fully charged, the charging speed decreases.

The base case results show morning and afternoon peaks in the weekdays, and a more constant profile during the weekend. However, the curves are quite different for each day, and exhibit a relatively high dependency on the single user, resulting in a segmented aggregate profile. The final output is a typical weekly profile, without any seasonality variation. Figure 2.1a shows an example of the resulting charging demand for Monday. In addition to this, also a scenario where charging during the night is favoured is simulated, generating a load curve with an evening peak that is even higher than the peak of the base case scenario, as can be seen in Figure 2.1b, this suggests that a smart charging solution should be implemented to avoid these issues.

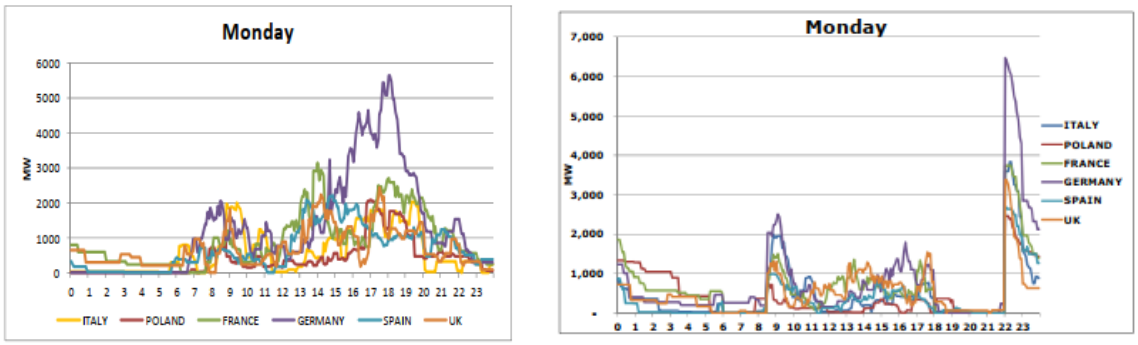

(a) Uncontrolled charging strategy.

(b) Night charging strategy.

Figure 2.1. Example of the results of the weekly average profile on Monday. The six considered countries are presented in both uncontrolled and night charging scenario [4].

The work conducted in 2014 by De Tena et al. [27] aims at simulating EVs' charging profiles, to study the impact of electric mobility on a future German power system with a high share of VRES. The load profiles are calculated developing the *VEnCo* model, while the integration with the power network is simulated with an energy model called REMix. The driving behaviours are retrieved from the extensive

survey Mobilität in Deutschland (MID), and consists of travel distance, purpose and type of vehicle used. Then, for each of the 8 defined trip purposes, a different charging point availability is assumed. With these inputs, the energy consumption of each individual car, the percentage of the fleet plugged into the power grid and the charging power demand are calculated. An example of the results can be seen in Figure 2.2 for a medium sized EV in 2050, where share of plug-in vehicles, mobility and uncontrolled charging load profile are shown. The gasoline consumption is shown in the legend simply because the model simulates also Plug-in Hybrid EV (PHEV), while the plot refers only to EVs. The shape of the curve shows two peaks, with the second being higher because a share of vehicles do not have any charging infrastructure available during the day, and can recharge the car only at home.

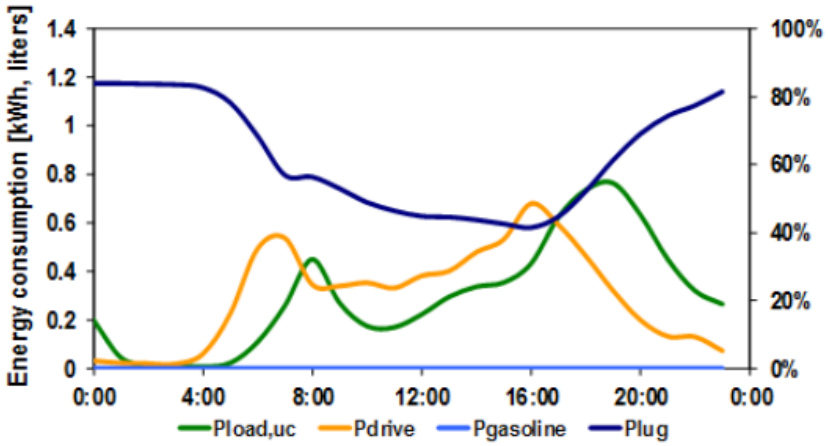

Figure 2.2. Result of plug-in share (in blue), mobility demand (in yellow) and total charging demand profile (in green) for a medium sized EV in 2050 [27]. The gasoline consumption is equal to zero as in the picture a fully electric vehicle is considered.

This study also elaborates a methodology to calculate the available battery capacity for flexibility purposes. This is done evaluating a maximum and minimum possible SOC, where the former corresponds to the uncontrolled charging case and the latter to the latest charging possible, while guaranteeing the feasibility of the last daily travel. Applying then a confidence interval to these two curves, the minimum fraction of the residual battery available can be computed. Therefore, the higher is the confidence interval, the lower the power balancing potential of the EV fleet. An example of this approach is show in Figure 2.3, where it is clear that if the confidence level overcomes a certain value, it is possible to have an intersection between the two levels, bringing to a null available energy.

This work develops an accurate model to simulate the load profile due to electric mobility, and proposes also a methodology to calculate the part of the battery fleet available for V2G purposes. However, neither the model nor the results are open-source, and therefore is impossible to use them as source of input for any energy system model. Furthermore, the model relies on the availability of statistics describing in depth the mobility behaviours of the population, and therefore extending it to other countries for an European wide energy system model might pose some challenges.

In 2018 Fischer developed a stochastic, bottom-up model to compute the additional electricity demand caused by a massive penetration of electric mobility, using Markov-

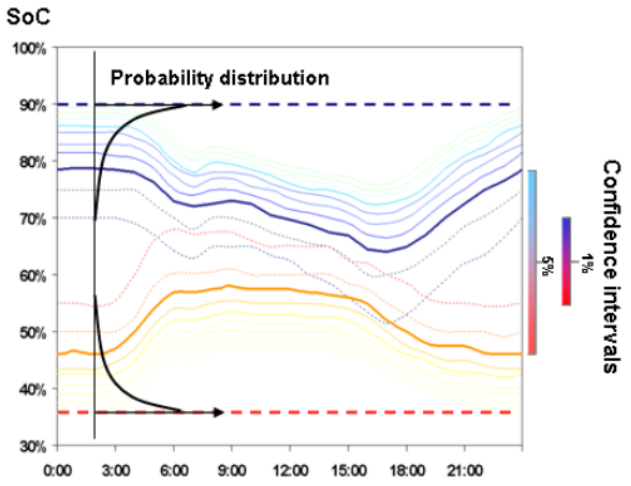

Figure 2.3. Example of the available battery capacity derivation, in blue the maximum SOC and in orange the minimum SOC. The available battery capacity is defined by the difference between the maximum and the minimum SOC level. The transparent lines report the confidence intervals of the two curves [27].

chain to simulate car usage [5]. Starting again from the conventional mobility data collected by the German survey MID, the trip related information is derived, such as travel purpose, location, distance and number of trips in the day. Then, a statistical analysis is conducted on the database to evaluate the influence of the household characteristics on mobility behaviours. The model relies on the synPRO load profile modelling framework, and simulates different behaviours for various socio-economic and demographic conditions. The main inputs of the model are of three groups, first the household specificities are determined, from this the car model is derived and the mobility behaviours related to the analysed group is drawn from the whole database. Then, the second inputs are technical parameters of the car and of the charging infrastructure at different locations, to compute the electric energy consumption. Lastly, mobility and charging assumption are set. These are the key inputs of the model, since they are used to derive the travel pattern based on Markov-Chain and to differentiate among different users' attitudes towards charging.

The inputs are then used to calculate the transport demand, the charging decision and the final load profile. The travel-related characteristics are sampled from the inputs distributions, while the Markov-chain builds the sequence of travels with their respective location and travel or parking times. After each parking, the charging decision is determined, depending on several factors. Clearly, the first necessary condition is the presence of the infrastructure, which is strictly linked to the parking location. This, in turn, is influenced by the trip index (number of the journey during the day), for example, on workdays employed users are assumed to travel to the workplace on the first daily trip and head back home on the last. Then, if the car is parked for a minimum time, the user charging style is simulated. This is modelled through a logistic function correlating the charging probability to the SOC of the car, in order to account for different attitudes towards the EV residual driving range. Figure 2.4 reports an example of the different shapes that the curve can assume. Additional aspects determining the charging probability are linked to charging price,

availability of different charging infrastructure and its distance. These factors are all incorporated in the logistic function, using a calibration parameter.

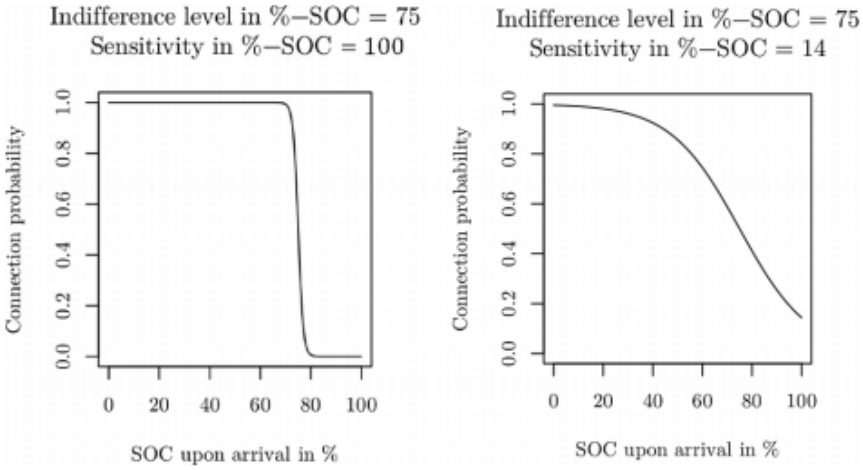

Figure 2.4. Example of different shapes of the logistic functions to model charging attitudes [5]. The two main parameters are varied to show the possible shapes of the function.

Once the car is connected to the grid, the battery is charged considering both the travel consumption and the self-discharge rate in the parking phase. In addition, the standard electricity consumption of the car is multiplied by a temperature-related factor, to account for higher air conditioning or heating consumption. The results show that the model simulates with good accuracy the mobility pattern described by the MID data, as can be seen in Figure 2.5 from the probability distribution of parking time. Here the two peaks connected to the commuting for working purposes are clearly visible.

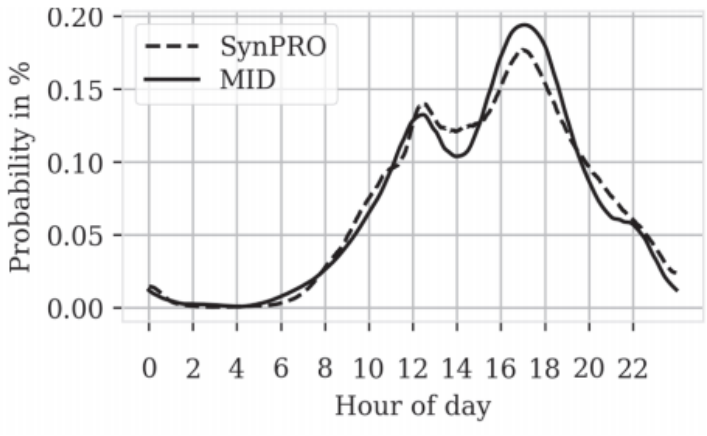

Figure 2.5. Comparison between the modelled weekday arrival time probability distribution and the MID data [5].

Moving to the load profiles, Figure 2.6 shows the aggregated results for 100 users over one year. The curve is simulated with the same probability of charging at the workplace and at home, equal to 80%. The solid line represents the average curve

over the year, the blue dots show the single users load profile, while the dashed and dotted lined are the results of a different study carried out by Schäuble in 2017, which will be presented in more detail in section 2.1.2. Focusing on the solid line, the typical shape with two peaks is visible, the first related to the arrival to the workplace, and the second to the travel to return back to home.

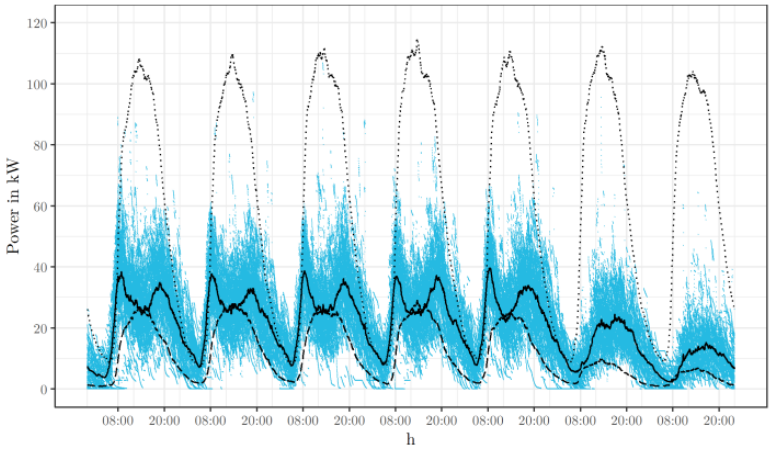

Figure 2.6. Charging profiles for 100 users over one year. The solid line shows the average result of the model while the blue dots represent the single users profile [28]. The dashed and dotted lines show a comparison with two different outputs of the work by Schäuble, that will be presented in section 2.1.2.

Overall, this work represents one of the most advanced modelling examples to calculate the EVs' load profiles from highly detailed inputs. Nevertheless, it poses similar challenges to the ones of the *VEnCo* model. These are, on the one hand, the lack of open-source availability of either the model or its results, and on the other hand, the high dependency on the availability of thorough and accurate statistics as reference for the mobility behaviours.

2.1.2 Models based on electric mobility data source

Studies using electric mobility data have opposite characteristics to the ones presented above. Indeed, the mobility patterns derived from these data are often not representative of the whole country behaviours. Since EVs are still in the early adoption phase, a large segment of the population is not captured neither by trial projects nor by measurements from actual charging point installed on the territory. Nonetheless, such studies do not need to rely on any assumption regarding the charging process, as the data directly provide information about most of the features needed to completely simulate charging events.

In 2016, Brady [6] developed a stochastic methodology to simulate the EVs mobility demand curve as well as the charging profiles. The input data are GPS information from a 9-month demonstration project carried out in Ireland on electric mobility. This consists of 15 small cars, of which both journey details and charging events are registered, for a total of more than 18 thousand travels. It is worth noticing that the users driving the cars are not the same along the whole analysed period. The focus of

this work is uniquely on the weekdays, and, due to the limited temporal scope of the data source, it does not capture seasonal variations.

The schedule of daily travels is modelled over two days with a Monte Carlo simulation. This is done analysing the correlation between six main variables, namely the departure time of the first travel, the number of travels, and the total daily distance of each of the two days. A non-parametric copula function describes the relational structure between the six variables. From this distribution, six values are sampled to start the simulation, which has a 5-minute time resolution. Then, the distance of each travel is simulated with an iterative method of conditional distribution. After this, a Bayesian inference approach samples the time of the first travel, depending on the time of the day when this happens and on its distance. The same approach is used also to sample the parking time before the second journey, that is affected by the characteristics of the parking, such as the time of the day and the travel number. This process is then repeated as many times as needed, to obtain the daily travel pattern. At the end of each travel, a probability of charging is calculated, based on the SOC, the parking time and the journey number, the latter being an indication of where the car is parked. The initial SOC is sampled from a distribution representing the inputs database, where around 50% of the users have fully charged battery at the beginning of the day. The simulation then assumes uncontrolled charging, therefore the car is charged at the beginning of the parking until full capacity is reached, with a regular 3.7 kW plug. After the last trip of the day the battery is not charged immediately, but a plug-in delay up to 5 hours is modelled, to replicate the behaviour indicated by the data. The charging point availability depends on the journey number, bringing to higher probability for the first and last travel, when, respectively, the user is arriving to work and returning to home.

This model manages to simulate quite effectively the travel patterns of the original database, as can be seen in Figure 2.7a. Nevertheless, some limits are visible when looking at the charging profile, as it is visible in Figure 2.7b. Here the data are not accurately replicated due to issues linked to limitations in the inputs database, and modelling of the parking time.

The work from Schäuble [7] starts from data measured in three electric mobility field trials in Southwest Germany conducted in the period from 2011 to 2015, overall recording around 500 EVs and almost 30 thousand charging events. The data from the three projects have differences in the level of detail of the information provided. However, the final database resulting from the processing of the data comprises information about car trips and charging events. This is used as source for the model, built to simulate the aggregate load profile for a defined number of days and car fleet size. The characteristics of the EV fleet are sampled from the database, along with the number of charges happening each day. Then, the starting time of each charging event and the final SOC, is drawn independently from the data, after checking that it provides a physical condition (SOC at the end of the parking higher than at the beginning). From the total battery capacity and the delta SOC, the energy absorbed from the grid is computed, determining the load profile with a minute temporal detail. The charging power is 3.6 kW in the base scenario, but also options with fast charging are analysed, with 22 kW and 50 kW infrastructure; anyway, the results do not show important deviations. Analysing the results, the model manages to simulate a charging profile close to the input data. However, it does not reproduce the typical passenger

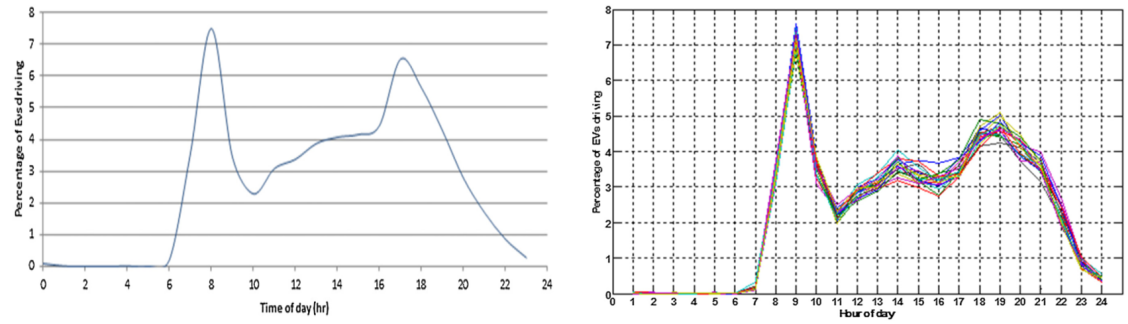

(a) Comparison between percentage of cars driving each hour.

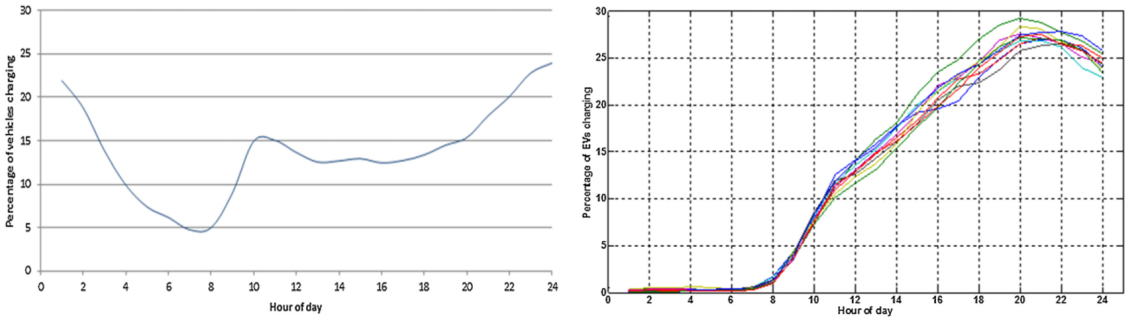

(b) Comparison between percentage of cars charging each hour.

Figure 2.7. Comparison of mobility and charging profiles from data (left) and simulated (right) [6]. The model presents different model runs, resulting in different curves due to the stochastic nature of the model.

mobility trend composed by two peaks, corresponding to work-related commuting, as can be seen in Figure 2.8. This result is mostly dependent on the type of users that compose the inputs database, mainly commercial fleet users. In addition, the author points out that the model can be applied only to conditions similar to the measured ones, both because of how the database was constructed, and due to the moderate amount of data available.

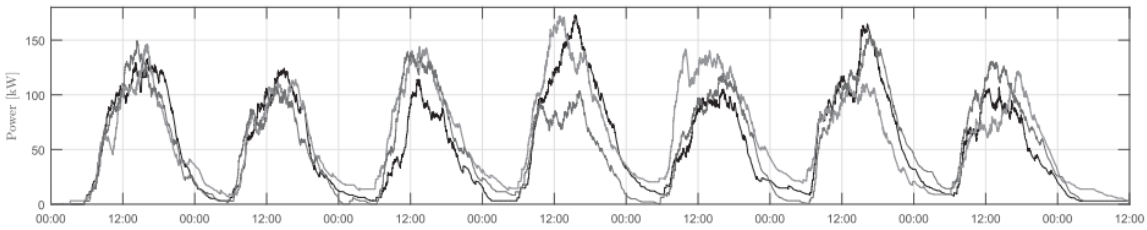

Figure 2.8. Results of three simulated load profiles over a week [7]. The three different shapes represent different model runs, and are different due to the stochastic nature of the model.

2.2 Electric vehicles in energy system models

There are not many studies about Europe-wide energy system models simulating the widespread adoption of electric transportation. This is due to the already presented

challenges linked to obtaining reliable profiles describing EVs power demand.

2.2.1 PyPSA-Eur-Sec-30

One of the first examples of EVs integration in an Europe-wide energy model is PyPSA-Eur-Sec-30, published in 2018 [3]. This work analyses both sector coupling and grid reinforcement potential to achieve 95% CO_2 emissions reduction compared to 1990. To overcome the lack of a unified dataset describing the transport profiles for Europe, the weekly mobility statistics developed by the German Federal Highway Research Institute (BASt) are used as basis to calculate the electric mobility load profiles [29]. This means that the same pattern is applied to the whole Europe and to the whole year, without any seasonal variation. The mobility demand is corrected considering the higher efficiency of the electric motors with respect to the thermal engines. Then, a linear temperature-dependant coefficient is applied, to consider the additional consumption related to heating and cooling. Hence, the electric demand from the grid is calculated assuming that the charging starts immediately after parking, considering therefore a widespread availability of Electric Vehicle Charging Points (CPs) both at the workplace, at home and in public spaces. The nominal charging power is at least 11 kW and the power demand is spread one third at the plug-in, one third one hour after the consumption and one third 2 hours after consumption. A weekly example of the resulting curve used in the model is visible in Figure 2.9, showing a slight temporal shift from the transport demand to obtain the final charging profile.

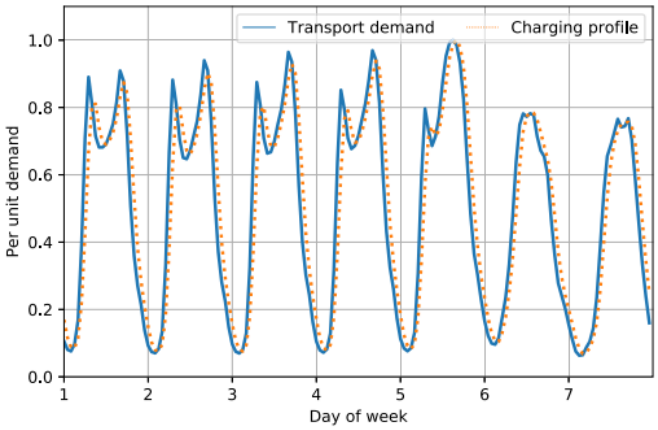

Figure 2.9. Mobility profile (in blue) and the derived charging demand (the dotted orange line) used in PyPSA-Eur-Sec-30 [3]. The curves are normalised with respect to the peak value.

In addition to this, also the V2G solution is modelled, assuming a 90% efficiency of charging and discharging, and a maximum nominal power of 11 kW. The percentage of the battery fleet connected to the grid is considered inversely proportional to the demand profile. This is between 95% and 60%, with an average around 80%. Half of the cars participate to the power exchange with the grid with only 50% of their battery capacity. Overall, the PyPSA-Eur-Sec-30 model offers one of the first examples of integration of electric mobility in a European-wide energy model, considering the

challenges linked to the absence of a dataset providing EVs load profiles with such a large geographical scope.

2.2.2 Dispa-SET "as-is" condition

This thesis work started from the need of generating reliable load profiles for EVs in the framework of the soft linking between the Dispa-SET and JRC-EU-TIMES models. It is therefore useful to analyse what was the solution adopted in the Dispa-SET framework before the development of the RAMP-Mobility model. The two main components that need to be introduced in an energy system model when integrating electric mobility are: i) the additional power demand; and ii) the storage option resulting from the adoption of a V2G solution. For the existing Dispa-SET version, the data source for both components of the model is a dataset containing historical data measured in the Netherlands in 2015, comprising charging events from around 2215 cars using the EVnetNL network [13]. Further details about the database are reported in Section 4.1.2, where these same data are used in the model validation. First, the resulting charging demand is reported in Figure 2.10, which exhibits the typical shape with two peaks caused by commuters. This profile is then scaled up to meet the total electricity demand computed by the JRC-EU-TIMES scenario, and assumed valid for all the analysed countries.

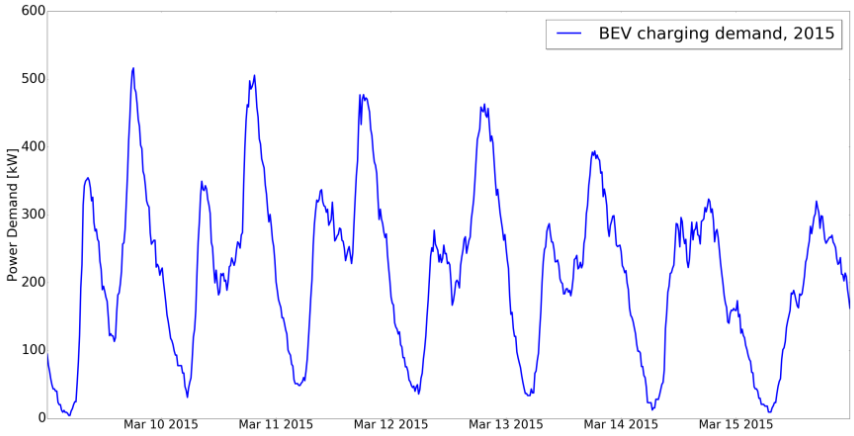

Figure 2.10. Weekly EVs power demand computed from ElaadNL historical data for a week in March 2015 [13]. It is visible the different charging demand in the weekdays and in the weekends.

Then, the share of flexible battery capacity in each hour is computed, starting from the electricity demand, to model the amount of storage available for V2G purposes. Two main hypothesis are considered:

- Limited battery availability: The total available storage capacity cannot be computed as the sum of all individually connected EV capacities. Minimum state of charge must be taken into account since battery charge should always ensure that customers have sufficient energy for the upcoming trips.
- Perfect foresight: EV users are fully aware of the time, duration and battery displacement of all future trips. They also deploy “just-in-time charging”,

where the minimum state of charge constraint is defined just before the time of departure. This value is the minimum required energy for the upcoming trip.

Figure 2.11 shows the methodology just outlined, where each vehicle has a minimum amount of energy that should be guaranteed, defined for each vehicle by the energy consumed in the next travel interval. The rest is available to the TSO for flexibility purposes. Because of the perfect foresight hypothesis, the computed battery capacity using the methodology is too optimistic and a security margin is therefore defined, called *Capacity margin* in the figure. While the modelling approach is valuable, the data source used is quite limited, since it accounts for only the behaviours of EV drivers in the Netherlands, which are reasonably not representative of the whole country. In addition to this, no differentiation in the working hours of the different European countries is included. The latter is instead an important parameter, since it might significantly influence the total load peak hours, which are critical to analyse the resilience of the power system.

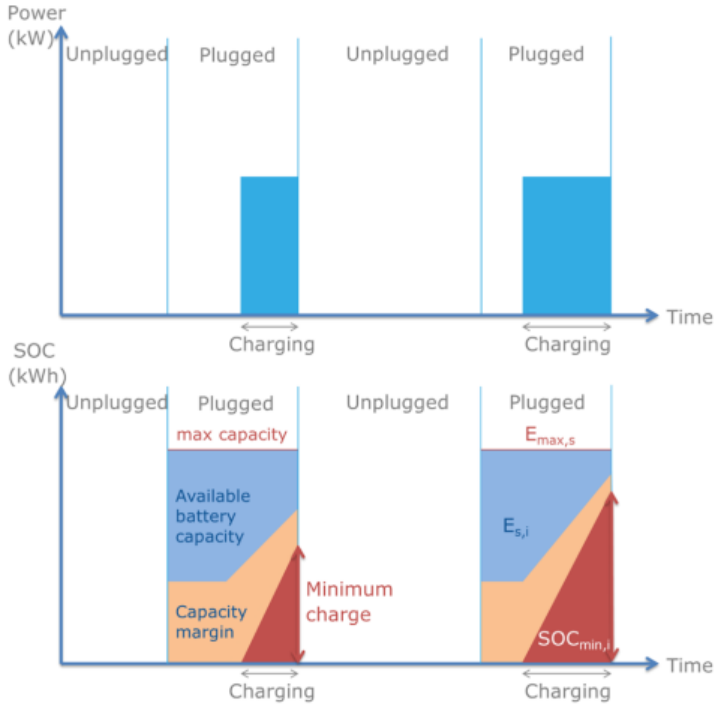

Figure 2.11. Calculation of the battery capacity of a single EV available to the TSO [30]. When the car is plugged the whole battery capacity is available to the system, minus the percentage reserved by the security margin. When charging, the share of battery available decreases according to the power requested to the grid.

Chapter 3

Methodology

Parts of this chapter were published as: Matija Pavičević, Andrea Mangipinto, Wouter Nijs, Francesco Lombardi, Konstantinos Kavvadias, Juan Pablo Jiménez Navarro, Emanuela Colombo and Sylvain Quoilin (2020). "The potential of sector coupling in future European energy systems: Soft linking between the Dispa-SET and JRC-EU-TIMES models". *Applied Energy*, vol. 267. doi: https://doi.org/10.1016/j.apenergy.2020.115100

The goal of this work is to develop a model, based on the RAMP stochastic modelling framework, to compute the mobility and charging electricity demand curves for the EVs. Here the main methods employed are described, the model is fully implemented in a Python environment and is released as open-source software. It can be freely accessed from the GitHub repository: https://github.com/RAMP-project/RAMP-mobility. The generation of reliable EV demand profiles with wide geographical scope is fundamental for energy system modelling. Therefore, a first application of this new model's results is implemented in Dispa-SET, via a soft-linking with JRC-EU-TIMES. Hence, the methodology adopted to link the two models, the simulation setup and an overview of the inputs is here provided.

3.1 Electric Vehicles charging profiles

The model consists of two main algorithms. First, starting from traditional mobility data, the mobility demand is computed, being the power consumption of the mobility appliance to satisfy the user's mobility needs. This results in a time series, with a minute time detail, composed by the travels undertaken by the user.

Then, the second algorithm takes the mobility profiles as input, and for each travel event calculates the amount of energy that the charging infrastructure transfers to the EV. The model aims at simulating both scenarios representing the present situation, with limited transport electrification, and scenarios projected in the future, like the ProRES simulated by JRC-EU-TIMES, with massive deployment of electric mobility. Therefore, the results can vary greatly. To capture the whole spectrum of possible evolutions of the system, different options and parameters are introduced, so that the user can adapt them to its own needs. Figure 3.1 presents an overview of the interaction between the different model components.

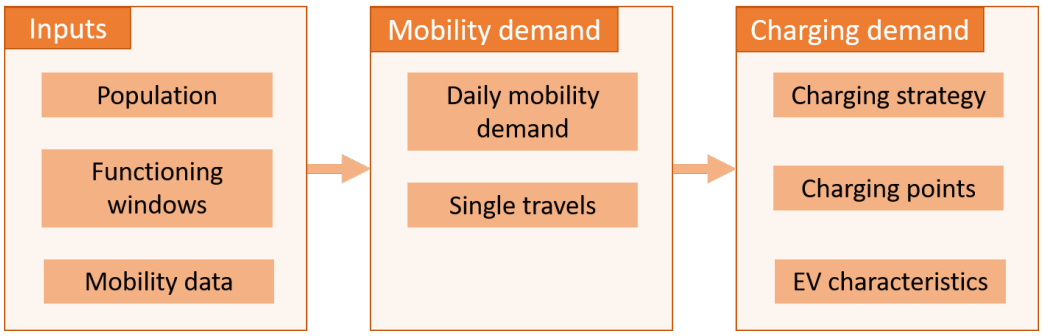

Figure 3.1. Conceptual scheme of the main components of the RAMP-Mobility model. The input data are first used to compute the mobility demand. Starting from that, the charging power requested to the grid can be computed under different assumptions.

In order to prevent problems related to transient model dynamics at the beginning and at the end of the simulation, a given number of additional days (by default 5 at the beginning and 5 at the end of the simulation) are simulated and then discarded.

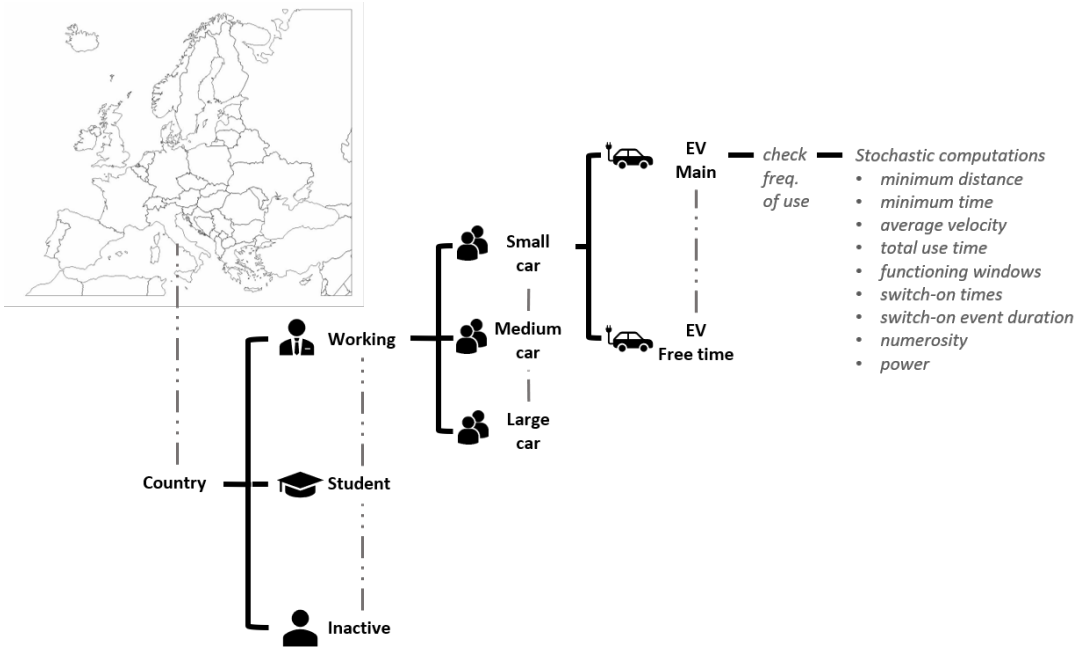

Figure 3.2. Graphical representation of the RAMP model composition, adapted from Lombardi et al. [8]. The country is divided in three users categories, and each is in turn differentiated by the size of the driven car. Each car is then modelled differently if used in the main functioning time or in the free time period.

The complete representation of the model setup for each country is presented in Figure 3.2. From the conceptual point of view, each country is divided in a certain number of *User types*, 9 in the default version. Then, the population is subdivided to assign n users to each *User type*. Each user drives one EV, characterised by different parameters according to type of day considered (Weekday, Saturday or Sunday) and to the hour of the day (peak or off-peak time).

3.1.1 RAMP modelling framework

Before presenting the detailed formulation of the RAMP-Mobility model, it is important to provide an overview on the RAMP modelling framework. RAMP is an open-source bottom-up stochastic model for the generation of high-resolution multi-energy profiles. The complete model description is available in the related publication [8], while source code can be freely accessed from the GitHub repository[1].

The model is based on three conceptual layers. First, a set of User types should be defined, representing a group of users with the same characteristics (for example Household, Commercial activities, Hospitals etc.). Then, a number of single users is associated to each User type. Third, the Appliances owned by each user are identified. The same set of appliances is associated to each User type. This setup allows to model each Appliance belonging to a single User, meaning that, within the same User type category, each User will have a different load profile. Aggregating all the User profiles, the total load is obtained. Due to the stochastic nature of the model, each run produces a different load curve, reflecting the randomness inherent in the behaviour of the real-life users. The main inputs necessary to setup the model are presented in Table 3.1. These refer to the main parameters needed to define the behaviour of the Users, along with the corresponding Appliances.

User type and Users		
$Usertype_j$		Name of the User type
n		Number of $Users$ within $Usertype_j$
Appliances		
$Appliance_{jik}$		Name of the k-th *Appliance* associated with the j-th *User type* and the i-th *User*
m_{jik}		Numerosity of $Appliance_{jik}$
P_{jik}	[W]	Power absorbed by a single item of $Appliance_{jik}$
tot_use_{jik}	[min]	Total time of use of the $Appliance_{jik}$ in a day
t_min_{jik}	[min]	Minimum time that the $Appliance_{jik}$ is kept on after a switch-on event
use_frames_{jik}		Time frames in which a random switch-on event of $Appliance_{jik}$ can occur
$frequency_{jik}$	[%]	Weekly frequency of use of $Appliance_{jik}$

Table 3.1. Overview of the main inputs necessary to setup the RAMP model.

3.1.2 Modelling mobility demand

The first necessary step is to adapt the general structure of the RAMP model to manage the particular case of mobility "appliances", i.e. vehicles. This is achieved passing from the definition of the power consumption cycles of the appliance, to that

[1] https://github.com/RAMP-project/RAMP

of the characteristics of the travel – a much easier information to be found in the transportation field – and then computing the power consumption for each travel, based on the car type.

A large amount of data is needed in order to model the whole EU minus Cyprus and Malta, plus UK, Switzerland and Norway. These data are related to the mobility behaviours, the population and car fleet composition, and the time habits of the different countries. This work relies on traditional mobility data in the evaluation of the travel patterns. This is preferred over the alternative of using electric mobility data, which fails at reproducing the whole population dynamics. Indeed, EVs are a technology still in the early development phase. Therefore, the population segment already driving electric cars is not representative of the whole country behaviours. A conceptual representation of the input data used in the mobility demand modelling and of the main algorithm outputs is presented in Figure 3.3.

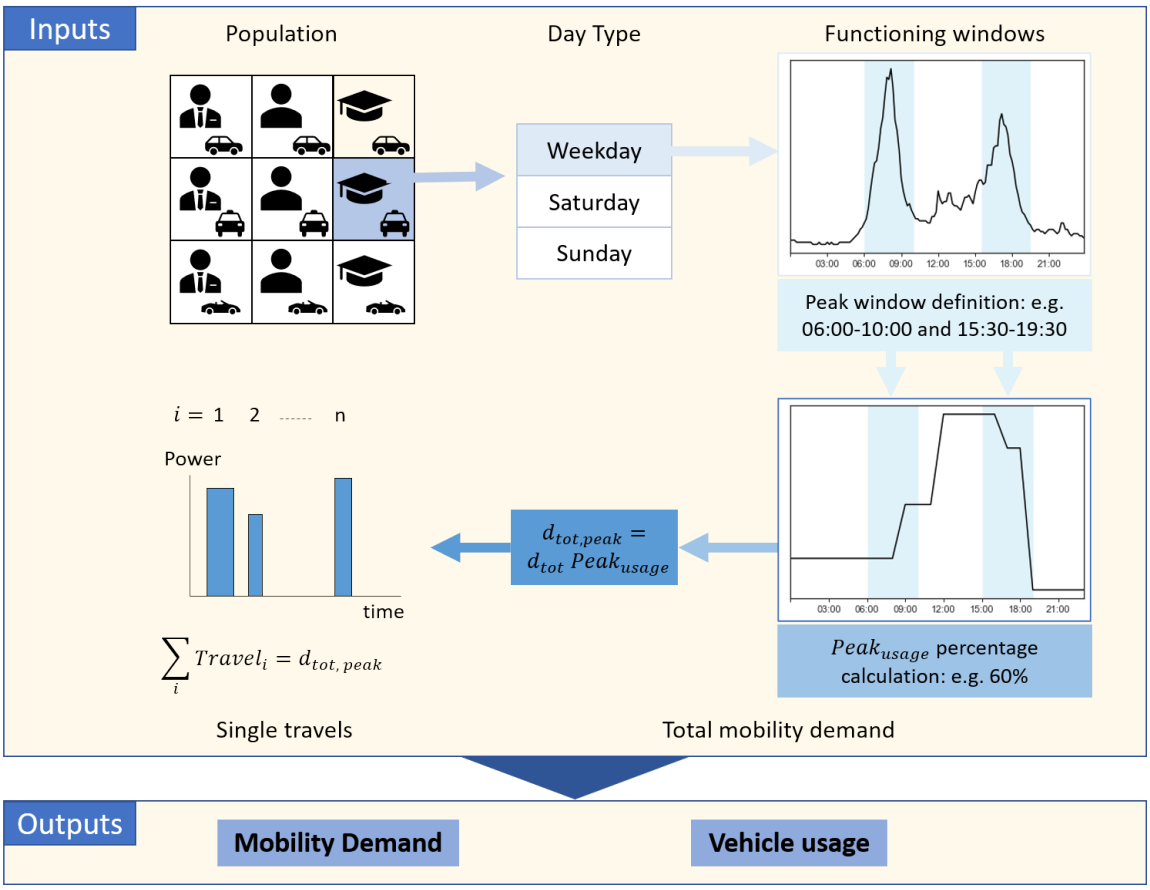

Figure 3.3. Conceptual scheme of the input data, their relations, and of the main outputs of the mobility demand algorithm. Each user belongs to a certain User type category. For each day type the peak and off-peak functioning windows are defined and the total daily mobility demand is subdivided accordingly. Then, the single travels are simulated until the total transport demand is satisfied. The result of the algorithm are two time series: the power demand to the vehicle battery and the percentage of vehicles travelling in each time step.

Population composition

Due to the bottom-up nature of RAMP, the first step in creating the model setup is the definition of the population composition, which in the model is implemented through the *User types* variable. An overview of the variables presented in this section is available in Table 3.2.

Population composition	
Population share	
Working	Percentage of people working
Student	Percentage of people enrolled in higher education
Inactive	Percentage of people unemployed or not looking for job
Vehicle share	
Large	Percentage of low power cars
Medium	Percentage of medium power cars
Small	Percentage of high power cars

Table 3.2. Overview of the variables used to calculate the population composition. Source: Eurostat [9], [10].

The population is divided in 3 main categories, namely *Working*, *Student* and *Inactive*. This is considered a good trade-off between the increasing complexity given by a too detailed population subdivision, and the reduced modelling accuracy resulting from a limited differentiation between different users behaviours. Indeed, the high effort in modelling very specific users, is likely to be jeopardised by the insufficient detail of most data sources. The population is further subdivided, based on the size of the mobility appliance. Again, 3 main car types are identified: *Small*, *Medium* and *Large* cars; these models will correspond to different power consumption of the electric motor, P_{EV}, and to different battery capacities, $C_{battery}$. Overall, the simulated country is subdivided in 9 *Users type*, each composed by a number of independent *Users*, with a uniquely simulated car usage profile. Indeed, RAMP allows to simulate for each *User* as many *Appliances* as needed, however, for the purpose of this work, each user owns only one single "appliance", this being a "mobility appliance", and in particular, an EV.

The data used in the default model version are the result of two datasets, namely the different occupation type, and the different car size. The working condition is the combination of two Eurostat databases. First, one showing the population composition by working condition (employed, unemployed and inactive) [9] and the second one indicating the number of students enrolled in tertiary education [10], the reference year is 2016. Considering only the population older than 20 years, the values for the three model categories are deducted, the *Working* category is composed by employed people, the *Student* by the number of enrolled students, and the *Inactive* by the number of people registered as unemployed or inactive, minus the number of students. Moving to the distribution of car size, the data source is again Eurostat, in particular the passenger cars subdivision by engine size, the reference year is again 2016. Since the data reflect the current situation, the division is related to combination of diesel and petroleum cars, which represent more than 90% of the total fleet, and can therefore

be considered a good indication of the car size distribution [31]. An example of the resulting population composition in Italy is shown in Figure 3.4.

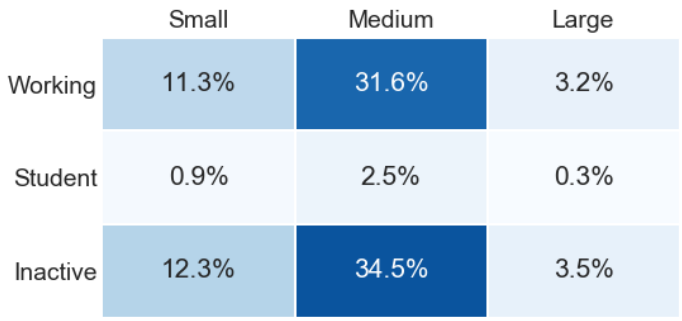

Figure 3.4. Example of population composition in Italy. It is visible the predominant share of working and inactive users with medium sized cars.

Day type

The model simulates the mobility profile independently for each day, but, in order to obtain a result that can represent the real EVs' consumption, it is important to represent the variability caused by the different days of the year. Therefore, in the model is implemented the possibility to simulate any year, with the proper differentiation between weekdays, Saturdays and Sundays. During the weekdays, different time behaviours are defined for *Student/Working* users with respect to the *Inactive*; on the weekend, instead, the whole population behaves according to the same daily patterns, equal to the *Inactive* user ones.

In addition, also the holidays are taken into account, modelled with the same behaviours as Sundays; this is done thanks to the open-source python library *holidays*, to which it was necessary to add the information related to Latvia and Romania, not included in the default version [32].

Functioning windows

In the model, each appliance has a predefined number of functioning windows, defining the time frames in which it can randomly start a travel. The most common trend observed in travelling behaviours is the presence of two peaks of car usage, one in the morning and one in the afternoon, corresponding to the commuting from home to the workplace. For this reason, the *Working* and *Student* users type are characterised by 5 functioning windows, 2 defining the peak hours, and 3 identifying the car usage for non-work related purposes. In the model these are called, respectively *Main* and *Free time* travel windows. An overview of the types of functioning windows implemented in the model is reported in Table 3.3. However, RAMP considers a maximum number of windows for each appliance equal to 3. Therefore, for each user type, two fictitious cars are modelled, one for the *Main* functioning time, with 2 windows, and one for the *Free time* parts of the day, with 3. This workaround is an effective way to simulate the full daily usage of the car for each user, without increasing the number of functioning windows to be defined for each vehicle. The *Inactive* user's functioning

Functioning windows	
Working or Student	
Weekday	2 Main and 3 complementary Free-time windows
Weekend	1 Main and 2 complementary Free-time windows
Inactive	
Weekday	1 Main and 2 complementary Free-time windows
Weekend	1 Main and 2 complementary Free-time windows

Table 3.3. Overview of time windows types used by the model to calculate peak and off-peak usage. Source: HETUS [11].

windows instead are more difficult to be defined, as no standardised behaviours can be identified. Hence, one single *Main* functioning window and two complementary *Free time* windows, for the early morning and early evening, are defined.

For this purpose, data coming from the Harmonised European Time Use Surveys (HETUS) are well suited. This is composed by national surveys with the goal of studying the way in which people spend their time in different activities. The surveys have been conducted two times so far, in 2000 and in 2010, with another round planned for 2020, not yet released at the time of writing. The methodology used in each country is as similar as possible, since common guidelines were provided, along with standardised questionnaires, which leads to comparable results among countries. Furthermore, the main methodology is the same over time, ensuring similar results among the two rounds of survey results [33]. This is particularly useful, since some of the countries modelled in this thesis are not present in the 2010 results, but participated to the 2000 survey. For the *Working* and *Student* users, the same functioning windows are used; the data determining them is the participation rate in the *Work and study* main activity, reported with a 10 minutes temporal detail [11]. An example of the derivation of the functioning windows starting from the HETUS data is shown in Figure 3.5: windows with the same length, equal to 4 hours, are taken around the travelling peak. The data for the *Inactive* functioning windows, instead, are more difficult to be found, due to the lack of regular pattern in the users' activities. However, it can be inferred, with the help of some indicators. First, in the HETUS results, the category *Unspecified time use and travel* gives a good approximation of when the activities start in the morning, indeed, the results of the survey show a significant delay in the rise of the curve, and a similar delay in the evening, when the curve falls. Since this category does not show only the unspecified travelling trends, but also more in general all the activities that do not fall under any of the main categories expected by the survey, it is important to have a confirmation of this trend from another source. As previously explained, the functioning windows for the *Inactive* users, are applied to the whole population during the weekend. Therefore, analysing the behaviour of the population in the weekend could be another index of the *Inactive* functioning windows also during the weekdays. In this regard, the survey conducted by the JRC in 2012, provides some useful insight [12]. There, the car trips distribution by time of the day are reported, divided by day type, showing during the weekend a much higher share of trips in the window between 09:00 and 12:00 AM

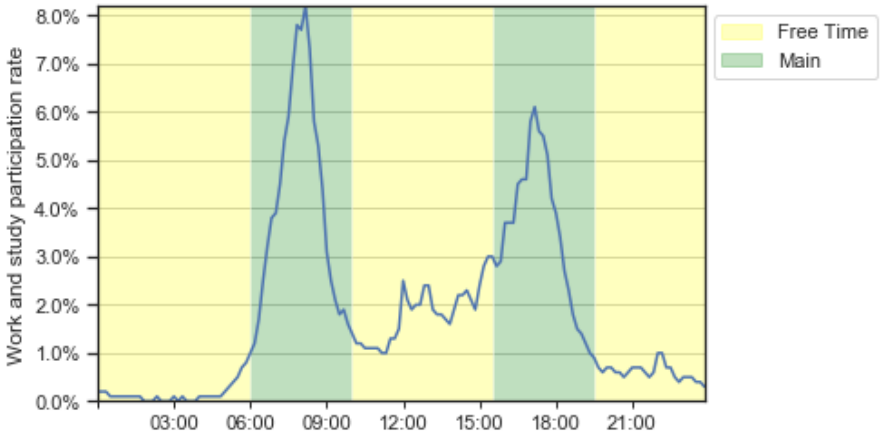

Figure 3.5. Example of functioning windows calculation for the Netherlands. The peak windows are highlighted in green, the rest of the day is considered as free time, and highlighted in yellow.

with respect to the weekday, and consequently also a lower incidence of travels before 09:00. In addition to this, since the activities tend to start later, they also finish later. It is however important to mention that the data show a less pronounced trend in this regard, with respect to the delayed start of the activities in the morning. Therefore, the idea that the weekend (and therefore *Inactive*) *Main* functioning window ends later is confirmed, but particular attention should be payed about this in the validation phase (Section 4.1).

Total daily mobility demand

In order to model the whole daily usage, it is necessary to define the total distance driven on average each day. This is done through the variable d_{tot}, that combined with the average velocity v_{av}, provides the total usage time that the mobility appliance has to run each day, t_{tot}. The stochastic algorithm randomly switches on the appliance in the allowed functioning window, as many times as needed to satisfy the total travelling distance d_{tot}.

Total daily mobility demand	
d_{tot}	Total average driven distance for each day
$usage_{perc}$	Percentage of total distance driven in each functioning window type

Table 3.4. Overview of variables used to model total daily mobility demand. Source: 2012 JRC Survey [12].

As previously explained, due to modelling reasons, the EV is divided for each day in two different appliances, one working during the *Main*, and the other during the *Free time* functioning windows. Therefore, the d_{tot} needs to be subdivided as well, in order to model correctly the total driven distance in the corresponding times. To do this, a new parameter is introduced, $usage_{perc}$, that determines the share of d_{tot} belonging to each functioning window type

The accurate modelling of mobility patterns for a large amount of countries relies on the availability of public data describing their main characteristics, such as the specific travelling behaviours of the population, and in particular for this study, private passenger cars mobility. A large number of European countries conduct a National travel survey (NTS), some with a regular basis and other less frequently, with the goal of analysing the aforementioned mobility trends. However, these surveys are not conducted with harmonised methodologies, hindering the possibility of using the results as a data source for an EU-wide study. In addition, most of the NTS are not detailed enough to be used as data source for the kind of model developed in this thesis, either because the surveys do not investigate all the necessary information, or because the results are reported on a too highly aggregated basis [34]. Therefore, in 2012 the JRC conducted a direct survey to analyse passenger cars travelling behaviours in 6 EU countries, namely France, Germany, Italy, Poland, Spain and United Kingdom [12]. These six countries combined represent around 70% of the whole EU passenger car stock [35], and almost 75% of total new registrations of passenger cars in EU in 2018 [36]. This study reports data on daily driven distance and time, on the average trip distance and time, on the distribution of trips along the day and other travel-related parameters. Furthermore, most of the information are divided by trip purpose and by day of the week, providing data that are at the same time detailed, but also easy to be used.

In the literature there are other reports presenting similar results. However, there are different reasons why they were not considered as the best data source for this work. For example, in 2015, the JRC conducted another study presenting mobility data from two average Italian cities, Modena and Florence, collected in May 2011, and also from the Green eMotion project, a quite large database of EVs usage information collected in six Demonstration Regions from March 2011 to December 2013 [37]. However, the former results come from data collected in a very specific case, while regarding the latter, it was decided not to use EVs' mobility data, as the technology is still in the early adoption phase. Therefore, it is difficult to obtain a complete representation of the whole country's population. Furthermore, the report provides a very detailed statistical analysis, which is important if an accurate description of the variables is needed, but is not very suited for a model like RAMP-Mobility, that was conceived to work with aggregated input data. Indeed, a too detailed statistical characterisation of the input data is avoided, because it could hinder the model's ease of use. This work is meant to be applied in different energy models, with different case studies and needs, therefore one of the priority in the development phase is to guarantee the usability of the model. It is anyway important to notice that in the described study, a comparison of the two aforementioned datasets with the 2012 JRC survey is performed, pointing out that the results are comparable to a great extent. Another survey published in 2015 from the JRC, instead, has the goal of understanding car (and other transport modes) usage, and deepening mobility trends in the EU. This study is interesting because is conducted as a direct survey in the all the 28 EU's member states, providing therefore specific results for each country [38]. Unfortunately, the level of detail of the analysis presented is too low to provide all the necessary inputs for the model developed in this thesis. It is indicated in the report that additional results were published in a file annexed to the report, however, this is not available on the publication website. Nevertheless, it is also

explained that the additional results are linked, for instance, to a higher detail in the respondents' population segment. Hence, there is no guarantee that additional travel-related variables were studied at all.

For all the reasons just outlined, the 2012 JRC survey is the main source for the input data needed to characterise mobility behaviours. The total daily driven distance d_{tot} is deducted from this survey, the values are presented in Figure 3.6, divided by weekday and weekend. The $usage_{perc}$ parameter is derived from the JRC survey as well. This is calculated thanks to the values of car usage percentage per hour, divided by day type. Thus, the model attributes the correct usage percentage to the *Free time* and *Main* time windows, according to the functioning windows. This parameter is then multiplied by the d_{tot}, to set the total amount of kilometres driven each day by the mobility appliance.

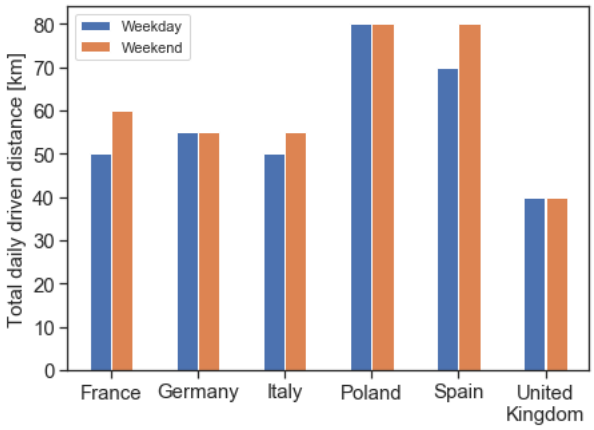

Figure 3.6. Value of total daily driven distance (d_{tot}) for different countries and day type (weekday or weekend) [12].

Single travel characteristics

After having defined the total distance driven by the car in each functioning window, it is fundamental to define the specificities of the average trip. This is used by the model to simulate as many switch-on events as needed to cover the total mobility demand. The main variables here described are summarised in Table 3.5.

Single travel characteristics	
d_{min}	Average distance travelled after a switch-on event.
t_{func}	Average duration of a switch-on event.

Table 3.5. Overview of variables used to model the single travel. Source: 2012 JRC Survey [12].

The average travel is implemented in the model through the variables d_{min} and t_{func}, which define the average distance and time of each travel performed by the EV. Then, the average trip velocity v_{av} is calculated, through Equation 3.1.

$$v_{av} = \frac{d_{min}}{t_{func}} \tag{3.1}$$

The values of the variables d_{min} and t_{func} are drawn from the 2012 JRC survey. The resulting values are shown, respectively, in Figure 3.7a and 3.7b. The data are differentiated for travel purpose, which can be either business or personal. Furthermore, the different day of the week is considered. For example, a general trend of longer personal travels towards the weekend is visible.

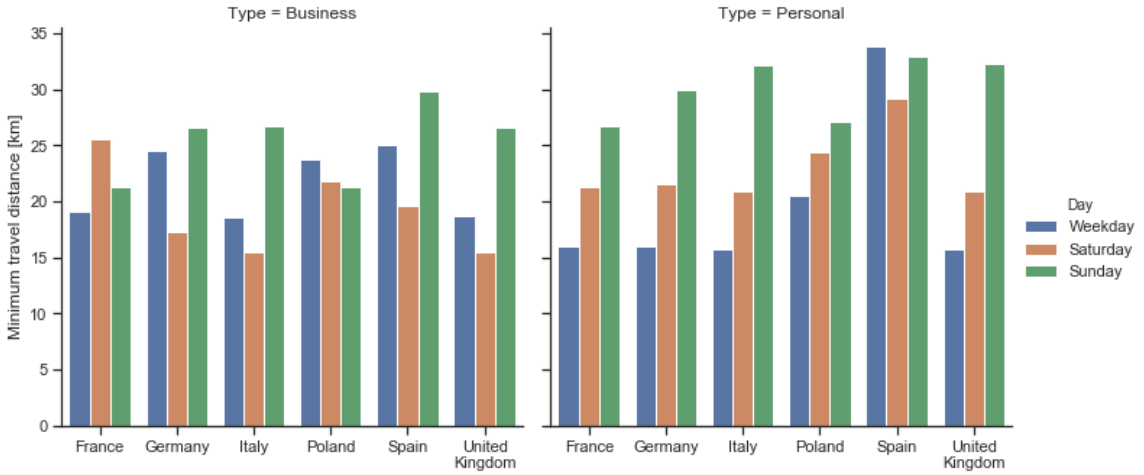

(a) Distribution of the data used as input for the minimum travel distance, expressed in km.

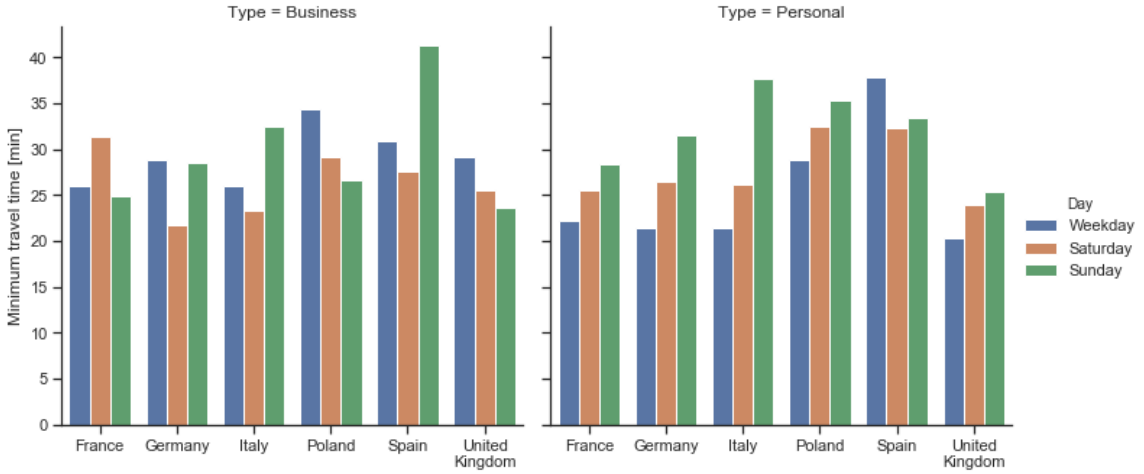

(b) Distribution of the data used as input for the minimum travel time, expressed in minutes.

Figure 3.7. Values of minimum travel distance and time for different countries, travel purposes and day of the week [12].

It is worth to explain in detail how these different data are assigned to the different user types and functioning windows. First, for the *Working* user type, the data related to business travels are the ones that characterise the mobility appliance in the *Main* functioning windows. Conversely, in the *Free time* windows the personal travels' information determine the minimum time and distance the appliance works once the travel starts. Then, regarding the *Student* user type, during the *Main* time frames a mean value between business and personal is taken, as the student behaviour can be considered halfway between the two purposes. In the *Free time* the personal travel data are used. Lastly, the *Inactive* user is fully defined by the personal travel data. This subdivision is consistent along the three types of day: weekday, Saturday and

Sunday.

Country	Mobility data	Functioning windows	Car Fleet
AT	Values from DE	Values from DE	Eurostat
BE	Values from FR	HETUS 2010	Eurostat
BG	Values from PL	HETUS 2000	Eurostat
CH	Values from DE	Values from DE	Eurostat
CZ	Values from DE	Values from DE	Eurostat
DE	2012 JRC Survey	HETUS 2010	Eurostat
DK	Values from DE	Values from DE	Values from DE
EE	Values from PL	HETUS 2010	Eurostat
EL	Values from IT	HETUS 2010	Eurostat
ES	2012 JRC Survey	HETUS 2010	Eurostat
FI	Values from DE	HETUS 2010	Eurostat
FR	2012 JRC Survey	HETUS 2010	Eurostat
HR	Values from IT	Values from SI	Eurostat
HU	Values from DE	HETUS 2010	Eurostat
IE	Values from UK	Values from UK	Eurostat
IT	2012 JRC Survey	HETUS 2010	Eurostat
LT	Values from PL	HETUS 2000	Eurostat
LU	Values from FR	HETUS 2010	Values from DE
LV	Values from PL	HETUS 2000	Eurostat
NL	Values from DE	HETUS 2000	Values from BE
NO	Values from DE	HETUS 2010	Eurostat
PL	2012 JRC Survey	HETUS 2010	Eurostat
PT	Values from ES	Values from ES	Eurostat
RO	Values from PL	HETUS 2010	Eurostat
SE	Values from DE	Values from NO	Eurostat
SI	Values from IT	Value from PL	Eurostat
SK	Values from DE	HETUS 2000	Values from CZ
UK	2012 JRC Survey	HETUS 2010	Eurostat

Table 3.6. Overview of the data sources for each country. Mobility data includes both the total daily mobility demand data and the single travel characteristics. The population share is not included as Eurostat provides the data for all the countries considered.

Vehicle power consumption

During the simulation of each travel, the model calculates the average trip speed based on the inputs just shown. Then, to calculate the power consumption, it needs a relation linking the car speed to the electricity provided by the battery. A simplified model developed by the JRC in 2013 is used, consisting of a quadratic function that calculates the power consumption based on the vehicle speed [4]. As can be seen in Figure 3.8, 3 groups of coefficients are suggested, to model the behaviour of small,

medium and large cars, in line to the type of modelling performed in this work. This is also useful as the coefficients can be adapted to future technology developments.

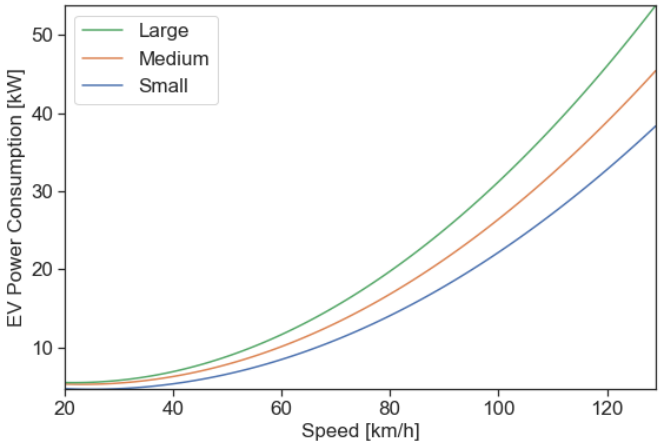

Figure 3.8. Power curve model implemented in RAMP-Mobility [4]. The three curves refer to small, medium and large sized cars.

In addition to the described consumption of the EV, a multiplication coefficient depending on the outdoor temperature, T_{amb}, is applied. This takes into account the effect of extreme weather on the battery performances and on the heat and cooling systems' consumption. The coefficient is computed as shown in Equation 3.2, according to the formulation proposed by Fischer [5].

$$\frac{P_{EV}\left(T_{amb}\right)}{P_{EV,\,nom}} = \begin{cases} 1.12 - 0.01\,T_{amb} & \text{if} \cdot\, T_{amb} < 15 \\ 1 & \text{if } 15 \leq T_{amb} \leq 20 \\ 0.63 + 0.02\,T_{amb} & \text{if} \cdot\, T_{amb} > 20 \end{cases} \tag{3.2}$$

In the default model inputs, the yearly temperatures from *Renewables.ninja* are used, these are composed by hourly values for each country, averaged according to the population. The years included span from 1980 to 2016 [39].

Optional stochastic parameters

All the variables presented above are subject to a random variability, whose extent is defined by the user. An overview of these additional inputs is presented in Table 3.7.

Stochastic parameters	
$d_{min,\,rand}$	Percentage random variability applied to the average distance.
$v_{av,\,rand}$	Percentage random variability applied to the average velocity.
$P_{EV,\,rand}$	Percentage random variability applied to the EV consumption.
$window_{rand}$	Percentage variability in the functioning windows length.
occasional use	Weekly frequency of use of the EV

Table 3.7. Overview of the optional stochastic parameters available in the model.

First, the mobility data are subject to a stochastic variability $d_{min,rand}$ and $v_{av,rand}$. The average velocity v_{av} determines also the total switch-on time that the EV has to satisfy. For this reason, also the t_{tot} is randomly varied. The same is applied also to the power consumption of the EV during the travel, $P_{EV,rand}$. The variability is calculated independently for each single user and each day, thus fixing the same values for all the daily travels. On top of this, also the functioning windows have a random variability parameter, $window_{rand}$, that shifts their starting and ending time around the user-defined average value. Again, the random variability can freely varied in the model, it is set to 1 hour in the default model configuration. Another important stochastic parameter in the model is the *occasional use*, which determines the probability that the appliance will be used in the simulated day; so, if it is equal to 1, there will be at least one switch-on event per day. In the model default version, during the *Main* windows, this value is set to 1 in the weekdays, to 0.6 on Saturday and 0.5 on Sunday. This choice is made to reflect the lower probability that the car is used on the weekend, due to the lack of working activities that cause the daily car usage. In the same manner, the value is set to 0.15 during the *Free time* windows, independently on the day of the week, to replicate an approximate probability of using the car once a week (1 out of 7 days) for free time activities. Clearly, it is very difficult to have any reference for the value of these parameters. Thus, they have a high degree of arbitrariness; for this reason, they can be freely modified by the user, and will be also subject to a sensitivity analysis, to study their impact on the final results, as discussed in Section 4.2.2.

3.1.3 Modelling charging demand

After a reliable mobility profile is calculated, it is possible to analyse the charging power demand, that is the electric energy the EV needs in order to recharge its battery. Several charging strategies are proposed and implemented. In addition to this, there are high uncertainties regarding the way in which the transport sector will develop with high share of electrification in the next decades. Therefore, several parameters of the charging process function cannot escape from having a certain degree of arbitrariness. Thus, they are explicitly reported, and are made easy to change for the model user, in order for them to be adaptable to different modelling purposes or assumptions.

Charging strategies

Due to the high uncertainty regarding the evolution of the EVs market, it is difficult to know how the charging process will be handled in 2030 or even 2050. Indeed, it is expected that the large-scale deployment of EVs is likely to cause high stress to the power grid, exacerbating the existing demand peaks. Therefore requiring high investments in the grid infrastructure and in the power production capacity [40]. For this reason the most recent literature discusses the possibility to introduce the so-called smart charging strategies. These consists of shifting the charging patterns efficiently, in order to prevent unnecessary investments, and possibly favour the coupling of the transport sector with Renewable energy sources (RES) power production [41].

Therefore, different charging strategies are implemented in the model, in order to

simulate the evolution of the EV demand profile in different ways. The most common smart charging strategies proposed in the literature consider either the presence of a centralised scheduling, or of a decentralised management system. In the former, the presence of EV aggregators is crucial in order to obtain an active integration in the market, leaving to them the task of defining the optimal charging pattern according to the system's conditions. In the latter, instead, the responsibility is shifted to the users, relying on the application of incentive strategies, such as electricity price mechanisms, that indirectly funnel the consumers' behaviour towards the desired pattern [42]. This level of optimisation is reached in energy system models, such as Dispa-SET, that simulate the whole power system and are able to manage the interactions between different sectors in the most cost-effective way. In this thesis, some less complex smart methods are implemented, in order to provide an halfway benchmark between the two extremes of uncontrolled charging on the one hand, and of complete optimisation on the other; overall, four charging strategies are implemented. Figure 3.9 shows a flow diagram presenting an overview of the whole charging algorithm:

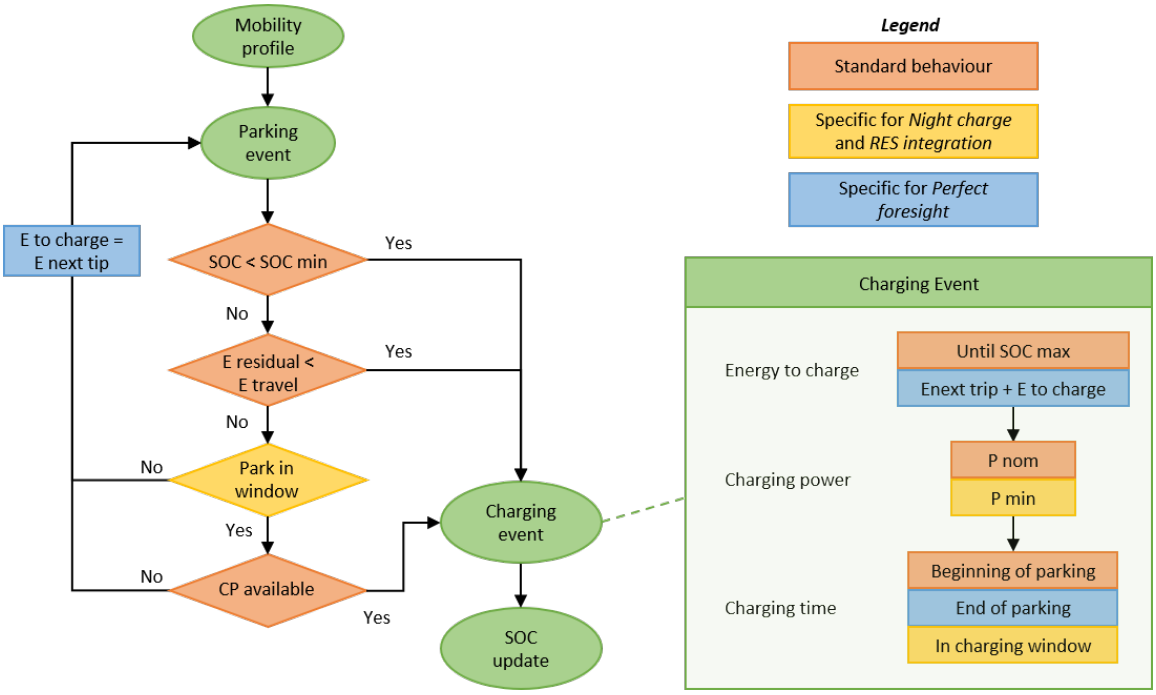

Figure 3.9. Flow diagram representing the charging process algorithm. The boxes represent different charging strategies: the common standard algorithm is in red, the specificities of the night charge and RES integration in yellow and the peculiarities of the perfect foresight are in blue.

1. *Uncontrolled*: this is the base case, where no control over the user behaviour is applied. The algorithm takes as input the mobility profile for each user, which is composed by the sequence of the travels made by the car, with the corresponding battery power consumed. Each time a travel ends, a parking event begins, and the presence of the CP is verified using the CP_{prob} function. If the charging infrastructure is available, the battery is charged, with a 90% charging efficiency at the CP nominal power, P_{CP}^{nom} randomly sampled from a

user-defined probability distribution. The charging event continues for the time needed to reach the user-defined SOC_{max}, that can be set to a value lower than 100% to avoid fast degradation of the battery and extend its lifetime [43].

2. *Perfect Foresight*: this strategy aims at quantifying the possibility to implement a V2G solution. After verifying the CP availability, the car is charged with the P_{CP}^{nom} right before the end of the parking. The energy transferred is the amount needed for the following journey, plus the energy lost in case of a parking event without charging. This strategy allows to compute the part of EV battery available to the system operator, without affecting the driving range available to the user once the travel stars [13].

3. *Night Charge*: it is the first smart charging strategy which, as the name suggests, aims at shifting the charging events to the night period, with the goal of flattening the load curve, charging in a time of lower electricity demand. The basic structure of the algorithm is the same: when the car is parked, the CP_{prob} function is evaluated. However, the CP availability is not enough to start the charging event. Also a check on the time of the day when the car is parked is performed; if that lies in a user-defined range (e.g. from 22:00 to 07:00), then the EV is charged. Furthermore, the power of the CP is not the nominal one, but is the minimum one that allows to completely charge the battery in the night charging window.

4. *RES Integration*: the second smart charging method developed has the goal of coupling the RES power generation with the transport sector. The charging algorithm is essentially the same of the *Night Charge*, the difference lying in the definition of the time windows where the charging is shifted. These are based on the residual load curve, $D_{residual}$, which is calculated as shown in Equation 3.3:

$$D_{residual} = D - P_{el}^{WIN} - P_{el}^{PHOT} \tag{3.3}$$

Where D is the total demand, P_{el}^{WIN} the wind energy production, and P_{el}^{PHOT} the power produced from solar energy. The charging is shifted to periods when the $D_{residual}$ is negative, which means that the power produced from RES is higher than the demand, and would be otherwise curtailed. Thus, this strategy enhances the usage of power from renewable sources. This strategy is a simplified version of what can be simulated in a complete energy model. Hence, it relies on the correct consideration of power demand, wind and solar availability, and their installed capacity. In the default version, European Network of Transmission System Operators for Electricity (ENTSO-E) data are used for the demand, while the the availability factors' source is the *Renewables.ninja* dataset [16], [17]. The installed capacities correspond to the PRORes JRC-EU-TIMES scenario. The user who wants to apply this charging strategy, should first carefully analyse the standard input data, and verify if they are suited also for different modelling purposes.

The mobility profile is computed without a feedback by the charging process. Hence, it is possible that the SOC reaches values lower than 0, which is clearly

a non-physical condition. For this reason, two different controls are implemented to detect this possibility, and prevent it. The first is the definition of the SOC_{min} value, below which the user necessarily charges the car as soon as the car is parked. This lower limit is also useful to extend battery lifetime. Anyway, is worth noticing that there is evidence that range anxiety plays a more important role in EVs' user acceptance, with respect to a lower consideration attributed to low battery lifetime [44]. Nevertheless, this might not be enough. Therefore, a further control is implemented, which guarantees that the energy stored in the battery is enough to cover the upcoming trip. It might happen that a trip is interrupted by a brief stop. To guarantee that the whole travel can be covered with the residual SOC, if the stop lasts less than 10 minutes, the two subsequent travels are counted as one.

Car battery capacities

The first of the arbitrary parameters defined is the battery capacity of the different types of EVs, $C_{battery}$. In the default version these are drawn from some of the most common models in the current market, as shown in Table 3.8.

Car Type	Reference model	Battery capacity [kWh]
Small	Volkswagen e-Up!	37
Medium	Opel Ampera-e	60
Large	Tesla Model X Long Range	100

Table 3.8. Reference models for car battery capacity depending on the car size [45]–[47].

Charging points

Together with the car, the other crucial components of the system are the CPs, characterised by their nominal power and relative distribution. In the default version there are 3 types of charging infrastructure. The P_{CP}^{nom} and their relative share is presented in Table 3.9.

Charging point type	Nominal power [kW]	Relative share
Standard plug	3.7	60%
Fast charge	11	30%
Supercharger	120	10%

Table 3.9. Reference values for the charging infrastructure nominal power and relative share in the country.

Charging infrastructure availability

The large-scale availability of charging infrastructure is a fundamental enabler to increase the electrification rate in the transport sector. Nevertheless, a high uncertainty surrounds the roll-out of this technology. Therefore, two modelling techniques are

proposed here for the CP_{prob} function, suited for different scenarios. The first assumes constant probability of finding the infrastructure at each parking, while the other considers a stepwise probability function:

- Nowadays, it is more likely to have a CP available at home, either as private infrastructure or as public point installed in the residential area. However, since there is no spatial information in the model, the closest approximation is to consider an higher probability in the early morning and in the evening, periods where most of the population is at home. The result is a piecewise probability function, as shown in Figure 3.10. Therefore, if the simulated conditions are similar to the current ones, the advised approach is to use this CP_{prob} function, taking into account also that its shape can be adapted to the users' needs. A clear example in which this approach is preferred, is the model comparison against historical data, as shown in Section 4.1.2.
- The second type of CP_{prob} function modelled is a constant probability throughout the day. Indeed, it is reasonable to assume that in a scenario where EVs become the main transport mean, a wide availability of charging infrastructure at home, at the workplace and in commercial buildings is guaranteed. This brings to a constant probability of finding a CP each time the car is parked. It is advised to use a high value (around 70-90%), but to keep this value below 100%. Indeed, that would bring to a simulation where the EV is plugged-in the grid at every parking. Anyway, as already explained, any kind of scenario can be simulated, varying this input accordingly.

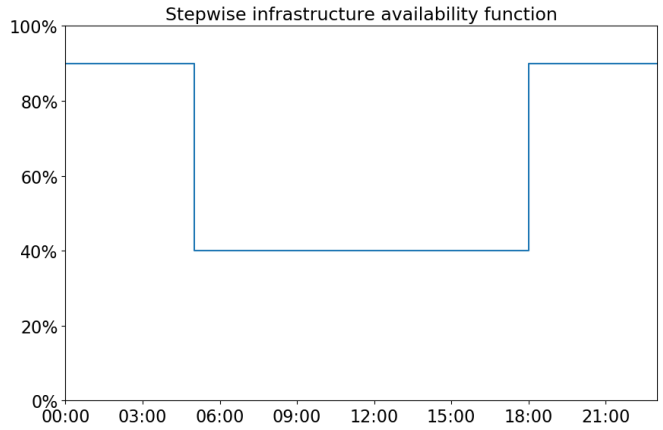

Figure 3.10. Default version of the stepwise probability function to model charging infrastructure availability.

User range anxiety

In order to model the behavioural characteristics of the user, it is included the possibility to define a logistic curve that correlates the plug-in probability to the SOC of the battery when the car is parked, according to the approach proposed by Fischer

et al. [5]. The function formulation is defined in Equation 3.4.

$$Prob_{plug-in}\left(SOC\right) = 1 - \frac{1}{1 + \exp\left(-k\left(SOC - \%_{SOC}\right)\right)} \tag{3.4}$$

where k is the gradient of the curve at the SOC defined by $\%SOC$. In the default version k is set to 15 and $\%SOC$ to 50%. The resulting logistic function is presented in Figure 3.11. The introduction of this feature aims at reproducing different EV user's dynamics, depending on the shape of the curve. This approach is not activated in the default version of the model, as its uncertainty is too high. Anyway, in case the model's user can rely on data that support certain assumptions, this feature can be activated.

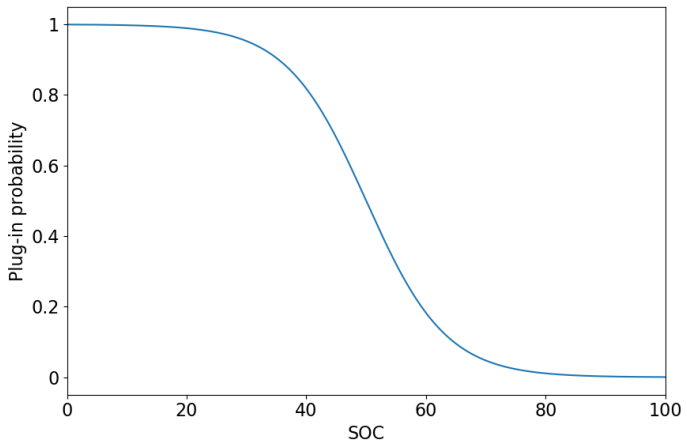

Figure 3.11. Shape of the default logistic curve implemented to model the relation between the battery SOC and the charging decision probability. By default this feature is not activated.

Vehicle-to-grid

Energy system models like Dispa-SET or PyPSA, often model the possibility for the system operator to use the storage offered by the EV fleet plugged into the network, to provide flexibility to the grid, in a V2G configuration. This can be represented in several ways in the optimisation model. RAMP-Mobility, providing the complete information about the mobility patterns and the charging curves, can be adapted to several modelling approached. Here a first example is reported, starting from the methodology shown in Section 2.2 and based on the specificity of Dispa-SET model. The V2G is modelled as an additional storage technology, with a variable nominal capacity defined by an Availability factors (AF). This is a time series indicating the percentage of the total battery fleet available for flexibility purposes. To define this, the *Perfect foresight* charging strategy is considered, to always ensure that the car users have sufficient energy for the following trips. In addition, a security margin is defined to cope with this optimistic assumption. Further details are reported in the Dispa-SET methodology description, Section 3.2.5.

3.2 Dispa-SET linking with JRC-EU-TIMES

In this section, the methodology adopted to simulate the future low carbon energy system is described. Here, the RAMP-Mobility EV load profiles are used as input for the Dispa-SET model, in the context of the soft-linking with the JRC-EU-TIMES model. The PRORes scenario simulated by the JRC-EU-TIMES long-term Energy System Optimisation Model (ESOM) is used as input for the Dispa-SET Unit-commitment and power dispatch model (UCM), where the flexibility needs of the system are analysed with a high temporal detail. The Dispa-SET model is first presented, then, the unidirectional soft-linking methodology between the two models is outlined. Subsequently, the metrics used to study the energy system performances are reported, and the simulated scenarios described. Finally, the main inputs and data used to model the different sectors are presented.

3.2.1 Dispa-SET model

Dispa-SET is a multi-sector energy system model which allows to define the flexibility requirements of an energy system characterised by high penetration of VRES. The model is defined as a mixed-integer linear programming (MILP) problem. Publicly available modelling approaches are the basis for the definition of the model. The key aim of Dispa-SET is to analyse complex, interconnected, electricity networks with a high precision.

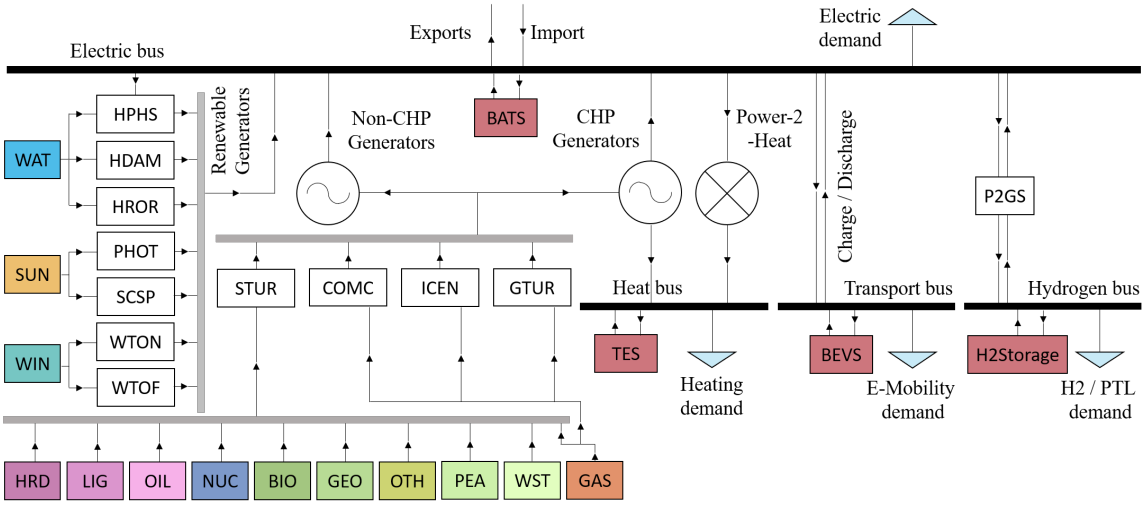

Figure 3.12. System structure for a single country. Each object symbolises a fuel, storage or energy production technology (boxes), buses (black lines) or demands (triangles). Adapted from Pavičević et al. [30].

A graphical representation of the model structure in one zone is presented in Figure 3.12. To facilitate the comprehension, a summary of the technologies and fuels used in the model is provided in Table 3.10, along with their description. An exhaustive explanation of the Dispa-SET model is out of the scope of this thesis. For a complete description of the model and its characteristics, the reader may refer to

Technology	Description	Fuel	Description
COMC	Combined cycle	BIO	Biomass
GTUR	Gas turbine	GAS	Gas
HDAM	Conventional hydro dam	GEO	Geothermal heat
HROR	Hydro run-of-river	HRD	Coal
HPHS	Pumped hydro storage	HYD	Hydrogen
ICEN	Internal combustion engine	LIG	Lignite
PHOT	Solar photovoltaic	NUC	Nuclear energy
STUR	Steam turbine	OIL	Petroleum
WTOF	Offshore wind turbine	SUN	Solar energy
WTON	Onshore wind turbine	WIN	Wind energy
BATS	Stationary batteries	WAT	Hydro energy
BEVS	Battery-powered electric vehicles		
P2GS	Power-to-gas storage		
P2HT	Power-to-heat		
SCSP	Concentrated solar power		

Table 3.10. Summary of the names of the technologies (left side) and fuels (right side) used in the Dispa-SET model, along with their description.

the model technical report [48] or to the official documentation[2]. The main features of the model are:

- Maximum and minimum power generation limits for each unit.
- Operational limits such as ramping rates, start-up and shut down intervals and minimum switched on and off times.
- The shed load possibility when the power supply does not meet the demand.
- Primary, secondary and tertiary upwards and downwards reserve requirements.
- Curtailment of VRES due to power grid constraints.
- Various storage technologies (thermal, hydro, electrical, hydrogen).
- Non-dispatchable power generation (e.g. from wind turbines, Solar photovoltaic (PHOT), Hydro run-of-river (HROR))
- Accurate representation of fixed and operational costs.
- Interconnections between different nodes, with limited values of maximum power exchanges for congestion analyses.
- Combined heat and power (CHP) units available both in flexible extraction mode and in inflexible back-pressure condition.

[2] Dispa-SET documentation: http://www.dispaset.eu

- Different heating supply technologies, such as Power-to-Heat (P2HT), CHP or backup heaters.
- Modelling of V2G technology considering the limited battery availability due to user mobility demand.
- Schedules of planned and unexpected outages for each unit.

The main equations regulating the optimisation are the objective function and the demand balance. Therefore, these are briefly outlined in the following sections.

Objective function

The target of the unit commitment problem consists of the minimisation of the overall system operational costs, in €. This is called $TotalSystemCost$ and is defined as the sum of different cost items. These are: shut-down and start-up and, variable, fixed, ramping and voluntary or involuntary load shedding costs. The demands are considered inelastic with respect to the price signal. Hence, the MILP objective function is the total system cost in the considered optimisation horizon. The complete formulation is as reported in Equation 3.5.

$$
\begin{aligned}
min\Big[& \sum_{u,i} CostFixed_{u} \cdot Committed_{i,u} \\
& + \sum_{u,i} CostVariable_{i,u} \cdot Power_{i,u} \\
& + \sum_{u,i} CostStartUp_{i,u} + CostShutDown_{i,u} \\
& + \sum_{u,i} CostRampUp_{i,u} + CostRampDown_{i,u} \\
& + \sum_{l,i} PriceTransmission_{i,l} \cdot Flow_{i,l} \\
& + \sum_{n,i} CostLoadShedding_{i,n} \cdot ShedLoad_{i,n} \\
& + \sum_{th,i} CostHeatSlack_{th,i} \cdot HeatSlack_{th,i} \\
& + \sum_{p2h2,i} CostH2Slack_{p2h2,i} \cdot StorageSlack_{p2h2,i} \\
& + \sum_{chp,i} CostVariable_{chp,i} \cdot CHPPowerLossFactor_{chp} \cdot Heat_{chp,i} \\
& + \sum_{i,n} VOLL_{Power} \cdot (LL_{MaxPower,i,n} + LL_{MinPower,i,n}) \\
& + \sum_{i,n} VOLL_{Reserve} \cdot (LL_{2U,i,n} + LL_{2D,i,n} + LL_{3U,i,n}) \\
& + \sum_{u,i} VOLL_{Ramp} \cdot (LL_{RampUp,u,i} + LL_{RampDown,u,i} + LL_{3U,i,n}) \\
& + \sum_{s,i} CostOfSpillage \cdot Spillage_{s,i} + \sum_{s} WaterValue \cdot WaterSlack_{s} \Big]
\end{aligned}
\tag{3.5}
$$

Where the variables with the *chp*, *p*2*h*2, *th* and u subscript refer to single the units. The time step is indicated as i, the transmission lines between zones as l, while n refers to the single zone.

Demand balance

The balance between supply and demand is the main imposed constraint. This is satisfied in the day-ahead market for each time step and zone. The formulation is reported in Equation 3.6.

$$\begin{aligned}&\sum_{u} Power_{u,i} \cdot Location_{u,n} + \sum_{l} Flow_{i,l} \cdot LineNode_{l,n} = \\ &\sum_{r} StorageInput_{s,h} \cdot Location_{s,n} + \\ &\sum_{p2h} PowerConsumption_{p2h,i} \cdot Location_{p2h,n} + \\ &Demand_{DA,n,h} - ShedLoad_{i,n} - LL_{MaxPower,i,n} - LL_{MinPower,i,n}\end{aligned} \tag{3.6}$$

The supply side is represented by the power generation by all the units present in the node, including storage (*Power*), plus the injections from neighbouring nodes (*Flow*). The demand is composed by the day-ahead load in the node, plus the power consumption caused by P2HT units for heating purposes (*PowerConsumption*) and the stored power (*StorageInput*). In case the balance is not satisfied, the load shedding (*ShedLoad*) and load interruption (*LL*) options are activated.

Mid-term scheduling

The Dispa-SET UCM simulates one year with a hourly time step. Therefore, if the entire problem was optimised at the same time, the complexity would be too high, bringing to computationally infeasible dimensions. For this reason, the problem is divided in few days loops that are run recursively for the whole year. The starting point of each loop is the final result of the previous optimisation loop. In order to prevent problems related to the end of the optimisation period, such as the complete utilisation of the storage plants, a number of look-ahead days are computed and then discarded. Nevertheless, some components of the simulation such as the storage units require a pre-optimisation to evaluate their minimum SOC. Thus, a simplified, perfect foresight version of the problem is run with a full year horizon. This is called Mid-term scheduling (MTS), and is important especially for countries with high presence of hydroelectric storage plants. The MILP problem is converted in a linear programming setup by removing the integer variables along with the following components of the model:

- Thermal sector variables and costs, for example heating demand, generation and storage.
- Operational limits of the plants such as ramping rates, start-up and shut down intervals and minimum times both switched on and off and unit commitment.
- Costs associated to the heating sector and operational plants limits.

3.2.2 Soft-linking with JRC-EU-TIMES

The EU version of the Dispa-SET model was previously validated with data from 2016 [49]. In this work, a scenario in 2050 is used to analyse the role of sector coupling technologies in an energy system with high penetration of VRES. With this aim, the PROREs scenario generated by the JRC-EU-TIMES model provides the overall figures used in the Dispa-SET simulations. These include the capacity of the installed generation units, the total yearly demands and the commodity prices.

JRC-EU-TIMES model

To assess the flexibility potential given by sector coupling in a future energy system characterised by extensive penetration of VRES, the results of the JRC-EU-TIMES long-term ESOM in 2050 are first considered. The JRC-EU-TIMES model is a linear optimisation bottom-up model developed by the JRC of the European Commission, based on the TIMES model generator. It represents the EU27 energy system with the main neighbouring countries (36 countries in total), from 2005 to 2050. Due to the high complexity of the model, each year is divided in 12 time-slices representing the average day, night and peak demand for each seasons of the year. The low temporal detail impacts significantly the capability of the model to asses the energy system flexibility needs. The main goal of JRC-EU-TIMES is to study energy technologies potential and provide recommendations on European energy policies. It simulates capacity expansion, considers investment and operation costs and calculates prices endogenously, based on supply and demand curves. The objective function of the linear programming is the maximisation of the discounted welfare in each region. In other words, the optimisation minimises the negative surplus, also called system cost. Several constraints are considered, both on the supply and on the demand sides, these are: primary resources supply curves, technical constraints for capacity expansion planning, balances regarding all energy and emission forms, investment timings and other cash flows and the satisfaction of several demands for energy services in all the sectors. The model considers seven sectors: primary energy supply, electricity generation, industry, residential, commercial, agriculture and transport [50].

The PROREs scenario includes the long-term objective of 80% reduction in energy-related greenhouse gases emissions by 2050, with respect to the 1990 levels. Further information about the considered PROREs scenario are available in the dedicated report [14]. A strong decarbonisation path is visible. Fossil fuels dependency is significantly reduced, at the same time also nuclear energy is phased-out, according to the existing programs. 70% of the gross energy comes from RES. In the considered system, carbon capture and storage plays only a minor role, as underground carbon storage is not considered. Massive deployment of RES is experienced, along with relevant efficiency improvements and wide electrification of the heat and transport sector. Global CO_2 emissions are about 4.5 Gt_{CO_2} in 2050, the primary energy consumption is around 430 EJ and RES account for 93% of the power demand.

Soft-linking methodology

Figure 3.13 provides an overview of all the data used in the proposed modelling framework and of their interlinkages. The main elements are five: Sources, Inputs,

Pre-processing, Simulation and Outputs. The JRC-EU-TIMES results are used as inputs for generation technologies mix, the commodity prices and the yearly energy figures. From these, the hourly demand profiles or the weather characteristics such as VRES AF are computed thanks to external data providing the shape of each curve.

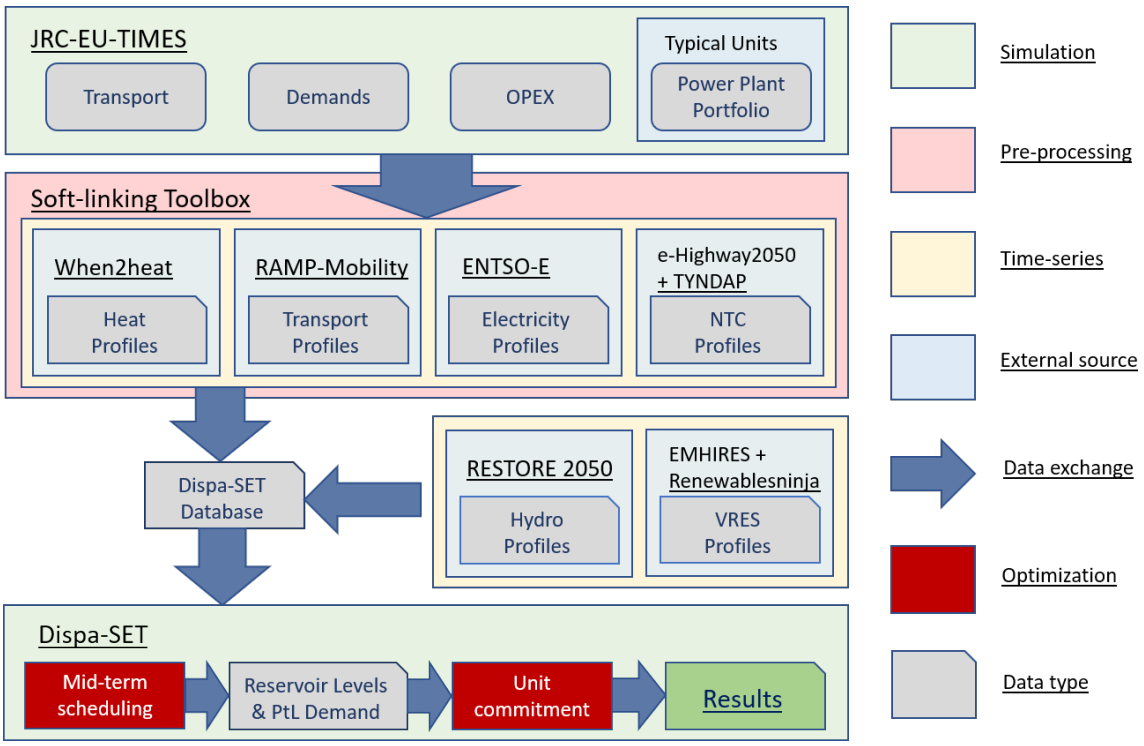

Figure 3.13. Block-diagram presenting the relations between models and various data sources used within this study [30]. JRC-EU-TIMES outputs (top) are integrated with several hourly profiles through the soft-linking toolbox (middle). Once the Dispa-SET model setup is completed, it is solved with the two stage process (bottom).

Being a uni-directional soft-linking, one key feature is related to the input files pre-processing. This is done thanks to a transition model with the aim of converting the JRC-EU-TIMES outputs into Dispa-SET readable format (included in the Dispa-SET SideTools toolbox[3]). The uni-directional soft-linking between the two models having different time scale is performed through a number of common variables.

- Total yearly electricity, heating and transport demand in each country.
- Total generation capacity installed in each country, divided by technology.
- Fuel and carbon emissions prices.

The above mentioned soft-linking toolbox is used to setup the Dispa-SET input database starting from these common variables. Additional parameters such as weather conditions (which are linked to VRES AF, ambient temperatures and hydro inflows) are considered equal to the 2016 values. Indeed, the calculation of different AF due to improvements in the technology or climate change is out of the scope of this work.

[3] DispaSET-SideTools: https://github.com/MPavicevic/DispaSET-SideTools

3.2.3 Metrics of system performance

The main parameters used to analyse the simulation results are outlined in this section. These allow to understand the performances of the energy system under different sector coupling options.

Total system costs and storage shadow price

Total system costs are the result of the optimisation objective function and include the operational costs for each considered technology. Storage shadow prices, expressed as €/MWh, are computed for each storage technology, time step, and for each zone. The storage shadow price is the dual value of the storage balance equation. It indicates the cost of an additional MWh of storage. Thus, if the storage shadow price is low, the storage capacity is enough to cover the system needs. Conversely, if the storage shadow price is equal to the shed load price, there is a lack of storage capacity.

Load shifting

The load shifting is an indicator of the storage capacity utilisation. It has the role of moving the power demand from one time step to the other. This condition is activated when the monetary benefit of reducing the load or participating in reserves is higher than the caused energy losses. Note that the total energy consumed is unvaried, even in presence of load shifting. The total load shifting is computed as the sum of the power used as input for the storage technologies.

RES curtailment

RES curtailment indicates the amount of electricity that could not be used because of network limitations. Both the total and the peak curtailed power are a relevant indicator of system adequacy. Indeed, the presence of high values of curtailment denotes a system where the available generation capacity is not fully utilised due to missing flexibility options. JRC-EU-TIMES considers more sectors than the one implemented in Dispa-SET. Therefore, what is visible as curtailed energy in the model results, might actually be used for other purposes. Nevertheless, this quantity is an important parameter to study the flexibility potential of the power sector.

Shed load and lost load

Shed load happens when there is an amount of electricity demand that the system does not manage to supply. Therefore, part of the load can be reduced in accordance to the load-shedding plans of the TSO or to the load interruption possibility agreed upon with large industries. This option is used in order to avoid system imbalance and the consequent blackouts. The cost of shed load is set to 800 €/MWh, and its maximum value is defined as the 25% of the demand.

If, after the load shedding operation, there is still a lack of generation, the energy balance equation is satisfied by the presence of the Lost load (LL) relaxing variable. A very high price is linked to this variable. Hence, it is activated only if strictly

necessary, ensuring that the problem does not result in an infeasible solution. For this reason, it should never be activated.

Transmission lines congestion

The congestion in the European electricity grid is computed as the number of hours when the amount of electricity that could imported or exported is higher than the technical maximum Net Transfer Capacity (NTC). The average and the maximum number of congestion hours is reported for all the scenarios.

Carbon emissions

Standard emission factors for each technology are used to asses the operational energy production carbon footprint. These account for both electricity and heat generation. No life-cycle analysis is performed, as it is out of the scope of this thesis.

3.2.4 Scenarios

With the aim of assessing the flexibility potential of each sector coupling option, the analysis is performed on four scenarios: NOFLEX, THFLEX, EVFLEX, ALLFLEX. Starting from one scenario with no sector coupling (NOFLEX), each one focuses on one sectors at a time (THFLEX for the thermal and EVFLEX for the transport), while the ALLFLEX studies the benefits of a smart energy system. An overview of the difference between the simulated scenarios, along with the main storage capacity assumptions, is presented in Table 3.11.

	Unit	NOFLEX	THFLEX	EVFLEX	ALLFLEX
Demand					
Electricity		✓	✓	✓	✓
Heating		✓	✓	✓	✓
Transport		✓	✓	✓	✓
Supply					
Hydrogen with storage		✓	✓	✓	✓
HPHS storage	[h]	6	6	6	6
Li-ion BATS storage	[h]	1	1	1	1
Lead acid BATS storage	[h]	4	4	4	4
SCSP TES	[h]	15	15	15	15
CHP TES	[h]	-	12	-	12
P2HT TES	[h]	-	5	-	5
V2G capacity	[kWh]	-	-	60	60
V2G share	[%]	-	-	50	50

Table 3.11. Summary of the characteristics of each simulated scenario. The main storage capacity assumptions are also reported.

An overview of the total installed generation and storage capacity in the ALLFLEX scenario for each country is presented in Figure 3.14 and 3.15, respectively. These are

subdivided by type of technology and exploited fuel. The generation capacity is the same in all scenarios, except for the Battery-powered electric vehicles (BEVS), which are present only in the ALLFLEX and EVFLEX scenarios, since are activated by the presence of V2G programs. In the same way, also the BEVS storage capacity is active only in those two scenarios. Furthermore, the Thermal energy storage (TES) provided by electric heating and CHP plants is active only in the THFLEX and ALLFLEX scenarios.

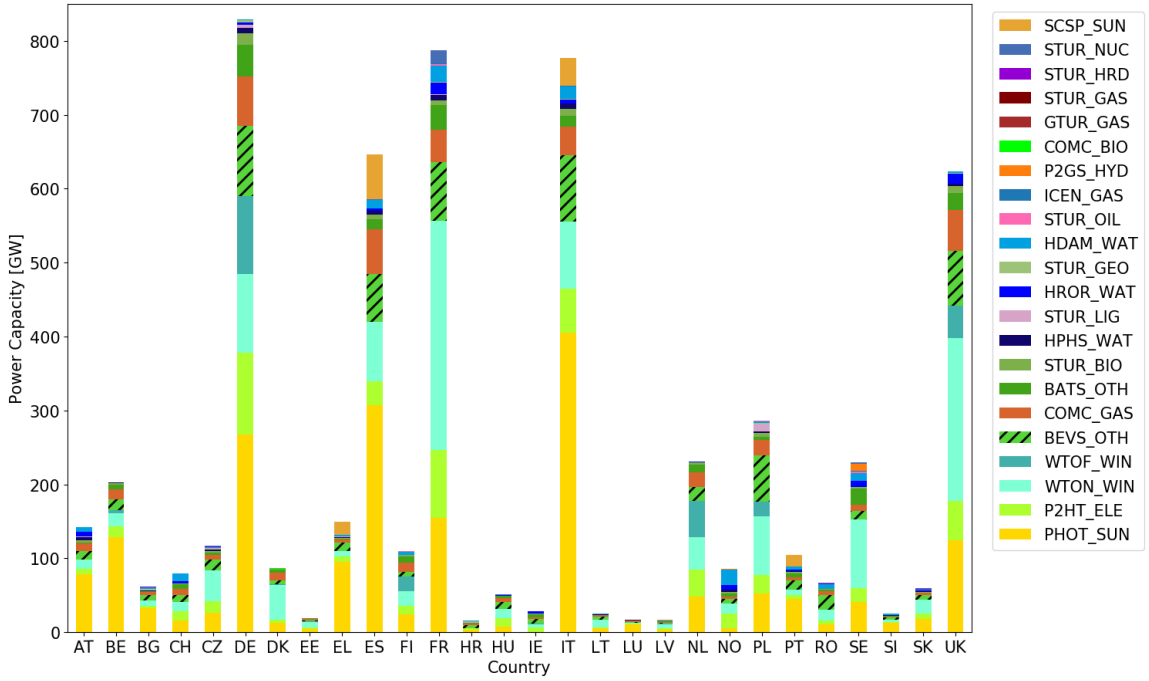

Figure 3.14. Overview of the installed power capacity in all the analysed scenarios. The only exception are the BEVS (identified by the slash hatch) which are active only in the EVFLEX and ALLFLEX scenarios.

NOFLEX

The NOFLEX case is the reference scenario of the study. It simulates an energy system as close as possible to the current state, without neither TES nor V2G options active. The main characteristics of the simulated system are the following:

- Non flexible back-pressure CHP plants, characterised by a fixed power-to-heat ratio, are used to satisfy the District heating (DH) demand. The P2HT heating demand is fixed. No TES option is installed.
- EVs are just an additional load, without any V2G feature.
- Concentrated solar power (SCSP) with overnight storage (15 h) is active, as it represents the current state of the technology in the energy system. The presence of molten salt storage coupled with a Steam turbine (STUR) increases the solar power generation flexibility, allowing power generation also when the sun is not present.

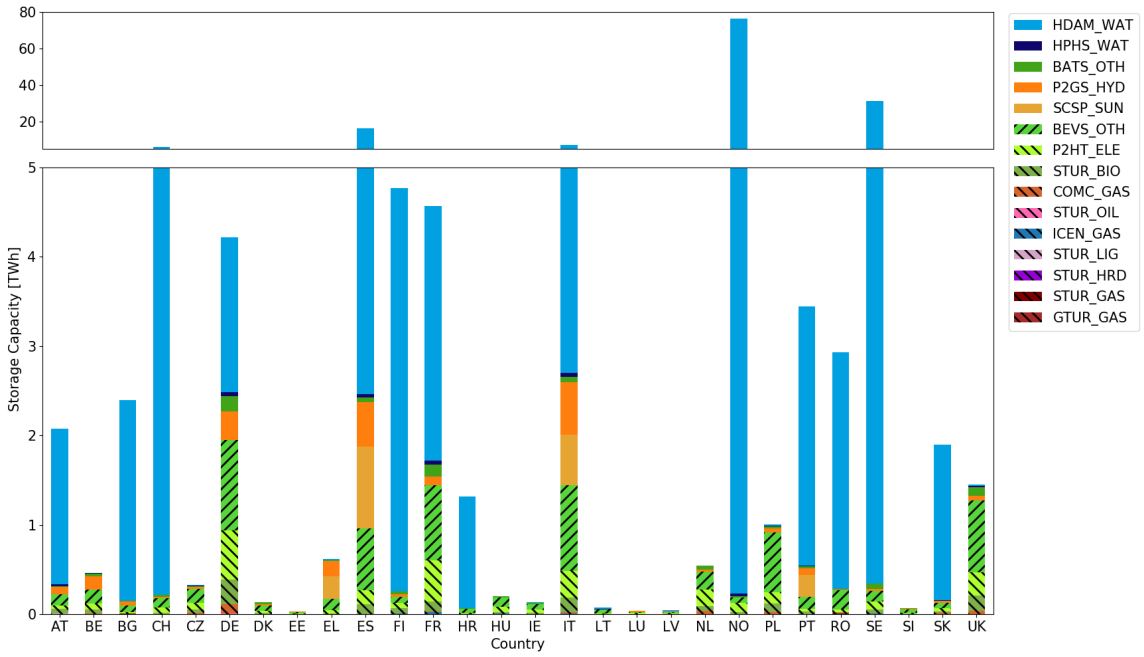

Figure 3.15. Overview of the installed storage capacity in the ALLFLEX scenario. The BEVS storage capacity is active only in the EVFLEX and ALLFLEX scenarios (identified by the slash hatch). The TES is active only in the THFLEX and ALLFLEX scenarios (identified by the backslash hatch).

- Storage options in the hydro power plants (such as Conventional hydro dam (HDAM) or Pumped hydro storage (HPHS)) are included, since are consolidated technologies. The high storage capacity is limited by the water evaporation losses, especially when using the reservoirs as seasonal storage. In addition, a certain reservoirs level should be guaranteed, in order to avoid problems on agriculture or downstream flooding.

- Hydrogen can be produced through electrolysis or through conventional systems, and stored. Then, it either satisfies a demand or it is converted back to electricity through fuel cells. The demand is divided in two parts: a rigid demand that needs to be covered at all time, and a Power to Liquid (P2L) demand. P2L needs hydrogen, but its demand can be shifted in time, as liquid fuels can be easily stored. However, the total available electrolysis capacity is limited compared to the demand. Therefore, the power sector contributes to the hydrogen production only partially, when there is an excess electricity production that would be otherwise curtailed.

- Stationary batteries (BATS) are considered in the share calculated by JRC-EU-TIMES, where both Li-ion and lead acid batteries are considered, with different storage capacities. These are then grouped in a single technology in Dispa-SET, with a weighted average capacity.

THFLEX

In the THFLEX scenario, the impact of flexibility in the heating sector is explored. The main differences in the scenario setup are the following:

- Introduction of extraction CHP plants with 12 h TES, as proposed by Jimenez-Navarro et al. [51]. This is opposed to the back-pressure units simulated in the NOFLEX scenario.
- Introduction of 5 h thermal storage for the P2HT units, which means 500 – 600 L water tank for a single-family house.

Two main impacts on the heating sector can be identified:

- The operation of CHP units is more flexible. This is obtained thanks to the activation of the extraction configuration and to the availability of TES, which is significantly more cost-effective than electrical storage [2].
- P2HT units flexibility is increased as well thanks to the introduction of TES.

EVFLEX

In the EVFLEX scenario, the impact of the transport sector flexibility through the V2G technology is analysed. The EVs' batteries are used as an additional storage option, with variable capacity. Even if the storage is characterised by a limited number of hours, the presence of a large vehicle fleet provides a significant flexibility contribution. Around 200 millions of EVs are considered in the simulated scenario. Only 50% of these participate to V2G programs, with an average battery capacity of 60 kWh. In each time step, only a fraction of the total battery capacity is available to the TSO, as the rest is reserved for travelling purposes. This percentage is defined by the AF time series, and is computed starting from the RAMP-Mobility results.

ALLFLEX

In the ALLFLEX scenario all the options introduced in the previous scenarios are available. This case simulates a smart energy system, where all sectors are coupled together.

3.2.5 Inputs and data sources

The core of the model inputs is composed by hourly time series. These are total power, heating and transport demands, hydro power reservoirs levels and VRES AF. Power plants inputs consists of power capacity, ramping rates, minimum up and down times, start-up times, efficiency and variable costs. For the sake of conciseness, only the main inputs are presented in this section. However, both the model source code[4] and the input data[5] are released with open licences, and can therefore be consulted for further information.

[4] Model source code: https://github.com/energy-modelling-toolkit/Dispa-SET/tree/PowerToGas
[5] Input data: https://github.com/MPavicevic/DispaSET-SideTools/tree/JRC_EU_TIMES

Power plant fleet

Considering the available computational power, it is impossible to simulate the whole number of power plants present in Europe. Therefore, it is necessary to apply a clustering technique, in order to reduce the dimensions of the optimisation problem. The technique applied in this simulations is called "Per-typical technology", and is described in detail by Pavičević et al. [15]. It consists of grouping similar plants into a single cluster of N units characterised by the same parameters. In this way, it is possible to group the several tens of thousands power plants available in the system, in few hundreds of units. The key technical and cost parameters for the typical units used in the simulations are presented in Table 3.12 and 3.13.

Fuel	Tech.	Power [MW]	Eff.	Min up/ down time [h]	Ramp Rate [%/min]	Part Load min	Start Up Time [h]	CO_2 Int. [t/MWh]
BIO	STUR	180	0.40	4/6	0.020	0.4	1	0.42
BIO	GTUR	64	0.33	1	0.167	0.2	0.167	0.32
BIO	COMC	420	0.51	3	0.070	0.06	1	0.22
BIO	ICEN	25	0.36	1	0.040	0.25	1	0.27
GAS	COMC	420	0.51	3	0.070	0.06	1	0.36
GAS	GTUR	64	0.33	1	0.167	0.2	0.167	0.68
GAS	STUR	120	0.37	1	0.020	0.4	0.167	0.53
GAS	ICEN	10	0.36	0	1	0.3	0	0.01
GEO	STUR	40	0.10	2	0.020	0	0	0
HRD	STUR	764	0.42	6	0.040	0.18	2	0.47
LIG	STUR	604	0.40	8	0.008	0.43	7	1.15
NUC	STUR	1008	0.34	24/48	0.050	0.25	12	0
OIL	STUR	386	0.33	5	0.020	0.4	1	0.73
OIL	GTUR	70	0.33	0	0.167	0.2	0.167	1.08
OTH	BEVS	–	0.95	0	1	0	0	0
OTH	STUR	70	0.33	0	0.167	0.2	0.167	0.80
OTH	P2HT	100	1	0	1	0	0	0
SUN	SCSP	150	0.25	0	0.020	0	1	0
WAT	HROR	-	1	0	0.076	0	0	0
WAT	HDAM	-	0.80	0	0.067	0	0	0
WAT	HPHS	-	0.80	0	0.067	0	0	0
HYD	P2GS	-	0.46	0	1	0	0	0

Table 3.12. Technical parameters for typical power generation units. The minimum up and down times have the same value, unless differently specified.

In addition to this, the time series for the wind [16] and PHOT [17] AF are obtained from the *Renewables.ninja* and EMHIRES datasets. Three main hydro power technologies are considered in Dispa-SET, namely HDAM, HPHS and HROR, along with the related inflow times series. These are obtained from the RESTORE 2050 project [18] for the year 2016. In order to compute seasonal storage, the yearly reservoir levels are pre-optimised using the Dispa-SET MTS module.

Fuel	Technology	Start Up Cost [€/MWh]	No Load Cost [€/MWh]	Ramping Cost [€/MWh]
BIO	STUR	120	12.5	1.30
BIO	GTUR	25	2.9	0.25
BIO	COMC	55	2.9	0.25
BIO	ICEN	24	0	0.63
GAS	COMC	55	2.9	0.25
GAS	GTUR	25	2.9	0.25
GAS	STUR	25	2.9	0.25
HRD	STUR	65	12.5	1.80
LIG	STUR	65	8	2.20
NUC	STUR	300	12.5	2.20
OIL	STUR	120	0	1.80

Table 3.13. Costs for typical power generation units. Only the units with non-null costs are reported.

Fuel prices

Table 3.14 presents an overview of commodity prices. Fuel and carbon emission allowances prices are aligned with the JRC-EU-TIMES output for the 2050 PRORes scenario [52]. No differentiation for the price of lignite is indicated. Therefore, the 2019 price ratio is used as basis, resulting in lignite having a price 25% lower than coal.

Commodity	Cost [€/MWh]
Nuclear	4
Lignite	15
Black coal	20
Gas	60
Fuel-Oil	78
Biomass	30
RES	0
CO_2	100 €/t_{CO_2}

Table 3.14. List of commodity prices and the assumed CO_2 price. All the prices are indicated in €/MWh, unless differently specified.

Electricity demand

The methodology adopted in this work aims at linking two models with different temporal detail. Therefore, an accurate analysis is necessary to derive the hourly power demand used in Dispa-SET from the total yearly electricity demand provided by JRC-EU-TIMES. The adopted approach is shown in Equation 3.7 and Figure 3.16,

where a precise graphical representation of the single steps performed are shown.

$$P_{n,i,2050} = \frac{P^{ENTSOE}_{n,i,2016}}{P^{TIMES}_{n,2016}} \cdot \left(P^{TIMES}_{n,2050} - P^{TIMES}_{ev,n,2050} - \frac{\Delta Q^{TIMES}_{p2h,n,2050-2016}}{COP_{p2h,2016}} \right) + P^{TIMES}_{ev,n,i,2050} \quad (3.7)$$

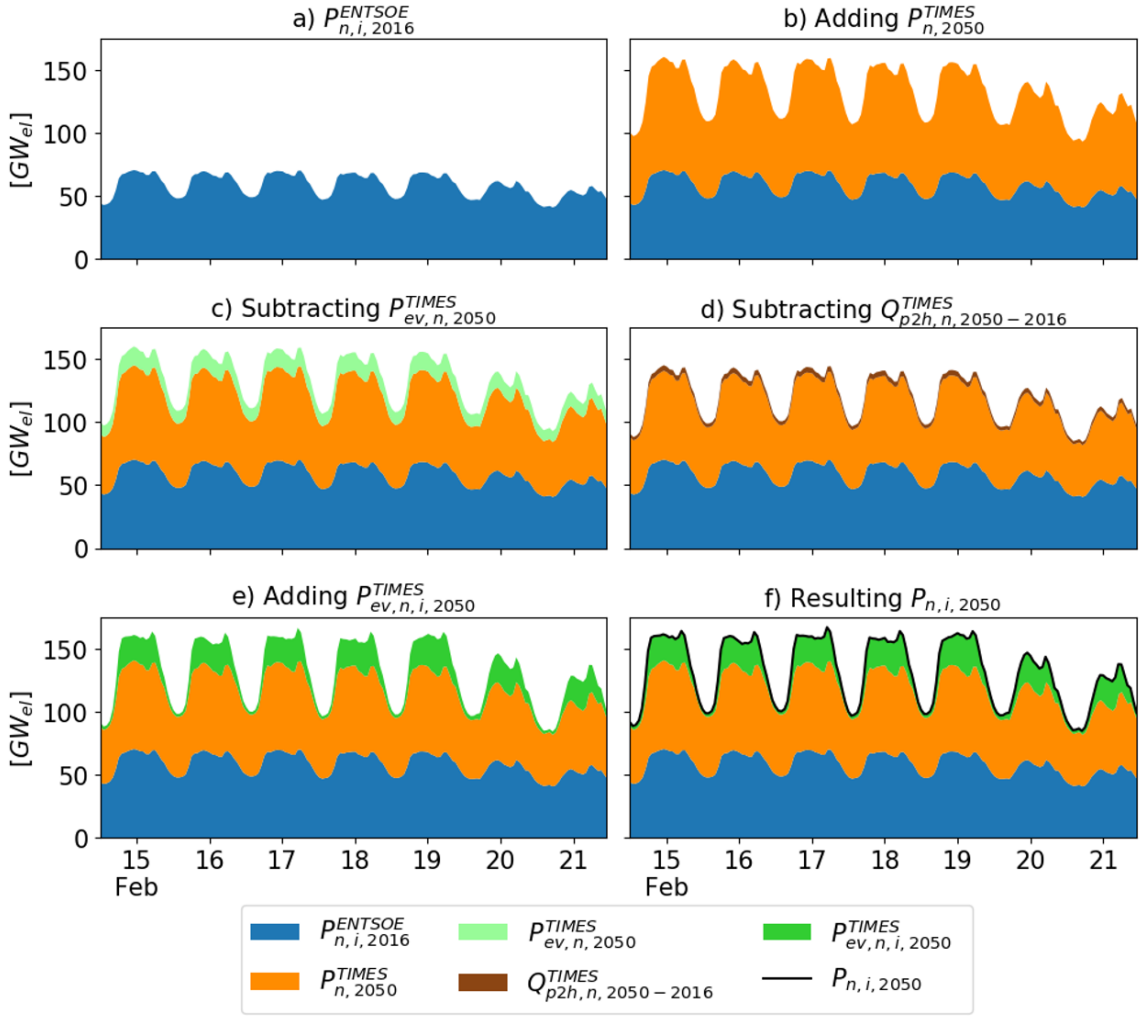

Figure 3.16. Electricity demand modelling steps for one week in February, in Germany. The resulting hourly load curve is composed of the ENTSO-E 2016 dataset, increased to match annual demand from JRC-EU-TIMES model, decreased by the amount of additional electric heating from 2016 to 2050. The shape of the EVs demand profile is computed using RAMP-Mobility and then added on top of the newly computed power demand.

It consists of scaling up the ENTSO-E 2016 data to meet the total demand in 2050. Indeed, the base curve ($P^{ENTSOE}_{n,i,2016}$) is multiplied by a country-specific coefficient accounting for the predicted increase of electricity demand by 2050. This coefficient is computed as the ratio between the power demand in 2050 according to JRC-EU-TIMES ($P^{TIMES}_{n,2050}$) divided by the total demand in 2016 ($P^{TIMES}_{n,2016}$). However, the transport and heating sector are not expected to have the same load profile as the one of the 2016 electricity demand. Therefore, both the amount of electricity dedicated

to EVs ($P^{TIMES}_{ev,n,2050}$) and the additional power demand caused by the electrification of the heating sector from 2016 to 2050 ($\Delta Q^{TIMES}_{p2h,n,2050-2016}$) are not considered in the calculation of the coefficient. Indeed, the transport demand profile is computed with the RAMP-Mobility model, scaled to the total 2050 levels considered in the PRORes scenario, and then added on top of the newly computed power curve. Instead, the power demand due to electric heating is endogenously added in the model, based on the heating demand assigned to the P2HT units. The resulting peak demand in the whole region is 1 361 GW.

Transport

The representation of the transport sector in an energy system model is the main focus of this thesis, therefore a whole section is dedicated to it. An original model was developed to simulate the mobility profile for each country, and the corresponding charging demand to the grid. Please refer to Section 3.1 for a complete description of the methodology used, and to Section 4.2.1 for the presentation of the load profiles used in the Dispa-SET simulations.

In addition to this, the V2G configuration is here implemented based on the specificity of Dispa-SET model, where it is modelled as an additional storage technology, with a variable nominal capacity defined by an AF. This is a time series indicating the percentage of the total battery fleet available for flexibility purposes each hour. The starting point is the methodology shown in Section 2.2, which is adapted to the new input data. First, it is necessary to consider two main assumptions:

- Limited battery availability: in the calculation of the available storage capacity, it should be considered that a minimum SOC has to be guaranteed to the vehicle user. This is defined by required energy for the upcoming trip, plus the energy that was not recovered if a parking without any charge happened. Indeed, the flexibility provided by the V2G technology should not interfere with the users' travelling habits.
- *Perfect foresight* charging strategy: the users have a complete knowledge of the future trips and their energy requirements. Furthermore, they charge the car right before the time of departure of the following planned travel.

Due to the optimistic assumption of perfect foresight, a security margin ξ is defined, to consider deviations from the ideal behaviour. In this study, the security margin is set to 50%, and defines the maximum battery availability. This brings to the definition of the total energy available to the system for each car i, $E_{sys,i}$, as shown in Equation 3.8.

$$E_{sys,i} = \xi \cdot (C_{battery,i} - E_{min,i}) \tag{3.8}$$

Where $C_{battery,i}$ is the total battery capacity of each EV and $E_{min,i}$ is the minimum energy in the battery to be guaranteed to the user. Aggregating each car's available energy, the total storage capacity for V2G purposes is computed. Then, the AF is calculated dividing the storage capacity available at each hour by the total installed EVs battery capacity. An example of the resulting AF is reported in Figure 3.17 for one week in Germany. It is visible that the average availability is around 40%, with

rather small fluctuations. Considering that the security margin ξ is set to 0.5, the result shows that the EVs are parked and plugged around 80% of the time. In the simulated region the total V2G power capacity is 650 GW, while the total storage capacity is around 7000 GWh. This is calculated starting from the total number of EVs available in the PRORes scenario. An average battery capacity of 60 kWh per car is considered, with only 50% of the fleet participating to the V2G program.

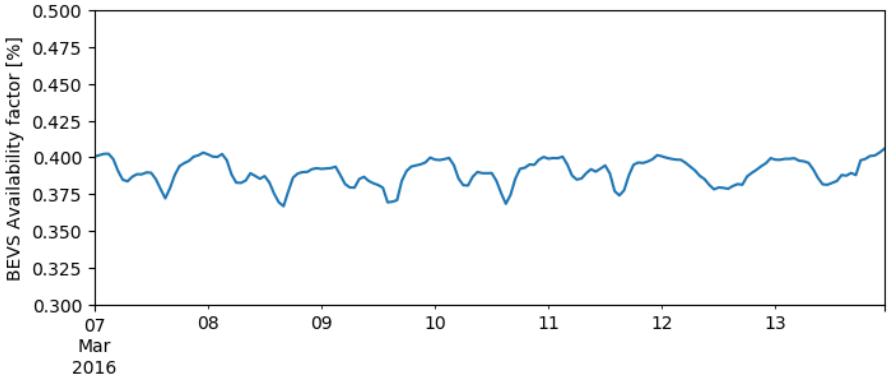

Figure 3.17. Example of AF result for one week in Germany. The maximum AF is limited by the security margin value of 0.5. The total installed BEVS storage capacity is slightly higher than 1000 GWh.

Heating

The mathematical formulation of the CHP and TES technologies in Dispa-SET is described in detail in Jiménez Navarro et al. [53]. In addition, in this work also the Heat pumps (HPs) and Electric heaters (EHs) systems are included, converting electricity into domestic hot water and space heating. These are represented in the model as a single technology, called P2HT, and considered subject to Direct load control (DLC) [19]. This means that these units can work in a flexible way, operating as a virtual power plant. The key assumption is that any heat generation unit is connected to a TES. Thus, the heat generated by both CHP and P2HT is first stored and then used to satisfy the heating demand.

HPs and EHs are aggregated in a single units type. Hence, a nominal efficiency (COP_{nom}) is derived from JRC-EU-TIMES [50]. This is computed based on the weighted average of the single technologies' nominal efficiencies, and on their relative shares in each country. Furthermore, the COP varies depending on the ambient temperature, T_{amb}. This relation is modelled as shown in Equation 3.9. A parametrisation around the nominal ambient temperature, T_{nom}, is performed, which is the temperature for which COP_{nom} is calculated, namely 5 °C. The two coefficients are different for each country, and are computed to obtain a value of COP_{nom} equal to 1 with T_{amb} at −10 °C, while at the same time having a positive concavity [54]. This temperature is the threshold under which HPs do not operate, being substituted by auxiliary heaters with efficiency equal to 1.

$$COP_{p2h,i}\left(T_{amb,i}\right) = COP_{nom} + C_1 \cdot \left(T_{amb} - T_{nom}\right) + C_2 \cdot \left(T_{amb} - T_{nom}\right)^2 \qquad (3.9)$$

In order to successfully model the heating sector, it is also necessary to obtain reliable data regarding the heat demand profile in each country, with an hourly detail. Among the several projects that were considered as a possible source of inputs, it was decided to use the "When2Heat" dataset. These heat demand profiles are based on German data regarding the gas standard load profiles, which are then processed in order to extend them to 16 European countries. The data regarding temperature and wind speed are taken from the global ERA-Interim reanalysis, and are used to calculate the heat demand in other countries. Then, the profile is weighted according to the population, based on Eurostat geodata, and scaled up to the total energy consumption provided by the EU Building Database. A final correction to consider the losses in the conversion from final energy to heat is applied [20]. The authors of the dataset perform a validation analysis for the United Kingdom (UK), that shows good results, even if the building properties are significantly different from the ones in Germany. As there is no other source of measured data for the heat demand profiles, by induction, it is advised to use the data only for the countries which have building properties in the range between Germany and the UK. However, due to the challenges in finding better data source for the heat profiles, for this work, the dataset is extended also to the countries that were not originally included. A qualitative validation with modelled heat demand profiles for Italy was attempted, providing good consistency, and supporting the decision of extending the geographical scope of the data. The structure of the "When2Heat" project provides already almost all the necessary data to extend the dataset to the whole geographical scope of this work. The only exception lies in the database of building properties from Eurostat, that does not comprise Switzerland and Norway. For this reason, it was assumed that their building properties are equal to, respectively, Austria and Sweden, being their closest neighbour. This assumption is supported by the fact that in the Eurostat database, countries with similar climates show comparable building properties.

The heating adimensional profiles are then scaled up to the total residential and commercial heating demand. This is supplied by P2HT or CHP technologies, their relative share in each country is derived from the PRORes scenario results. An example of the total heat demand profile for one week in Germany is shown in Figure 3.18. Low-temperature industrial heat supplied by CHP units is considered in the

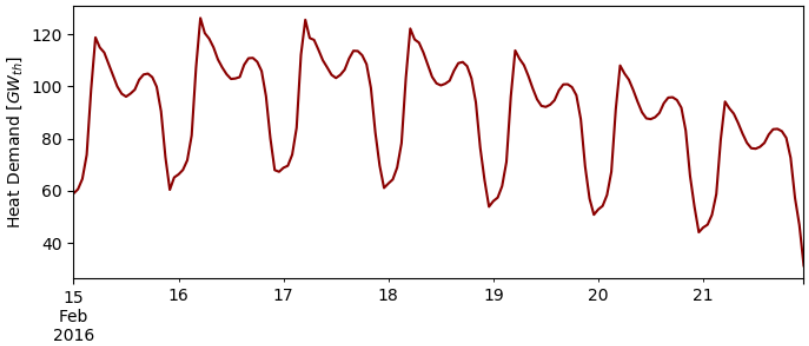

Figure 3.18. Example of heating demand in Germany for one week in February.

heating demand. Instead, process heat covered by electricity and cooling are already considered in the power demand. P2HT covers 1780 TWh of annual useful space

heating demand, the peak value is 595 GW. CHP units account for 277 TWh of total annual heating demand, with a 91 GW peak. In addition to CHP and P2HT units, heat can also be generated by backup gas heaters. The cost linked to this technology is 112 €/MWh. This value is computed starting from a gas price of 60 €/MWh and a CO_2 price of 100 €/t, as proposed in the Heat Roadmap Europe project [55]. Table 3.15 presents the parameters for the CHP plants in the THFLEX and ALLFLEX scenarios. In the NOFLEX and EVFLEX cases, only back-pressure CHP units are considered, with a power loss factor equal to 0. All other cost and technical parameters are the same already presented in Table 3.12 and 3.13.

Fuel	Technology	CHP Type	Power to Heat ratio	Power loss factor
STUR	BIO	Extraction	0.45	0.24
GTUR	BIO	back-pressure	0.55	0
COMC	BIO	Extraction	0.95	0.21
ICEN	BIO	back-pressure	0.75	0
COMC	GAS	Extraction	0.95	0.21
GTUR	GAS	back-pressure	0.55	0
STUR	GAS	Extraction	0.47	0.23
ICEN	GAS	back-pressure	0.75	0
STUR	GEO	Extraction	0.22	0.17
STUR	HRD	Extraction	0.45	0.26
STUR	LIG	Extraction	0.45	0.24
STUR	OIL	Extraction	0.45	0.11
GTUR	OIL	back-pressure	0.55	0
STUR	OTH	back-pressure	0.55	0

Table 3.15. Technical parameters for CHP units.

Net Transfer Capacities

In the Dispa-SET model, the commercial NTCs are the maximum amount of energy that each country can exchange with the neighbouring countries. Since the electricity network is expected to develop significantly until 2050 to withstand a high penetration or RES, it is important to properly account for these variations. The most reliable source of analysis for the expansion of the European electricity network, is the Ten-Year Network Development Plan (TYNDP), published by the ENTSO-E every two years. This plan indicates how the electric grid will change in the following 10 or 20 years. After having evaluated projects for grid reinforcement, and having conducted both regional and European analysis, some scenarios are developed in order to explore different options for the future power system. In the TYNDP 2014, 4 visions are developed. Therefore, in this work the data related the vision closer to the scenarios indicated by JRC-EU-TIMES are used. This corresponds to either the Vision 3, called "Green Transition" or the Vision 4, called "Green Revolution". It is not relevant to determine which of the two is closer, as the reference values for the grid development in 2030 are the same [56]. Unfortunately, the TYNDP provides grid reinforcement

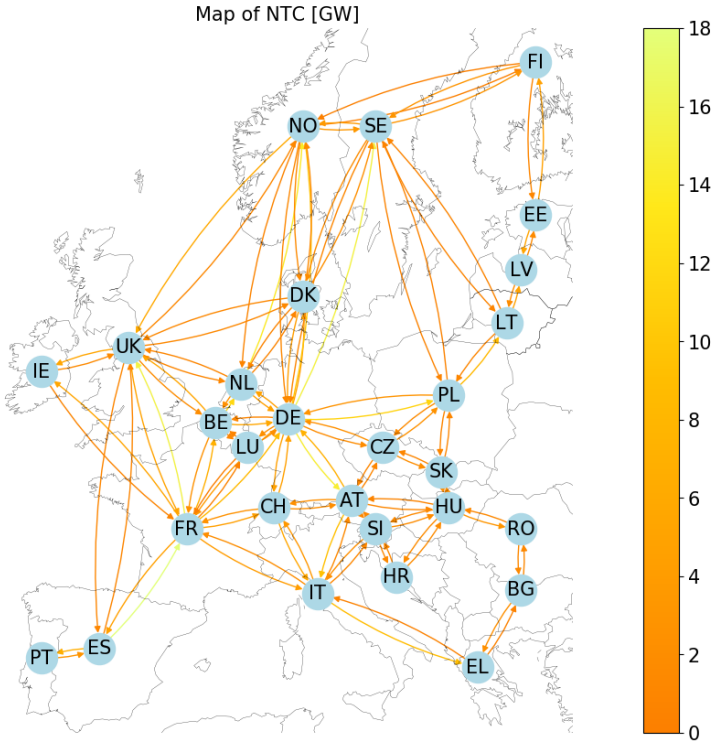

Figure 3.19. Map presenting the maximum electricity transfer capacity between the simulated countries.

plans only until 2030. Thus, it is necessary to rely on another source to obtain the NTCs data for the year 2050. The e-Highway2050 project, supported by the EU Seventh Framework Programme, starts from the TYNDP 2014 basis. Considering the reference grid in 2030 as the starting point, evaluates the additional reinforcements necessary to operate the grid in 2050 under different generation scenarios [57]. There are 5 different scenarios, each dealing with different assumptions regarding generation capacity, energy demand, and power exchanges with neighbouring countries. The three scenarios where nuclear energy has a major role are excluded, as the PRORes scenario does not consider it predominant. These are the "Fossil and nuclear", "Big & market" and "Large-scale RES" scenarios. Hence, only the "100% RES" and "Small & local" scenarios are left. In particular, the former relies only on RES for power production, and considers high electrification rates and an important role for storage technologies. Instead, the latter gives priority to decentralised energy generation, considering lower grid reinforcement, and discouraging exchanges between countries. In addition, the "Small & local" scenario assumes low electrification rates both in the transport and in the heating sector, which is not in line with the sector-coupling approach adopted by this work. For all these reasons, the "100% RES" scenario was the one selected as data source for the NTCs values in 2050 necessary for Dispa-SET. The final map of the NTCs between each country is visible in Figure 3.19. It is visible that most of the lines are below the 10 GW level. Only few exceptions reach almost the 20 GW, for example the line from Spain to France, due to the high RES capacity available in the Iberian country, or several lines leaving Germany.

Chapter 4

Results and discussion

In this section the thesis results are presented and discussed. First, the RAMP-Mobility model is validated, comparing the results of both the mobility and charging demand algorithm against measured data. Then, the general RAMP-Mobility results are reported. These consist of the European database of EV load profiles, along with a sensitivity analysis on both the mobility stochastic parameters and on the customizable features available in the charging process. Finally, the results of the Dispa-SET simulations are analysed, starting from the overall performances of the system, and then focusing on the role of the transport sector flexibility.

4.1 RAMP-Mobility validation

Due to the nature of the EV technology, still in an early adoption phase, the validation of a model generating electric mobility demand profiles is a challenging task, as data are not easily available. Furthermore, even when data are measured, they often refer to databases collected during trial projects, which are usually of limited scope. Thus, can scarcely represent the mobility dynamics of a whole country. Nevertheless, two different kinds validation are performed, first the results of the mobility profile are tested, comparing them with the vehicle counting statistics collected by the BASt. This can be helpful in understanding if the mobility inputs provided to the model generate accurate results. Then, to validate the charging process, the ElaadNL database, is used. This is composed by historical values collected in the Netherlands from the public charging points managed by EVnetNL. This was chosen as data source mainly for two reasons. First, it is the result of real world data and not of a trial project, and second, because it is one of the largest databases of private electric cars' charging demand available in Europe.

4.1.1 BASt mobility profiles

Since the model is composed by two main sections, it is important to perform a first validation on the simulation of the mobility profiles, as these are the basis for the charging profiles calculation. The mobility input data refer to conventional passenger cars, hence, it is possible to validate them with data related to conventional mobility.

Source data

The mobility profile is retrieved from the data collected each year by the German institute BASt, which measures the number of vehicles passing through automatic highways and motorways counting points. The data are then averaged to weekly profiles, considering that small variations in traffic habits are registered in different seasons. The system is able to recognise nine different types of transport means, from freight transport to passenger cars [29]. The statistics computed from 2017 data are considered in this section, filtered to account only for passenger cars (identifiable by a specific label), in order to mitigate the relevant share of freight transport, out of the scope of the present analysis.

Validation results

No specificity is identified regarding the population composition or time related behaviours in the BASt statistics. Thus, the simulated conditions are the model default ones. The BASt data record hundreds of millions of cars passing through the automatic counting points. Due to computational limits, it is impossible to simulate millions of EVs in RAMP-Mobility. For the sake of this comparison 10000 cars are simulated, as this is a number of users that abundantly covers the whole population dynamics. In order to allow an easier comparison among the different number of users considered, both curves are normalised with respect to the peak value.

Figure 4.1 shows the comparison between the simulated values and the reference data for a representative week. It can be noticed that the peak and off-peak time windows are represented with a rather high degree of accuracy, proving that the HETUS survey provides reliable information regarding the time habits of the population. Nevertheless, also some inconsistencies are visible, especially regarding the difference between the two peaks and the in-between central window. This is an expected behaviour, linked to the inherent difference between highway traffic measurements, and urban mobility, that is the main focus of the model. In particular, it is reasonable that a higher share of continuous travels are registered on the highway, both because of longer travels, and because the statistics include people that frequently travel for working reason, that therefore use much more the highway than the urban roads.

4.1.2 ElaadNL charging profiles

After having verified that the mobility profile provides a satisfying representation of the real world data, it is possible to move to the second part of the validation, looking at the charging demand. The first analysis performed on the BASt data is important, because it allows to focus on the charging process algorithm during the comparison with ElaadNL data. This means that any result can be directly ascribable to the charging process, removing all doubt that it is caused by inaccurate mobility profile.

Source data

The validation dataset is composed by charging transactions registered in the Netherlands from January 2012 to May 2016. The analysed year is 2015, as the most recent and complete one. The database covers around 1750 charging points, that represent

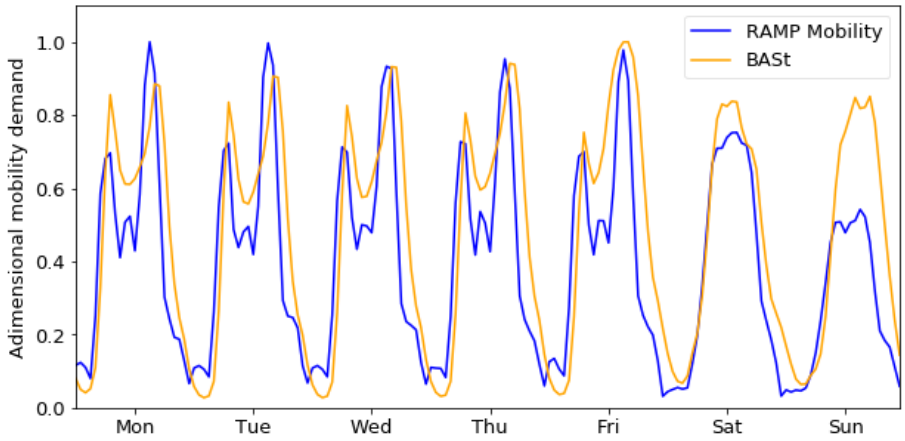

Figure 4.1. Comparison between the simulated and measured usage profile for a typical week. Peak and off-peak time windows are represented with a high degree of accuracy.

approximately 16% of the whole public charging infrastructure available in 2015. The data are recorded based on a ID code which refers to a card used by the customer to start and end the charging transaction, these will be referred to as "ID card". The processing of the database follows the methodology described in the work conducted by Beltramo et al. [13], where PHEV are divided from EV as the transactions having maximum charging power lower than 4 kW and maximum energy charged lower than 12 kWh. Furthermore, the data are filtered to consider only the ID cards having more than 10 transactions recorded, with the goal of limiting the analysis to the usual customers, better representing the overall charging behaviours. This brings to consider 2215 charging ID cards, of which 60% are small vehicles, and 40% big ones. It is important to highlight two points about the data analysed:

- The ID cards are not necessarily linked to a single user, bringing to two possible cases. First, one person might use more than one charging cards, second, more people could use the same card. The former case corresponds to a person losing the card or shifting to another charging service. Hence, this does not have a relevant effect on the profile derived. The latter case could be due to different cards corresponding to different charging tariffs. Anyway this is not expected to impact significantly the profile, as different tariffs would likely be used for different CP providers, while this database only analyses data from one provider [58].

- The users might charge the EV also in a station not belonging to the EVnetNL network, or at a private charging point. Therefore, the profile derived from this database is not representative of the whole charging demand associated to each user [13].

Overall, it is expected that these two effect have a limited impact on the final results. In addition to this, it is important to point out that, from to a survey conducted on around 300 drivers who requested a CP from the EVnetNL network, it is found out that the population of the Dutch EV drivers differs quite significantly

from the national average [59]. Indeed almost all the users interviewed are working people, more than 90% of the users are males, and the 77% has a higher education background, with a relatively high income. Also, around 60% of EV users have a private parking space, against a national average of 25%. This points out clearly that the sample of the ElaadNL dataset is hardly representative of the whole country. All the aspects just outlined should be taken into account during the model validation.

Modelling in RAMP

The validation of the model against the real world data relies on the possibility to simulate conditions that are as close as possible to the experimental ones. Therefore, both the input data and the optional parameters should be carefully revised, to get closer to the conditions of ElaadNL database. As previously said, from the maximum energy charged by each car, it is possible to obtain an approximation of the car fleet composition, composed by 60% of small cars and 40% of large ones, therefore this is changed in the model accordingly. Also, from the data recording the charging power of each transaction, it is possible to derive the relative distribution of CPs' nominal power P_{CP}^{nom}, and represent those accurately in the model. The distribution shows that the CPs have a maximum nominal power of 12 kW, that the vast majority works at 3.7 kW (around 80%), and approximately 15% charges in the 8-12 kW power range. The rest is evenly distributed along the other values.

All the other inputs of the model correspond to the default version. Some of these, such as the travel specifications, are considered reliable also for this validation purpose; others, for example the population composition and the functioning windows, are left unchanged only due to the lack of specific information about the ElaadNL dataset. The last parameter to be considered is the CP_{prob}, for which the piecewise option is selected, as, as previously explained in Section 3.1.3, it is likely that charging point availability is higher in residential areas, even if the database consists only of public charging points. This hypothesis is supported also by the research performed by Helmus et al. [58], where this same database is analysed from the CPs' perspective. In the study, two kinds of infrastructures are identified, the first, called *demand-driven*, is composed by the installations carried out due to an explicit request by an EV driver, asking for a CP near to home. The second type is called *strategic*, and represent the applications carried out upon governmental roll-out plans, to obtain a widespread presence of CPs also in locations where might be necessary, even if are not in residential neighbourhoods This study shows that the demand-driven CPs weekly energy transfer is around 50% higher than the strategic ones, in spite of being less present on the territory (they are only around 40% of the total). Thus, they prove to be used more intensively. Furthermore, the analysis shows that demand-driven CPs are used as alternative to private charging, for situations such as overnight charging, while strategic CPs are more commonly adopted for daily charging. This is important because supports the hypothesis that the profile generated by RAMP-Mobility, which virtually account for all the CPs in the country, both private and public, can be reliable also in modelling the ElaadNL database. Indeed, this exhibits both the characteristics of private and of public charging, despite being composed only by public CPs.

Sensitivity analysis

The choice of adopting the piecewise CP_{prob} function introduces a high degree of uncertainty, since it is impossible to have data neither regarding the time frames when the probability is higher, nor about the probability values. Hence, to cope with this, a sensitivity analysis is performed on the piecewise curve, to evaluate the influence that the variation of this parameter has on the final results. The shape of the curve is defined by 4 parameters, two defining the probability characteristics of the function, namely p_{max} and p_{min}, and two identifying the time of the day when the probability first drops from p_{max} to p_{min}, and then rises again to p_{max}. The two time-related parameters are called t_1 and t_2. As shown in Table 4.1, 8 cases are identified, starting from the default assumptions of Case 1, and varying one parameter at the time. Note that the Case 9, with t_2 anticipated to 18:00 is not reported, as it proved to be too far from the conditions measured in the ElaadNL database.

	Case 1	Case 2	Case 3	Case 4	Case 5	Case 6	Case 7	Case 8
p_{max}	0.9	1	0.8	0.9	0.9	0.9	0.9	0.9
p_{min}	0.4	0.4	0.4	0.3	0.5	0.4	0.4	0.4
t_1	06:00	06:00	06:00	06:00	06:00	05:00	07:00	06:00
t_2	19:00	19:00	19:00	19:00	19:00	19:00	19:00	20:00

Table 4.1. Overview of the eight cases analysed in the sensitivity analysis on the piecewise probability function. These are the result of the variation of the 4 parameters defining the shape of the curve.

In addition, it is expected that the curve simulated by RAMP-Mobility, will have a total value higher than the measured data. This is due to the fact that, even if the number of users simulated is equivalent, the model accounts for all the charging transactions performed by the users. Instead, the ElaadNL database only records the charging events happening in certain CPs, in particular in 16% of the total public charging infrastructure available in the Netherlands. This brings to the definition of an additional parameter, specific for this validation, called *scale factor*, defined as the ratio between the ElaadNL curve and the curve simulated by the model. This will not be equivalent to the share of CPs considered in the database. Indeed, among the users recorded, some performed hundreds of transactions, suggesting that they use predominantly the ElaadNL charging network, while other account only for around 10 transactions, indicating an occasional use of the infrastructure analysed. As the scale factor will have a different value each minute, it is expected not to be constant along the year. Therefore, a sensitivity analysis will be performed also on this parameter, around the median value. Figure 4.2 shows the distribution of the scale factor for each of the 8 cases simulated. It is clear that there is a high concentration around 0.4, as proven by the blue band, representing the median value for the different cases. The median is chosen as measure of central tendency as more indicated for skewed distributions than the mean. Hence, a scale factor equal to 0.4 is taken as reference. Around it, a sensitivity analysis is performed, considering also scale factors equal to 0.35 and 0.45.

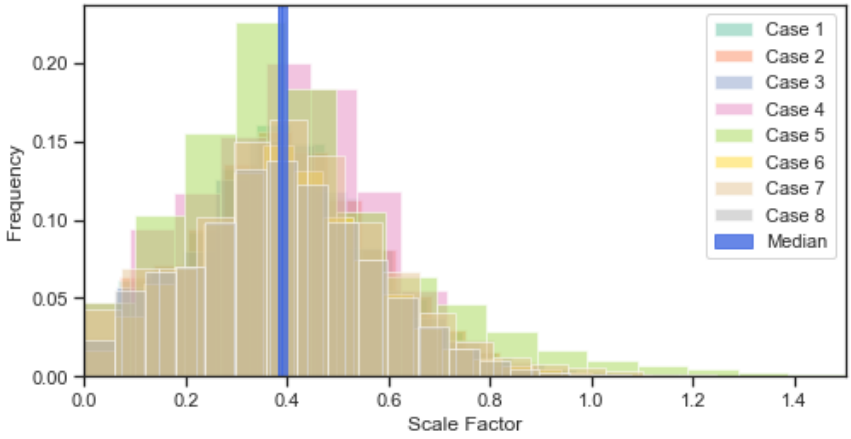

Figure 4.2. Histogram of the scale factor for the different cases linked to the piecewise probability function sensitivity analysis. The blue band represents the median values.

Validation results

Having set the two layers of uncertainty regarding the model, it is possible to present the results of the validation, comparing the ElaadNL data with the uncertainty cloud generated by the sensitivity analysis on the RAMP-Mobility's simulations.

The first comparison is performed on the load duration curve, as shown in Figure 4.3, where the three different scale factors are first plotted individually, and then aggregated in the final uncertainty cloud. A satisfying match can be noticed, except for the lower loads, that are overestimated by the model. This is due to a sharp decrease in the car usage experienced in July and August. The reason lies in the presence of summer vacations, which are not simulated in RAMP-Mobility, as a conservative choice made in the developing phase. Both the period of vacation and the extent of demand reduction are characterised by a very high uncertainty. Therefore, it was decided to model only the national holidays, that have a more predictable behaviour. Furthermore, the lack of detailed information about the time-related habits of the sample considered in the database increases the discrepancies between the model and the data. Considering more in detail the effect of the different scale factors on the final result, it is clear that the 0.35 value follows only loosely the data, and is not even as accurate as expected at low powers. The scale factor equal to 0.45, instead, seems to better represent the data, both in high and medium charging powers. As expected from the analysis conducted before, the 0.4 scale factor is a good trade-off between high and low powers, and can be further analysed to understand the impact of the 8 different cases.

Looking closely at one of the load duration curves the specificities of the 8 cases can be identified. Here the case with 0.4 as scale factor is depicted in Figure 4.4. However, the patterns of the 8 different cases are the same for any scale factor. The first trend that can be observed is that the peak values of the Case 8 curve are clearly lower than the average. This can be explained by the fact that this is the only case with a lower CP_{prob} during the afternoon's mobility peak window, which ends around 19:30, bringing to a lower number of simultaneous connections to the grid, and shaving

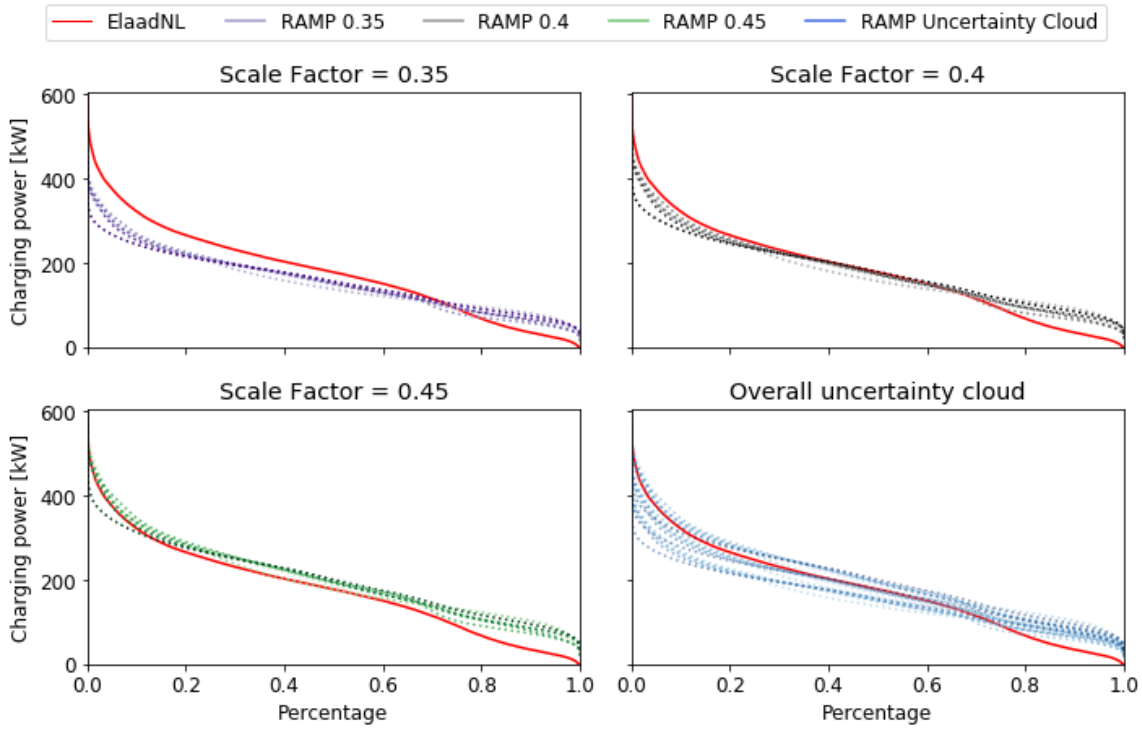

Figure 4.3. Comparison of load duration curves for different values of scale factor. To each scale factor value correspond eight cases linked to the sensitivity analysis performed on the piecewise probability function.

the peak. Case 5 shows another clear pattern deviation, having reduced low power frequency. This case has the highest CP_{prob} set during the central window, which results in a more frequent coincidence of car connections, bringing to a lower frequency of low power values. The third interesting case is number 4, that has both a higher share of low power values, and a lower share in the medium powers region. These two aspects are linked, because as a lower probability of plug-in is set during the 06:00-19:00 window, coincident connections to the grid are less likely, and this flattens the profile, causing a higher share of low power demand windows, and consequently a decrease of medium power ones. The remaining 5 cases do not exhibit particular deviations from the average behaviour. Therefore, can be regarded approximately equivalent. This is an important finding, proving that not all the parameters of the piecewise function have the same impact on the final results.

It is important also to evaluate the evolution of the comparison in different months, to understand if there are major discrepancies linked to either the different climate conditions or to the changes in the daylight hours, causing gaps in the time behaviours. Figure 4.5 shows for each month, the detailed comparison in the central week. The whole RAMP-Mobility uncertainty cloud is reported, as the contribution of the single sensitivity cases has already been exposed above. First, it is possible to investigate the impact of different climate conditions on the EVs consumption. In this regard, the first visible trend is an increase in the peak values of the ElaadNL database in the winter period. This is in line with the temperature factor applied to the consumption of the vehicle in RAMP-Mobility, as explained in Section 3.1.2. Looking

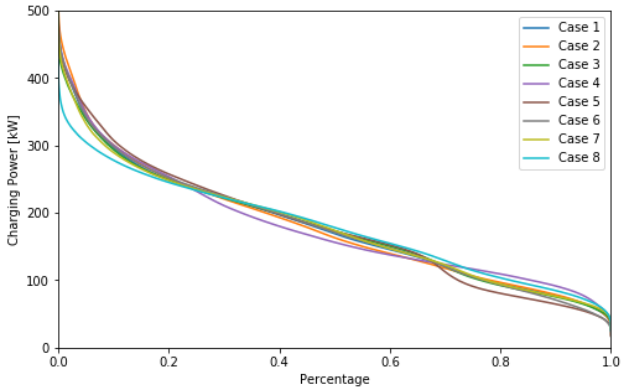

Figure 4.4. Load duration curve for a scale factor = 0.4. The eight cases linked to the piecewise probability function sensitivity analysis can be seen in detail.

at May, an interesting aspect can be noticed. Indeed, May 14 is a national holiday in the Netherlands (Ascension day), and its peculiar trend is well captured by RAMP-Mobility. The day after, which is a Friday, is treated as a normal day by the model. Nevertheless, its vacation-like behaviour is clear when looking at the ElaadNL data. These two days show both the strength of the model in reproducing correctly the holidays, and at the same time its limit in not capturing the non-official vacation days. Then, looking at July and August, it is possible to notice a lower demand, with the peaks being almost half of the rest of the year. As already explained, the variation due to summer vacations is not simulated in the model. The introduction of this feature could potentially bring more problems than benefits, considering the large amount of assumptions needed to model both the summer time period and the related behavioural peculiarities for a large amount of countries. Moving to the time behaviours, some minor deviations from the simulated results is noticed, however, the overall precision in representing the peak windows can be considered satisfactory.

It is important also to evaluate some quantitative parameter, that can help to capture additional insights that are not clearly visible from a visual comparison. The rate of accuracy of the model is computed with the Normalised Root-Mean-Squared Error (NRMSE), defined as shown in Equation 4.1.

$$NRMSE = \frac{\sqrt{\frac{\sum_{x}^{N_t}(P_{model}(x) - P_{measured}(x))^2}{N_t}}}{P_{measured,max} - P_{measured,min}} \quad [\%] \tag{4.1}$$

Where $P_{model}(x)$ and $P_{measured}(x)$ are, respectively, the values of the power calculated by the model and the measure from the ElaadNL database at each minute, N_t is the total number of observations. The denominator is the difference between $P_{measured,max}$ and $P_{measured,min}$, being the maximum and minimum values measured in the ElaadNL database. This is preferred over the alternative of having the average power at the denominator, since the load profile is a periodical function, and therefore the average value would not capture this trend. Another important parameter to compare energy time series is the Load Factor (LF), that allows to evaluate if there is wide variability in the charging demand [21]. It is computed as ratio between average demand $P_{average}$,

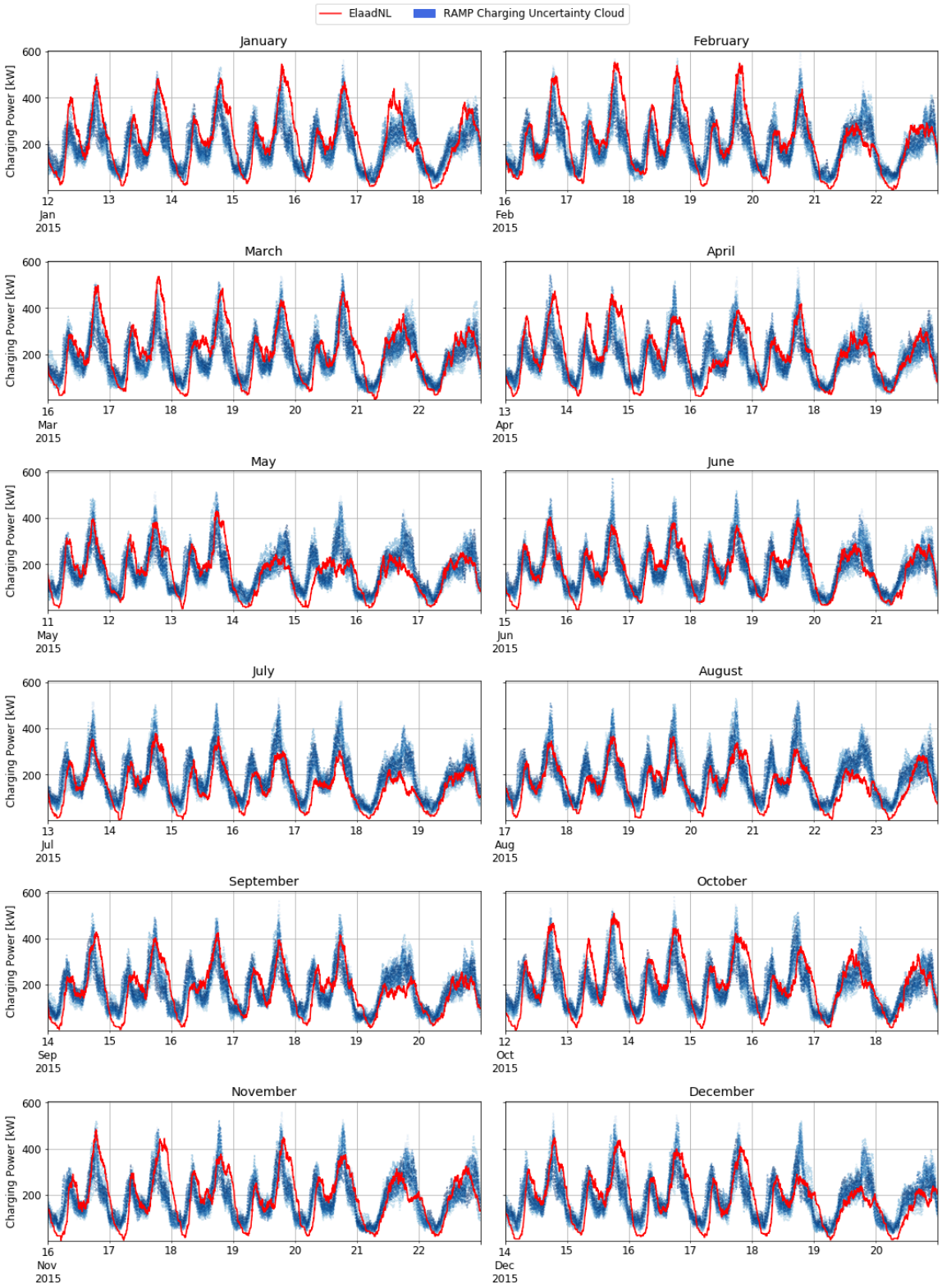

Figure 4.5. Charging profile comparison between the ElaadNL data and the model results for the central week of each month.

and peak demand P_{peak}, as shown in Equation 4.2.

$$LF = \frac{P_{average}}{P_{peak}} \tag{4.2}$$

In Table 4.2 the quantitative parameters calculated are presented for all the 8 cases, together with the median. First, the LF is calculated for both curves, and the error is computed. Being the LF an intensive parameter describing the shape of the curve, it does not change when applying different scale factors. Analysing the error, it can be seen that Case 3, 7 and 8 are quite far from the ElaadNL data, while the other 5 values are quite similar, around 10%.

	LF [−]	LF Error [%]	NRMSE LDC [%]
ElaadNL	0.302	-	-
Case 1	0.345	12.54	3.86
Case 2	0.334	9.54	3.79
Case 3	0.365	17.39	3.98
Case 4	0.336	10.28	5.00
Case 5	0.336	10.26	2.70
Case 6	0.336	10.18	3.39
Case 7	0.357	15.39	4.17
Case 8	0.421	28.32	5.98
Median	0.341	11.41	3.92

Table 4.2. Summary of the load factor, the load factor error with respect to the data and the NRMSE calculated on the load duration curve. The NRMSE values refer to a 0.4 scale factor, while the load factor is constant for each scale factor.

Then, the NRMSE is computed on the load duration curve, to understand which case better reproduces the ElaadNL data. A different value of NRMSE is computed both for each case and for each scale factor, resulting in 24 cases. However, as it was already analysed, the 0.4 scale factor is the most representative. Hence, the values reported refer only to this family of cases. The curve with the lowest NRMSE is the Case 5, probably because better follows the trend of low power values, that as seen before, is the region that the model has more challenges in reproducing. The LF error presents marked discrepancies, especially in Case 8, meaning that delaying the window of high CP_{prob} does not correspond to the real conditions measured in the Netherlands. Moreover, it can be noticed that the NRMSE results are limited in a narrow range, showing that the model provides quite robust results.

4.2 RAMP-Mobility results

In this section different model results are presented. First, the database of European EV load profiles is reported. This will then be used to represent the transport demand in the power system simulation performed with the Dispa-SET model. Then, a sensitivity analysis is performed on the stochastic parameters, to study the robustness

of the model to variations of these arbitrary inputs. Lastly, the charging process is analysed. The differences between the four charging strategies implemented are first shown. Afterwards, a sensitivity analysis on the arbitrary parameters necessary to calculate the charging demand is performed.

4.2.1 European EV profiles database

Here the results of the load profiles simulated with the RAMP-Mobility model are presented. First, an analysis is conducted to evaluate the optimal number of users to be simulated in order to capture the whole country behaviours while limiting the computational time. Then, the profiles are presented, along with some comparison to understand the differences between countries. This can help in determining the impact of different input data such as mobility patterns, climate conditions, time-related habits or population and car fleet composition.

Analysis on the number of users

Before presenting the results of the European charging profiles, it is relevant to perform a brief analysis on the impact that the number of simulated users has on the shape of the curve. This is useful to study the trade-off between obtaining a smoother profile when simulating more users, and the resulting computational time increase.

Table 4.3 shows the simulation time when varying only number of users. One month is computed and from that the total time for one year is estimated. The computer used is a Intel® Xeon® W-2155 CPU @ 3.30GHz, 32 GB RAM machine. In addition, only for 2500 and 5000 users the whole year was simulated, to test the actual total computational time. Results show that the time increases proportionally with the number of users, meaning that it takes roughly twice as long to simulate twice as many users. Instead, the time necessary to simulate a whole year is around 4 times more than estimated from the one month simulation.

Number of users	1 Month	1 Year (estimated)	1 Year
500	00:00:39	00:07:48	-
1000	00:01:09	00:13:48	-
2500	00:02:46	00:33:12	02:21:02
5000	00:05:31	01:06:12	04:34:06
7500	00:08:30	01:42:00	-
10000	00:12:46	02:33:12	-

Table 4.3. Computational time for different number of users simulated [hh:mm:ss]. One month is simulated and from that the time to simulate the whole year estimated. Only for the 2500 and 5000 users cases the actual time to simulate the whole year is computed.

The corresponding profiles are plotted with the standard RAMP-Mobility minute time detail in Figure 4.6a. Then, since energy system models have usually a hourly time step, the profile is re-sampled and presented in Figure 4.6b. This additional analysis is useful to understand the level of detail available when passing to a lower

time resolution. It is clear from the results that up to 1000 users the aggregate curve is highly segmented, as can be noticed both in the minute and hour detail plot. Starting from the 2500-5000 users range, instead, the profile reaches a more stable trend. Some minor deviations are still visible, anyway these are lost when looking at the hourly profile. Therefore, if an hourly profile is needed, any value in the 2500-5000 users range can be considered a good trade-off, depending on the computational power available. Otherwise, if a higher time resolution is relevant, then a higher number of users is advised, around 7500. Finally, no significant improvement is noticed for the simulation with 10000 users, which brings to a much higher calculation time. Hence, it is not advised to simulate more than 7500 users.

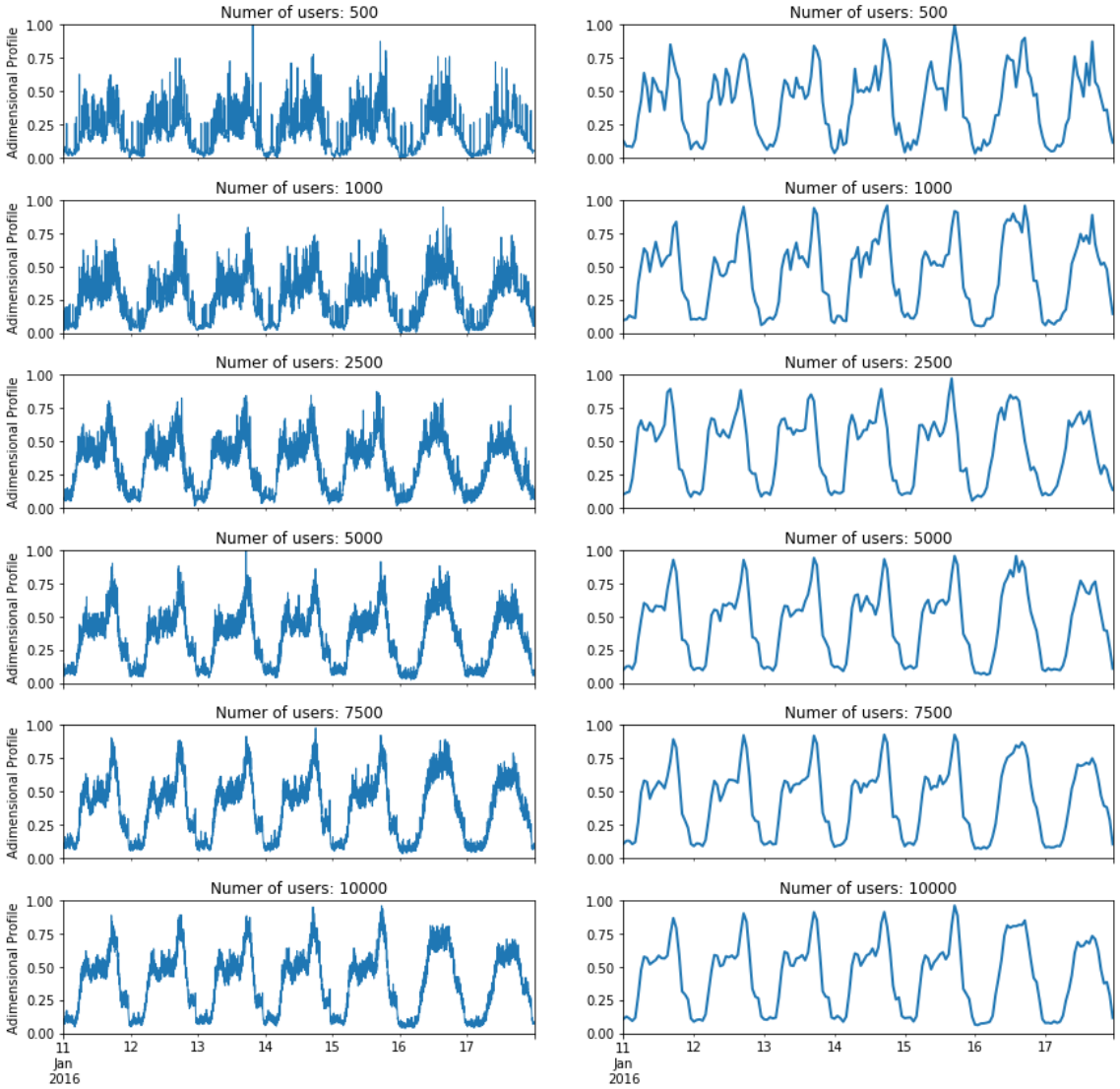

(a) Minute detail.

(b) Hour detail.

Figure 4.6. Comparison of the adimensional charging profile for one week for different number of users simulated. Both the minute and hourly time detail are reported.

Charging profiles results

After defining the optimal number of users to be simulated, the complete European database of EV charging demand is computed. This is used to represent the transport demand in the power system simulation performed with the Dispa-SET model. For this reason, some of the parameters used in RAMP-Mobility are set to meet the specificities of the energy model, especially regarding the V2G modelling. The *Perfect Foresight* charging strategy is used, to compute the AFs of the battery fleet, necessary to activate the V2G option in Dispa-SET. The CP_{prob} is constant and set to 80%, as in the 2050 system a massive deployment of charging infrastructure is expected. Charging stations are distributed as in the default version of the model, with a higher share of 3.7 and 11 kW nominal power, and a limited amount of 120 kW superchargers. The logistic function to model the user attitude towards the SOC of the car is not activated, since a too high uncertainty is linked to the value of this parameter in 2050. As a trade-off between accuracy and computational tractability, 2500 users are simulated for each country, bringing to a total of 70000 users. This, as previously explained, is a value that allows to obtain smooth results on an hourly basis, while avoiding a too high simulation time.

The results of the simulations for 28 European countries (EU27 minus Cyprus and Malta, plus UK, Norway and Switzerland) are now presented. In order to allow an easier comparison of the results, the 28 countries are grouped in 8 macro-regions. Table 4.4 presents the definition of the 8 regions, along with a country considered representative. Their graphical representation is depicted in Figure 4.7. The choice of the representative country starts from the six regions for which mobility data are available from the JRC survey (see Section 3.1.2 for further details). In addition to this, Norway and Romania are included to capture on the one hand extreme climate effects, and on the other differences due to specific time habits. In addition, these countries were chosen as do not rely on car fleet or functioning windows data from other countries.

The first comparison is performed on the load duration curve, to capture the overall yearly trend. The eight resulting curves are presented in Figure 4.8. This plot allows to evaluate mainly the differences in the mobility data and in the climate conditions. Another factor that can influence the results is the different population

Region name	Countries	Representative country
Central	AT, CH, CZ, DE, SI, SK	DE (Germany)
West	BE, FR, LU, NL	FR (France)
East	EE, LT, LV, PL	PL (Poland)
South	EL, IT	IT (Italy)
North	DK, FI, NO, SE	NO (Norway)
South-East	BG, HR, HU, RO	RO (Romania)
South-West	ES, PT	ES (Spain)
North-West	IE, UK	UK (United Kingdom)

Table 4.4. Definition of 8 macro-regions with their representative country. For each region, only the results from one country are presented.

Figure 4.7. Graphical representation of the 8 macro-regions used to present the results[1].

composition, reported in Figure 4.9 and divided by population type and vehicle size. In some specific cases, also the weekly profile is shown, to investigate with higher detail the differences between the curves. Several trends can be highlighted.

First, it is visible that the curves of Poland and Romania are almost overlapping. This is clearly due to the fact that mobility data collected in Poland are used also for Romania. Furthermore, the two countries have similar climate conditions. In addition, the highest power demand is registered, in particular in the peak region. This can be explained by Poland having the highest average mobility demand. Indeed, the total daily travel distance per car, d_{tot}, reaches the highest values for Poland, as already presented in Figure 3.6. This is intensified by the increased car consumption due to cold climate. Subsequently, Spain shows a similar trend to the one of Romania for the low power values, whereas a lower one for the peak zone of the curve. To better visualise the trend, the weekly charging profile is reported in Figure 4.10a. It is clearly visible that prominence of the daily peaks is much lower in Spain than in Romania. The reason for this might lie in the user type distribution. Indeed, Spain (together with Italy) is the country where the highest number of inactive people are registered. Since the peaks are mainly determined by the travels made by Working and Student users, this brings to low peak values. In addition, also climate conditions might play a role. Indeed, also Romania has a rather high share of Inactive users, but presents higher peaks than Spain. This is possibly due to the colder climate causing a higher multiplicative factor in Poland. The result is a more stretched curve. From the weekly profile plot is also possible to notice the peak values happening later in the evening in Spain. The possibility to capture time-related habits is an important feature of the

[1] Map created with mapchart.net ©

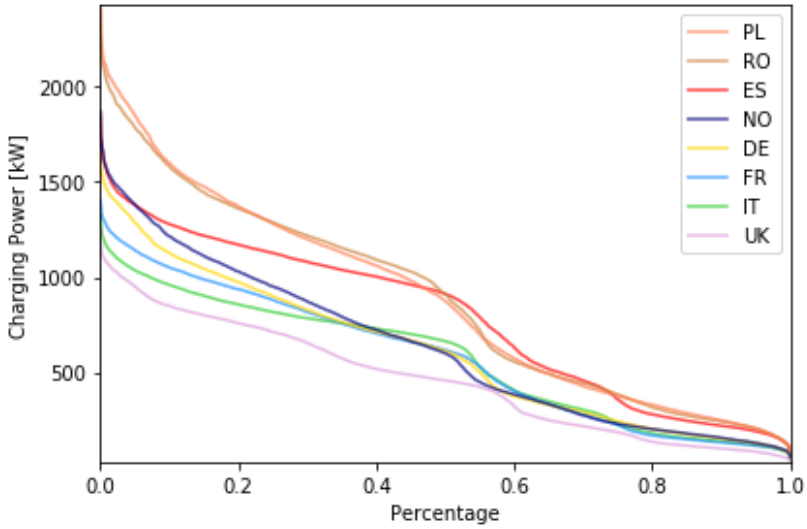

Figure 4.8. Comparison between the charging demand load duration curve in the 8 selected countries.

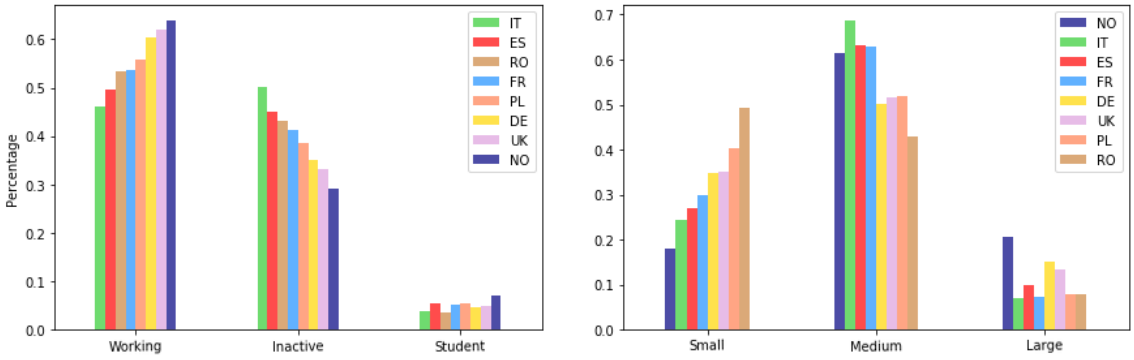

(a) Population category

(b) Vehicles size

Figure 4.9. Comparison of vehicle and population composition for the 8 analysed countries.

RAMP-Mobility model.

Moving to the lower curves, Norway and Germany have almost the same trend. This is an expected result, since German mobility data are used also for Norway. Then, also France and Italy have roughly the same curve shape for medium and low power values. The reason is that these three countries all have very similar d_{tot} values. Nevertheless, a declining trend can be noticed in the peak region, starting from the highest values registered in Norway to the lowest peaks displayed in Italy. The explanation can be twofold. On the one hand, going from Scandinavian countries to Italy there is a continuous trend towards warmer climates, that brings to lower power consumption. On the other hand, there is also a downward trend in the Working and Students users, indeed Norway shows the highest share, while Italy the lowest. As already seen for Spain, a higher share of Inactive users contributes to soften the charging profile peaks. To understand in detail this trend, Figure 4.10b shows the comparison between Norway and France. Here two interesting aspects can be observed. First, it is confirmed the the difference in the peak height due to different shares of

Inactive users. Second, the earlier peaks in Norway show again the potentiality of the model to reproduce the country-specific time habits.

Lastly, the United Kingdom is the country with the lowest values of charging power. This is clearly due to being the nation with the lowest daily mobility demand, as is visible from the values of d_{tot} presented in Figure 3.6.

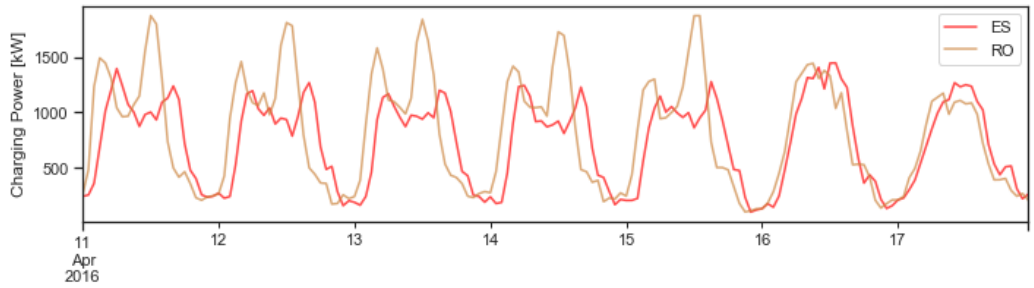

(a) Comparison between Romania and Spain

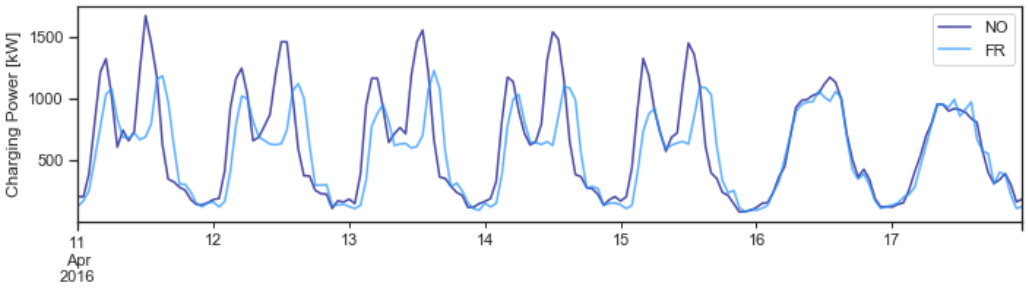

(b) Comparison between Norway and France

Figure 4.10. Charging demand weekly comparison between some of the selected countries. One week in April is presented.

4.2.2 Sensitivity analysis on stochastic parameters

After showing the differences between countries, this section will focus on just one, to present a sensitivity analysis on the main stochastic parameters. The country used for this case is Germany, as among the two that were validated, is the only one that does not rely on data from the closest neighbour. All the results reported in this section refer to a population of 5000 users. The stochastic parameters directly affect only the mobility demand. Therefore, in the results only the mobility profile will be shown. This choice is made as no additional information would be obtained from showing the charging demand simulated with constant conditions. Three groups of parameters are identified, and a specific analysis is conducted on each of them, keeping the default value for the others (equal to the value used in the Case 1).

Travel-related characteristics

The first group of parameters are the ones linked to the travel characteristics. These are: the variability applied on the car power consumption, $P_{EV,rand}$, on the average travel distance, $d_{min,rand}$ and on the travel velocity $v_{av,rand}$. The conditions of the seven different cases simulated are show in in Table 4.5.

	Case 1	Case 2	Case 3	Case 4	Case 5	Case 6	Case 7
$P_{EV,rand}$	0.1	0	0.2	0.1	0.1	0.1	0.1
$d_{min,rand}$	0.3	0.3	0.3	0.2	0.4	0.3	0.3
$v_{av,rand}$	0.3	0.3	0.3	0.3	0.3	0.2	0.4

Table 4.5. Sensitivity analysis on travel-related stochastic parameters.

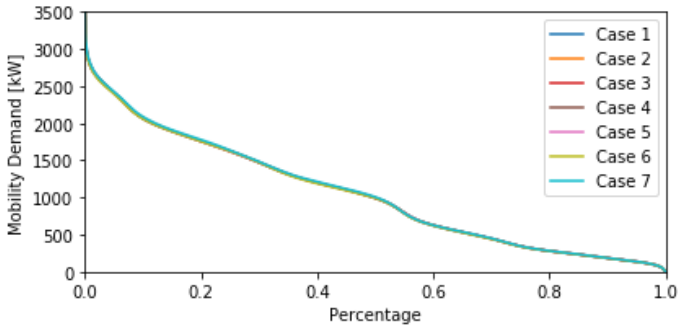

(a) Load duration curve.

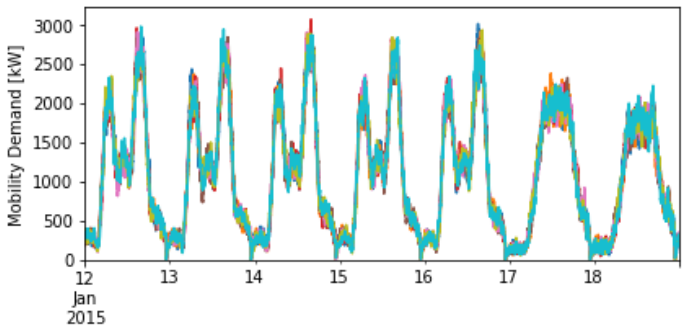

(b) Weekly detail.

Figure 4.11. Comparison of the results for the sensitivity analysis on the travel-related stochastic parameters. The seven cases correspond to different combinations of the values of random variability in the EV power, the average travel distance and the average travel velocity.

To compare the results, two different plots are reported. First, the load duration curve shown in Figure 4.11a gives an overview of the whole yearly mobility demand. All the seven cases are almost overlapping, showing that the model is quite robust with respect to these parameters. Then, to observe closer the differences, one week is selected and also its profile is presented (Figure 4.11b). Again, no significant trend is visible. This shows that the travel-related stochastic parameters do not influence significantly the final result.

Functioning windows variability

The functioning window variability $window_{rand}$ is the second group of stochastic parameters evaluated. Its role is to define a random variability in the starting and ending time of each functioning window. Three types of parameters are defined, one for each *Main* window, and a final one for the *Free time* windows, with no differentiation

by user type.

Functioning window	Case 1	Case 2	Case 3	Case 4	Case 5	Case 6	Case 7
Main - Student/Working	0.25	0.15	0.35	0.25	0.25	0.25	0.25
Main - Inactive	0.2	0.2	0.2	0.1	0.3	0.2	0.2
Free time - Any user	0.2	0.2	0.2	0.2	0.2	0.1	0.2

Table 4.6. Sensitivity analysis on functioning windows variability.

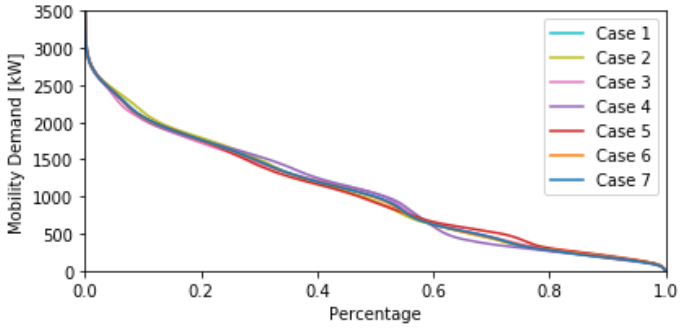

(a) Load duration curve.

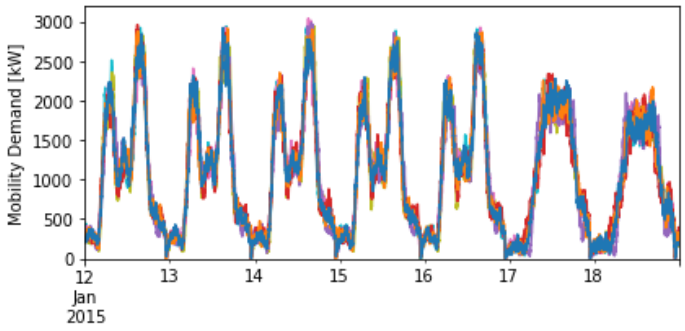

(b) Weekly detail.

Figure 4.12. Comparison between different functioning windows variability. The seven cases correspond to different combinations of the values of random variability in three types of functioning windows: Main - Student/Working, Main - Inactive, Free time - Any user.

Again, two different plots are reported. The load duration curve (Figure 4.12a) shows some minor deviations, especially for Case 4 and 5, that correspond to the sensitivity on the *Main - Inactive* window. This is the parameter affecting most the final curve since in the weekend the whole population behaves according to the *Main - Inactive* window. In particular, when the variability is lower (Case 4), the mobility is concentrated in a smaller windows. Therefore, there is a higher probability of simultaneous travels, bringing to lower frequency of low mobility periods. The opposite trend is observed for Case 5, with a wider window causing higher frequency of isolated travels. In the aggregate curve these are visible as low power values. However, it is worth noticing that in the weekly profile shown in Figure 4.12b, no important trend is visible. Hence, the deviations just described have a rather limited impact on the daily profile.

Occasional use

The last group of parameters is the occasional use, which determines the probability that the user starts at least one trip each day. Overall, five types of occasional use are defined, one for each day type *Main* window (namely weekday, Saturday and Sunday) and two for the *Free time*, one in the weekdays and one in the weekends. Since the effect of this parameter is the same on each functioning window, the sensitivity analysis reported refers only to two exemplary parameters. The first refers to a *Main* window and the second to a *Free time* one. Any consideration drawn in this section applies also the other windows of the same type.

Occasional use	Case 1	Case 2	Case 3	Case 4	Case 5
Main - Saturday	0.6	0.5	0.7	0.6	0.6
Free time - Weekday	0.15	0.15	0.15	0.05	0.25

Table 4.7. Sensitivity analysis on occasional use.

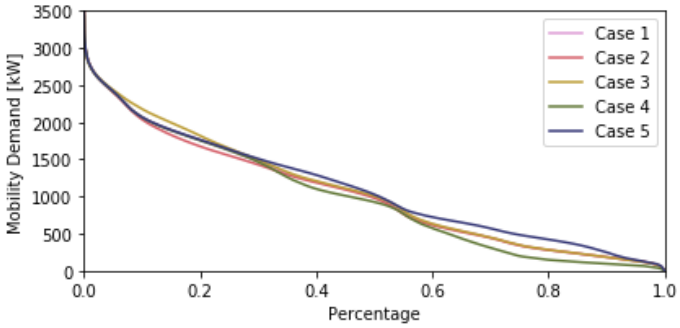

(a) Load duration curve.

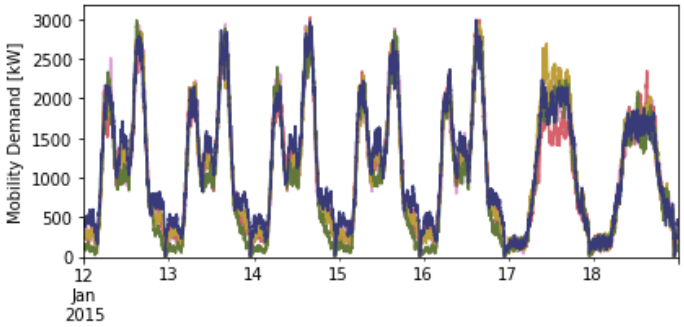

(b) Weekly detail.

Figure 4.13. Comparison between different occasional use values. The five cases correspond to different combinations of the values of occasional use in two types of functioning windows considered: Main - Saturday, Free time - Weekday.

Figure 4.13a reports the load duration curve for the 5 cases simulated. It is immediately visible that this is the parameter that affects the most the results. Indeed, it results in shifting the demand curve upwards or downwards, depending if it is higher of lower. In particular, the largest effect is visible for Case 4 and 5, where

the *Free time - Weekday* occasional use is varied. This brings to a shift in the free time usage, modifying the distribution of low power values. The same trend is visible in Figure 4.13b, where both the Saturday peak and weekdays free time values are clearly shifted. Thus, particular attention should be payed when varying the default values of this parameter, since they were already validated with a satisfying degree of accuracy.

4.2.3 Charging process analysis

In this section the charging process is analysed, to understand the impact of the different customizable features presented in Section 3.1.3. Note that a sensitivity analysis on the parameters of the piecewise CP_{prob} function has been already conducted in Section 4.1.2, therefore is not replicated here. Following the reasoning of the previous section, all the simulations refer to 5000 users in Germany. The mobility stochastic parameters are set to the default values.

Charging strategies comparison

The four different charging strategies already presented in Section 3.1.3 are here compared, to analyse the possible evolution of smart charging solutions. An overview of the strategies along with their main characteristics is presented in Table 4.8.

Charging Strategy	**Time**	**Energy**	**Power**
Uncontrolled	Immediately after parking	Until SOC_{max}	Nominal
Perfect Foresight	Right before next travel	Demand for the following journey	Nominal
Night Charge	Night period	Until SOC_{max} or end of night time	Minimum
RES Integration	During negative residual load	Until SOC_{max} or end of optimal time window	Minimum

Table 4.8. Overview of the main features of the charging strategies. All the charging events start only if the charging infrastructure is available and end if the parking time is over.

Figure 4.14 shows the comparison between the four different charging strategies. The *Uncontrolled* case shows the expected slight delay in the charging profile with respect to the transport demand. The opposite trend is visible in the *Perfect Foresight*, where the power demand to the grid is shifted earlier with respect to the mobility profile. This is due to the charging happening right before the start of the travel. Moving to the smart charging strategies, the *Night Charge* shows the load shifting potential offered by simply postponing as many charging events as possible in the 22:00 - 7:00 time window. This condition helps avoiding the coincidence of the EVs power demand peak with the base electricity demand peak. It is worth noticing that,

even if the time available for charging is lower than the *Uncontrolled* case, the peak load is comparable because the *Night charge* works at the minimum possible power. The *RES Integration* charging strategy requires a deeper analysis. In this case, the time window in which the charging is shifted depends on the calculation of the residual

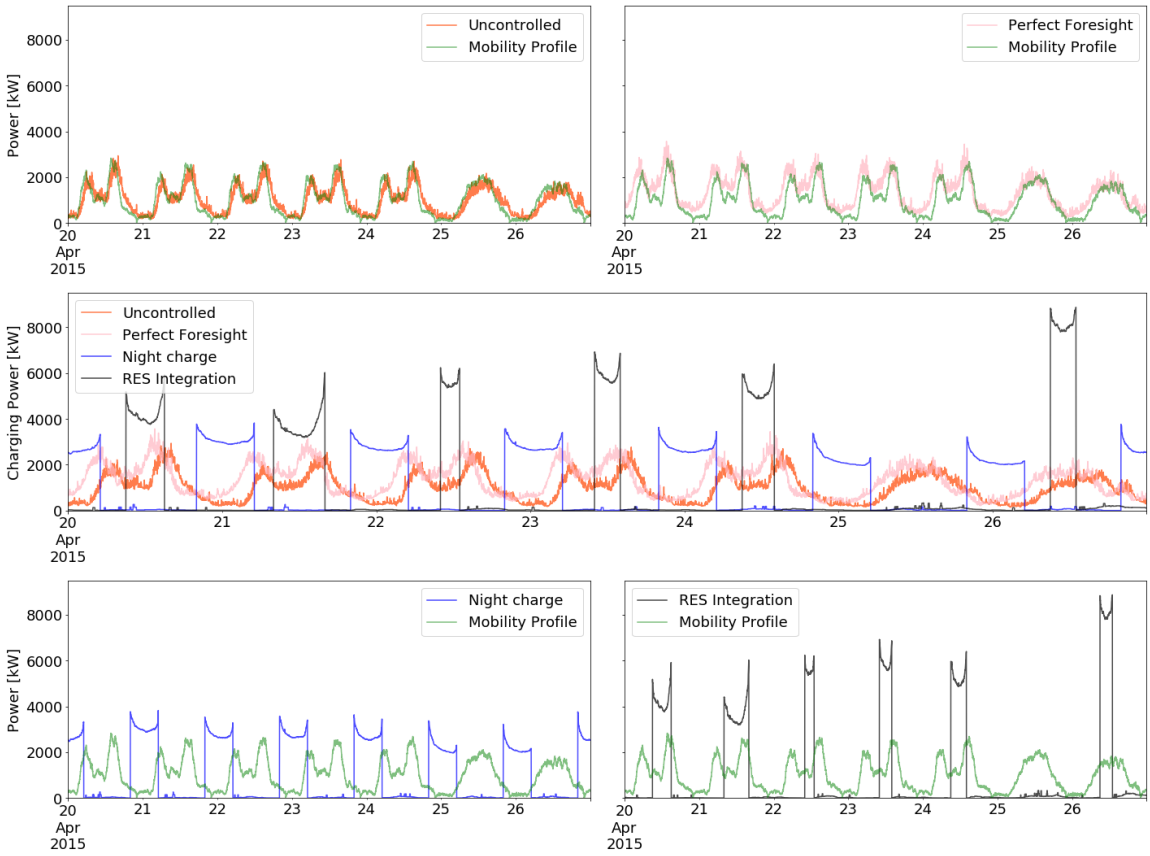

Figure 4.14. Comparison between the different charging strategies. The plots in the corners show each single strategy along with the mobility demand. In the centre the 4 strategies are compared against each other.

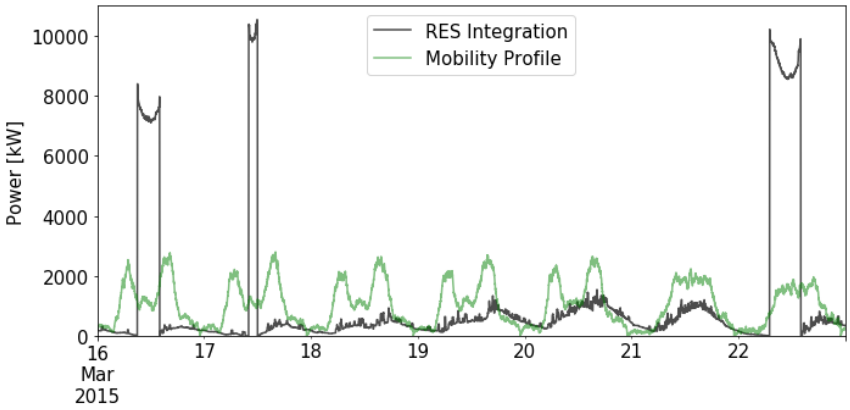

Figure 4.15. Focus *RES Integration*, showing one week with mostly positive residual load. This brings to a very high charging demand peak when the charging time window is available, as is visible on Sunday.

load curve. This is an indicator of when the VRES electricity production is higher than the load curve, causing curtailment of the excess electricity. Usually, as visible in the week presented, this condition happens in the central part of the day, when the solar power production peaks. However, on Saturday the residual load is never lower than zero. This causes almost no charging events to start, as the battery capacity is enough to cover the whole day mobility demand. The consequence is that the peak demand on Sunday is higher than the weekly average, to compensate for the missing charging events of the previous day.

It might happen that the residual load is positive for several consecutive days. In this case, the charging events start only because of EVs reaching the extremes conditions of either *SOC* lower than the minimum value, or of residual energy lower than the consumption required by the following travel. An example of this condition is presented in Figure 4.15. Here four consecutive days with positive residual load bring to a very high peak on Sunday. The charging demand is almost 4 MW higher than the average 6 MW demand in the week presented in Figure 4.14. The residual load curve shape is strongly dependent on the combination of load demand, weather conditions and VRES total installed capacity. Therefore, it varies significantly, depending on the country and on the considered year. In this section the base year 2015 weather was simulated, while the power demand and the installed renewable capacity refer to the 2050 ProRES scenario from the JRC-EU-TIMES model.

Comparing the two smart charging strategies implemented in the model, the *Night Charge* solution allows to completely shift the power demand in the off-peak time window, while the *RES Integration* is highly dependant on the system conditions. A possible solution could be the combination of the two, to exploit on the one hand the periodic pattern of the night charging and on the other hand avoid the curtailment of excess renewable electricity during the day. It is important to point out that the analysis here conducted is just a simplified version of what can be simulated by a complete energy model, where the whole power system is optimised. Anyway, the results here obtained provide an halfway condition between the uncontrolled charging pattern and the high complexity of a fully optimised system. This can be used as a benchmark to evaluate the extent of additional precision brought by a complete charging patterns optimisation, with respect to the higher computational burden.

Impact of the User range anxiety

The impact of the logistic curve to model the relation between charging decision and *SOC* of the car is here studied. The comparison will be between two main cases, with and without the activation of this feature. The default logistic relation is used, as already presented in Section 3.1.3. All the other charging parameters are set to the default value. The *Uncontrolled* charging strategy is simulated.

The introduction of an additional condition in the charging event decision results in a different distribution of the charging power. Figure 4.16 presents both the load duration curve and the weekly profile results. Here, both a reduction in the peak power and an increase in the lower power area are visible. These two trends are linked, because the introduction of the logistic curve determines a lower probability that the car is charged with a *SOC* higher than 50%, causing a lower coincidence of charging events in the peak windows. Consequently, this results in a slightly higher probability

in the low power zone, because the charging events skipped in the peak time frame are shifted to the off-peak periods. Also, being the logistic curve symmetrical, it increases drastically the probability that the EV is charged with SOC lower than 50%. As a result, the average total energy absorbed from the grid is lower, since there is a lower number of cases when the battery is charged from the SOC_{min} to the SOC_{max}.

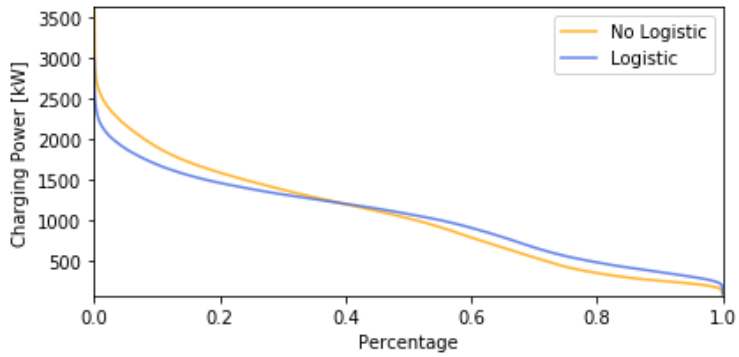

(a) Load duration curve.

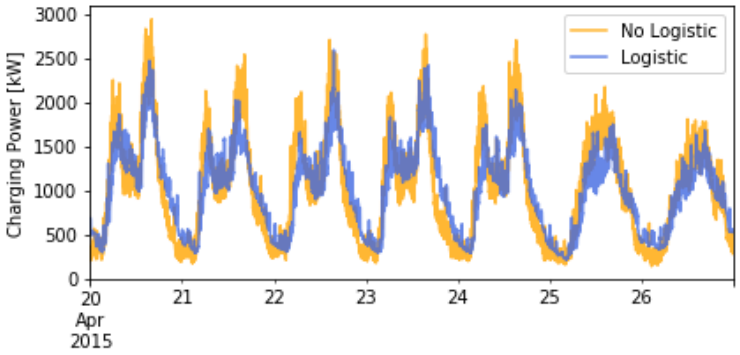

(b) Weekly detail.

Figure 4.16. Comparison between charging demand considering or not the logistic curve to model user's range anxiety.

Constant infrastructure availability

Then, the impact of a different probability of finding a CP is studied. Since the piecewise probability function has been already object of a sensitivity analysis in Section 4.1.2, here only the option with constant probability is studied. Two cases are explored, one with a medium penetration of CPs (0.5 probability), and one that simulates an extensive roll-out of charging infrastructure (0.8 probability). Almost doubling the CP availability does not seem to change drastically the results. The major effect visible in Figure 4.17 is that a lower availability of charging infrastructure brings to moderate decrease of simultaneous charging. Nevertheless, the results are comparable to a great extent.

Charging points technology evolution

The last parameters that can be set by the user in the charging process are the nominal power of the CPs and their relative distribution. Three main cases are analysed, as

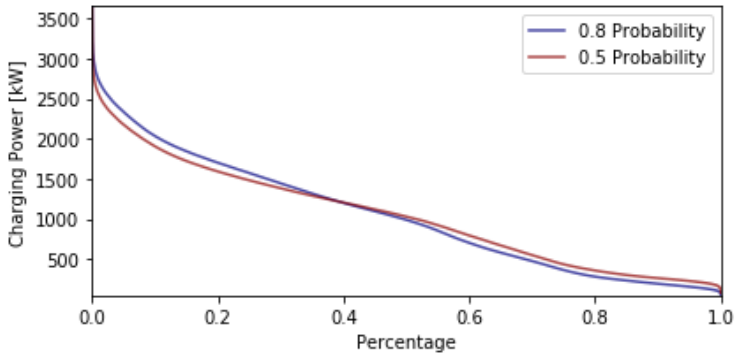

(a) Load duration curve.

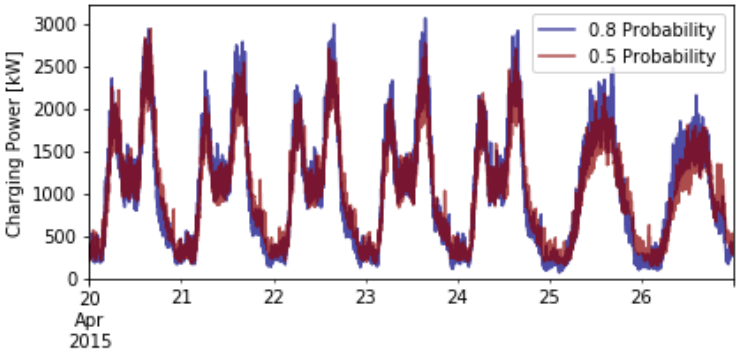

(b) Weekly detail.

Figure 4.17. Comparison between the two different constant infrastructure availability values, equal to 0.5 and 0.8.

reported in Table 4.9. First the default condition is simulated, with higher standard plugs availability. Then, the second case is an intermediate situation with higher share of fast charging stations. Finally, Case 3 explores a scenario with massive deployment of supercharging solutions.

P_{CP}^{nom}	Case 1	Case 2	Case 3
3.7 kW	0.6	0.2	0.2
11 kW	0.3	0.6	0.2
120 kW	0.1	0.2	0.6

Table 4.9. Sensitivity analysis on the charging point type distribution.

The results show an expected trend. When the relative share of stations with high nominal power increase, higher peaks are visible, as shown in Figure 4.18. However, when looking at the load duration curve in Figure 4.18a, the three cases are almost overlapped, indicating that this parameter does not severely affect the results in the low and medium power region. Indeed, it is necessary to zoom on the high power region of the curve to visualise the different peaks reached by the three cases. It should anyway be kept in consideration that the increase in the peaks is significant, as visible in Figure 4.18b.

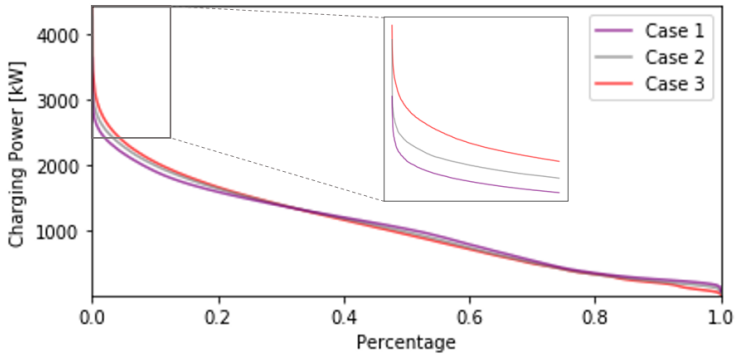

(a) Load duration curve.

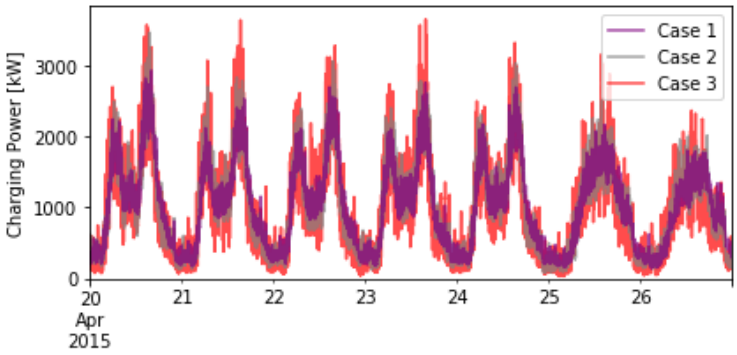

(b) Weekly detail.

Figure 4.18. Comparison between 3 different charging stations development scenarios. The three cases correspond to majority of: 3.7 kW normal plugs, 11 kW fast charge, 120 kW supercharging.

4.3 Dispa-SET simulations results

The final results of the Dispa-SET UCM simulations are here presented and discussed. The metrics of system performance presented in Section 3.2.3 are used as a guidance in the results discussion. After presenting the overall system results, a section is dedicated to a more detailed analysis on the storage technologies in relation to the flexibility needs of the system. Particular attention is dedicated to the contribution of the transport sector coupling on the competition among different storage technologies, and on the storage dynamics.

Scenario	Simulation time [hh:mm:ss]	Total system cost [billion €]	Average generation cost [€/MWh]
NOFLEX	05:57:55	840.6	93.5
THFLEX	10:36:39	804.2	88.1
EVFLEX	08:06:38	822.0	91.3
ALLFLEX	12:46:07	794.0	87.0

Table 4.10. Overview of simulation results. Computational time, total system cost and average electricity cost are presented.

It is first worth noticing that increasing the sectors integration brings to a higher computational time. The resulting simulation times are reported in Table 4.10, ranging from 6 hours in the NOFLEX case, to almost 13 hours in the ALLFLEX scenario. Again, the simulations are run on a Intel® Xeon® W-2155 CPU @ 3.30GHz, 32 GB RAM machine[2].

4.3.1 Overall system performance

In this section the main metrics to evaluate the system performance are reported and commented. These consist of analyses on operational costs of the system, power and heat production from the considered units, curtailed electricity and load shedding, congestion on the power network and finally the operational carbon emissions of the units.

Total system costs

A detailed costs breakdown of power plants operational costs, divided by technology and fuel, is presented in Figure 4.19. First, it is clear how the system cost decreases when integrating additional sector coupling option. Indeed, the ALLFLEX scenario proves to be the most cost-effective solution among the four considered conditions. Additionally, the introduction of extraction CHP plants, coupled with TES results in a significant increase in the usage of cogeneration technologies. This can be explained by the fact that the extraction plants have a much higher operational flexibility with respect to the back-pressure turbines, which are forced to work at fixed power-to-heat ratio. The trend is intensified by the presence of TES, which provides even more flexibility, thanks to the addition of the heat storage option.

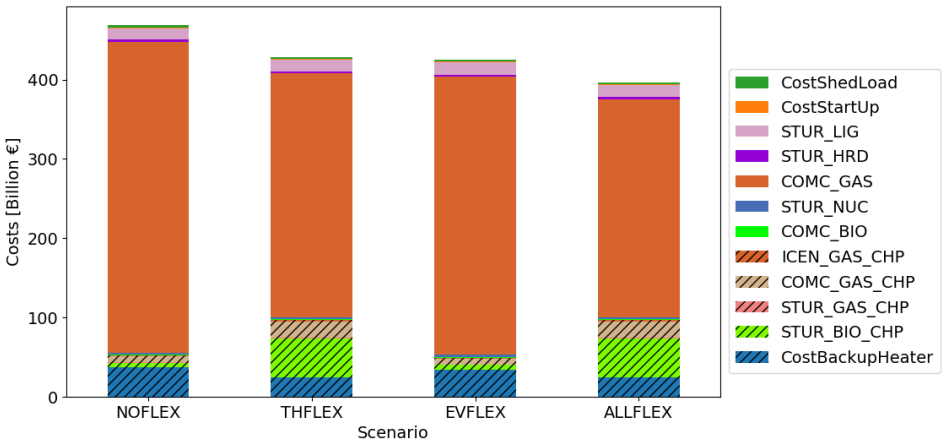

Figure 4.19. Costs breakdown in all scenarios. Variable fuel costs are presented per fuel and per technology type, the backup heaters cost is represented in blue.

[2] Due to memory issues, few loops did not provide feasible optimisation solution. Therefore the whole week was replaced by the previous week, to guarantee continuity in the results. These loops are: 14-15 August in the EVFLEX scenario, 9-10 July and 16-17 November in the ALLFLEX scenario.

Power and heat generation

Total electricity output divided by technology and exploited fuel is reported in Figure 4.20. The total generation varies among the scenarios mainly because of the presence of P2HT, which directly impacts the endogenous demand, as its functioning is strictly linked to the electricity price. The curtailment is quite low in all the four scenarios, for this reason the VRES penetration does not increase drastically when moving towards further the sector coupling integration. It is visible that electricity production from gas units is lower in the THFLEX and ALLFLEX scenarios. The reason is that the presence of additional storage capacity supplies electricity during periods of low VRES production. This avoids the need of using gas power plants to cover the peak demand of the system.

Subsequently, in Figure 4.21, the heat production divided again by technology and fuel, is shown. It is visible that the total value is similar across the scenarios. The

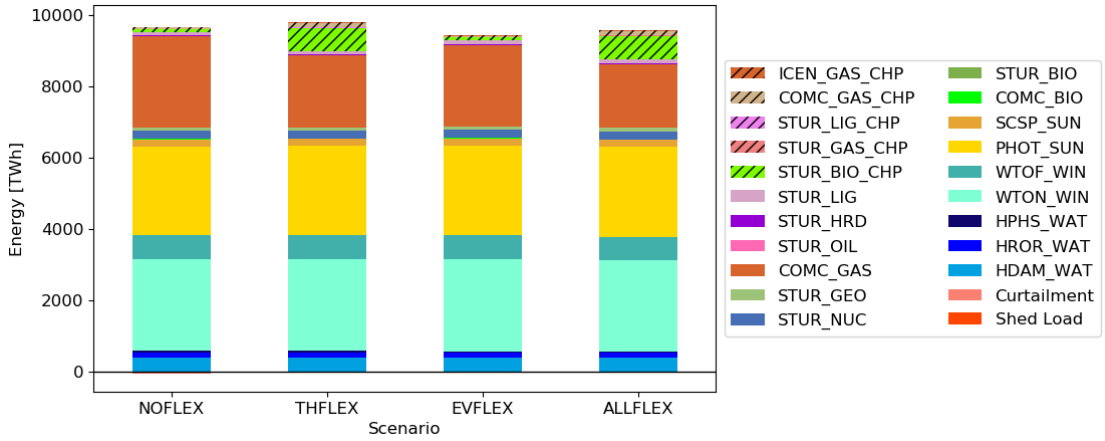

Figure 4.20. Electricity output per fuel and per technology type in all scenarios. Positive values on the indicate generation, while negative values indicate shed load and VRES curtailment.

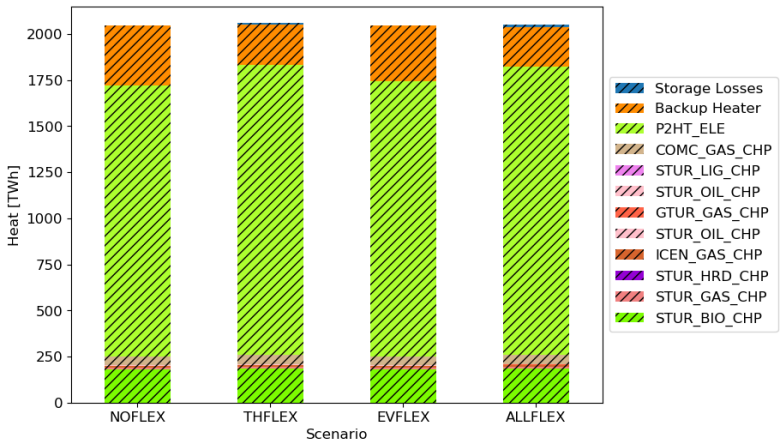

Figure 4.21. Heat output per fuel and per technology type in all scenarios. The presence of backup heaters is a signal of either missing heat generation capacity or high electricity price.

biggest difference lies is the utilisation of P2HT technology, which is in competition with the backup heaters. This means that when the electricity price is high, the backup heater is used instead of the electric heating. The thermal storage availability in the THFLEX and ALLFLEX scenarios balances the electricity price variability, bringing to more stable and lower prices. Therefore, these conditions favour the usage of P2HT technologies.

The power dispatch plots for the NOFLEX and ALLFLEX scenarios are presented in Figure 4.22. The comparison is provided, as a representative example, for the case of Italy, for a week in March. On Tuesday 22nd of March the presence of curtailment can be observed. This is due to fact that the full storage capacity available already meets the minimum *SOC* values imposed by the MTS calculations. Moving to the ALLFLEX scenario, it is visible how the full sector integration allows to completely avoid the

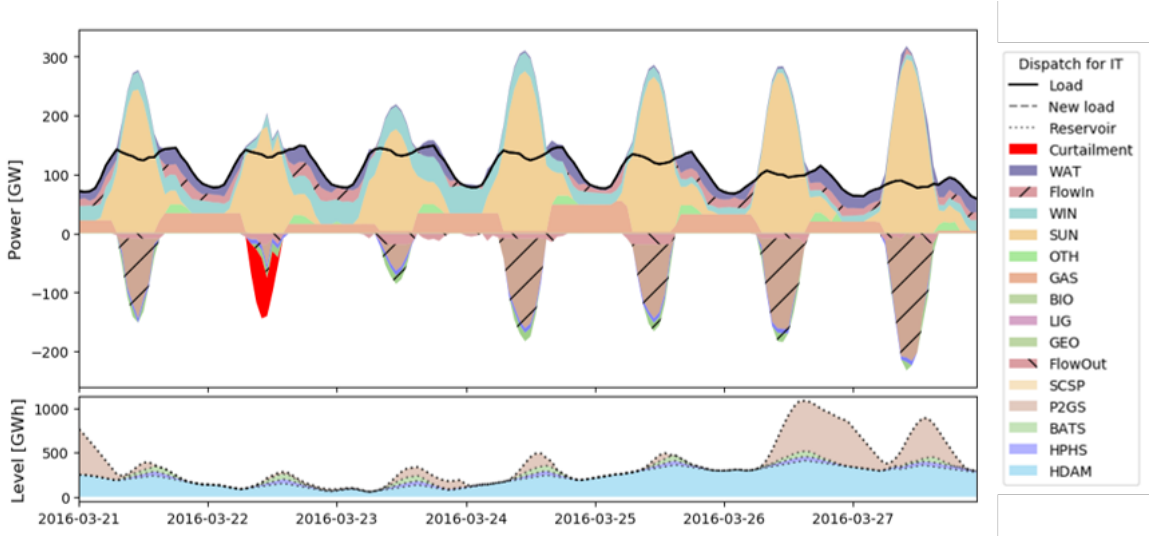

(a) Dispatch plot in the NOFLEX scenario.

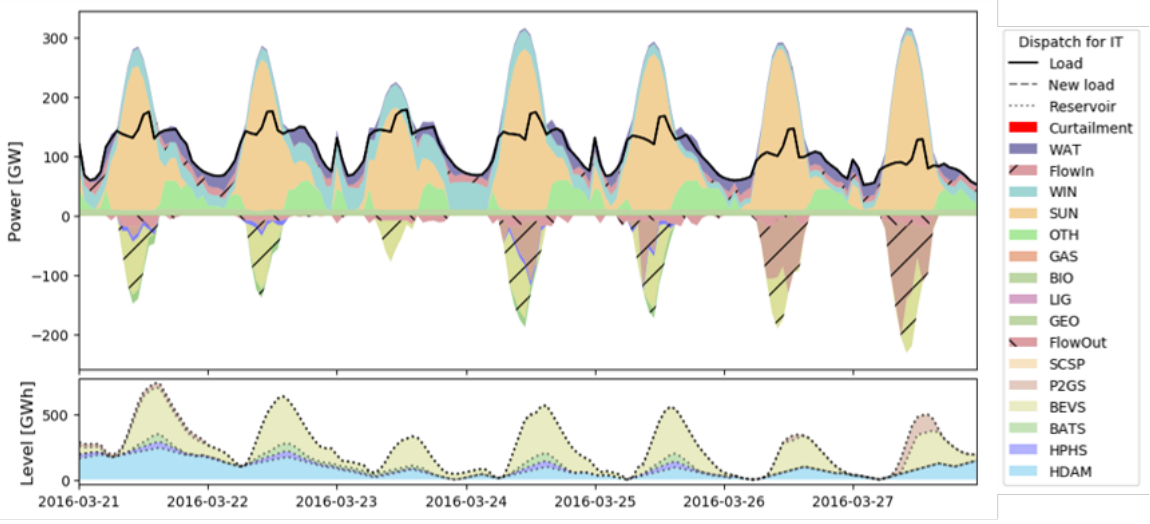

(b) Dispatch plot in the ALLFLEX scenario.

Figure 4.22. Power dispatch and reservoir levels for a week in March in Italy. Positive values indicate power generation, negative values indicate exported or stored power.

above-mentioned curtailment. This is the result of two main contributions. First, when more storage options are activated, the electricity price is lower, making the P2HT solution cheaper than the backup heaters. Therefore, the additional electricity demand requested by electric heating causes the visible increase in the load demand profile. Second, the additional storage capacity provided by the BEVS allows to absorb completely the excess electricity production. Indeed, in the analysed week the NOFLEX scenario mainly exploits Power-to-gas storage (P2GS) technologies to store the large amount of solar energy produced. However, when introducing BEVS, which is a cheaper and more efficient storage technology, the system shifts towards utilising it as much as possible.

Curtailed energy

The total and the maximum curtailed power is presented in Figure 4.23, as a percentage of the total and peak VRES power production, respectively. Overall, the amount of electricity curtailed is quite low across the four scenarios. This indicates that the system, even in the base scenario, manages to absorb most of the VRES power production, thanks to the available storage options. It is anyway relevant to analyse the benefits, in terms of curtailment reduction, when introducing the sector coupling options. Looking at the total curtailment, there is a clear downward trend when activating the TES and the V2G technologies. The biggest contribution to curtailed power reduction is provided by the transport sector. However, in the ALLFLEX scenario the total reduction is lower than the sum of individual contributions. This is due to fact that the available storage capacity cannot be fully exploited by the system because of limits in the European power grid. Instead, the trend is different when looking at the maximum curtailed power. Here the heating sector does not contribute significantly, while the transport sector decreases the maximum curtailment value by around 25%. Anyway, when combining the transport and heating sector flexibility, the maximum curtailment decreases more than the sum of the individual contributions. This might be explained by the exploitation of synergies generated by the availability of the maximum number of storage technologies possible.

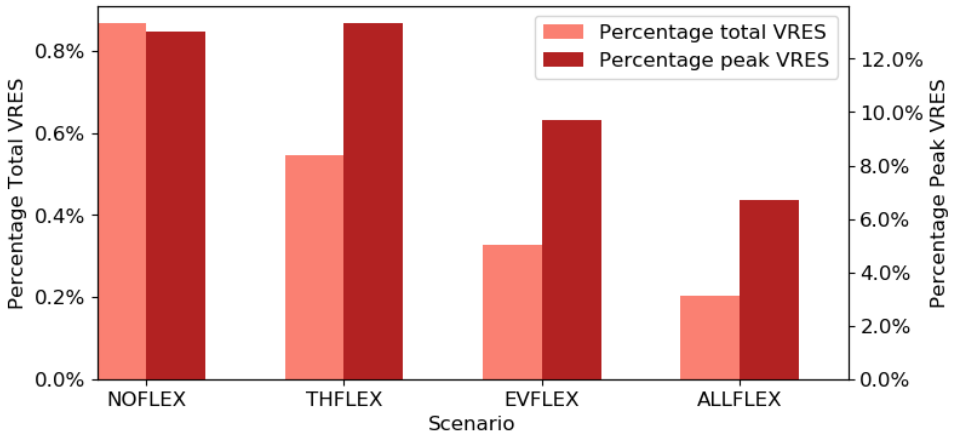

Figure 4.23. Total annual and maximum aggregated hourly curtailment as percentage of total and peak generation from VRES in all scenarios.

Load shedding

The total and maximum load shedding results are presented in Figure 4.24, as a percentage of the total load and of the peak load, respectively. It is visible that the overall level of shed load is quite low across the four scenarios. Furthermore, the maximum load shedding value follows a similar trend as the one noticed in the curtailment, where the transport sector coupling manages to reduce the most the shed load. Nevertheless, looking at the total load shedding value, it is visible that the thermal sector contributes to the reduction more than the transport sector.

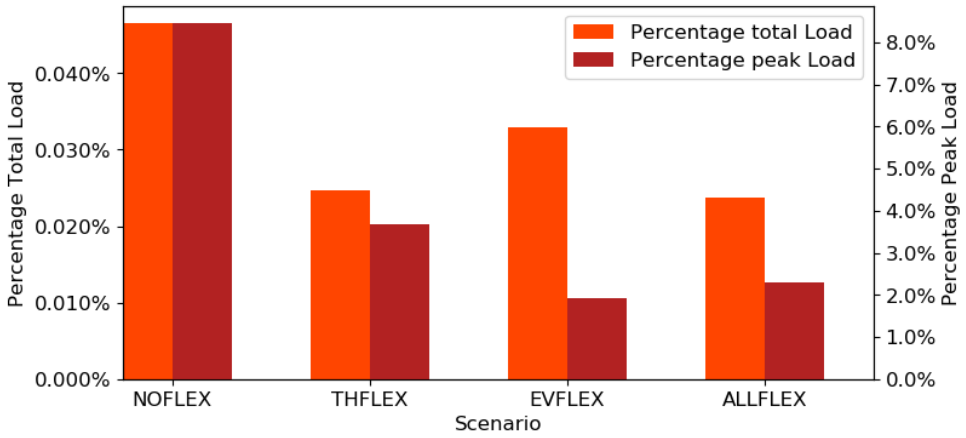

Figure 4.24. Total annual and maximum hourly shed load in all scenarios as a percentage of total and peak load.

Environmental impact

The operational carbon emissions from thermal units, both CHP and non-CHP is shown in Figure 4.25. Gas units are the major source of carbon emissions, followed by lignite units. The flexibility provided by the TES reduces the necessity of backup heaters, thus reducing the related CO_2 emissions. Overall, increasing the flexibility

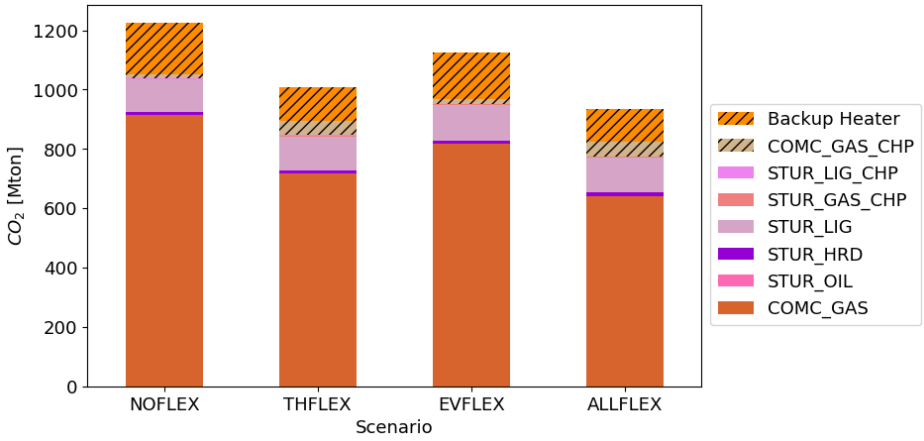

Figure 4.25. Summary of CO_2 emissions grouped per fuel and per technology type in all scenarios.

potential proves to be beneficial, as can be seen by the reduction of total carbon emissions. In particular it can be observed that the thermal sector coupling contributes the most to emission reduction. This is due to the higher utilisation of CHP technologies which brings to a significant reduction in the CO_2 emissions from gas units.

Congestion

The overview of the number of congestion hours in the power network is presented in Figure 4.26. Overall, the lines are rather congested. This is a clear signal of the fact that limits in the power grid are one of the main reasons why the system does not manage to exploit the complete flexibility potential available. Indeed, the presence of high storage capacities in some countries makes it convenient to exchange power in order to exploit the flexibility potential where possible. Another reason that causes

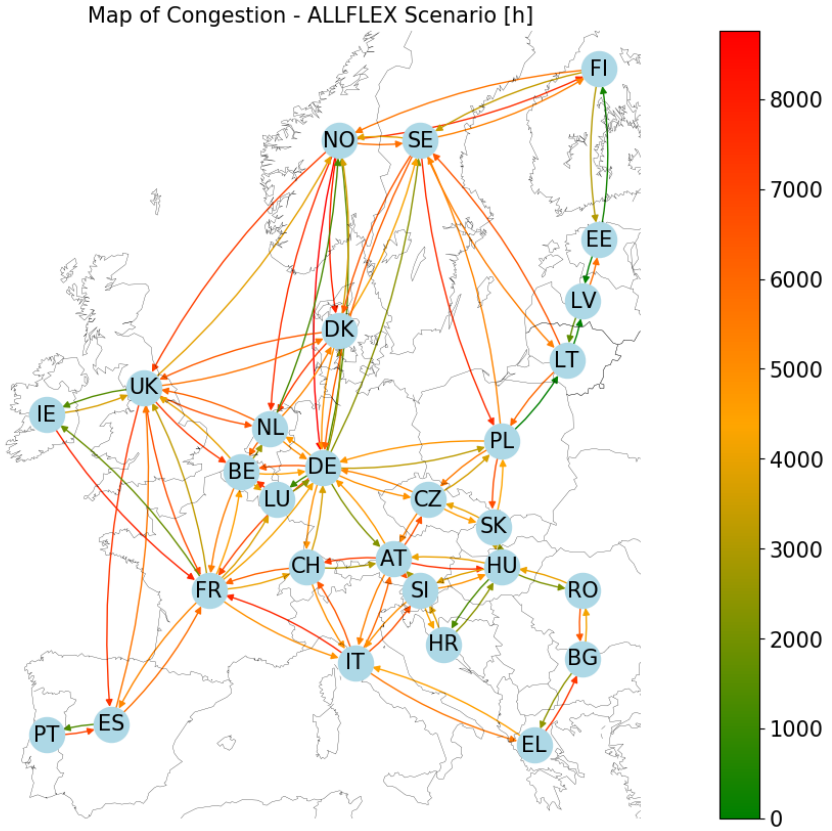

Figure 4.26. Number of hours of congestion power network lines. Red lines indicate high congestion levels (too low NTC value), green values low congestion levels (sufficient NTC value).

Congestion hours	NOFLEX	THFLEX	EVFLEX	ALLFLEX
Average	2988.2	3075.9	3032.2	3115.3
Maximum	5573.0	5648.0	5595.0	5802.0

Table 4.11. Average and maximum congestion hours in all cross-border lines from all scenarios.

high utilisation of transfer capacity is the presence of excess generation from VRES in countries such as Italy, Spain, France, Germany. In addition, also the lines between Norway or Sweden and their neighbours are highly used, due to the very high storage capacity installed through HDAM units.

The differences in grid utilisation are moderate among the four scenarios, as can be seen in Table 4.11. Both the maximum and the average number of congestion hours are higher when increasing the sector coupling option. Indeed, when the flexibility options increase, the power curtailment is reduced, increasing the overall VRES absorption and therefore causing a higher exploitation of the power grid.

4.3.2 Focus on transport sector flexibility

After having presented the overall performances, this section focuses on the flexibility needs of the system, with particular attention dedicated to the contribution of the transport sector coupling. This is conducted through the analysis of the shifted load by each storage technology in the four scenarios. Then, the storage shadow prices are studied in order to understand whether the available storage capacity is enough or not. Finally, the BEVS *SOC* dynamics are reported to understand the differences among scenarios.

Storage utilisation

The shifted load is presented in Figure 4.27, it indicates the extent of exploitation of the available storage technologies. It can be analysed that, with respect to the NOFLEX scenario, the introduction of BEVS in the EVFLEX and ALLFLEX scenarios causes a reduction in the usage of competing technologies such as BATS, HPHS and P2GS. This could be explained by the fact that the transport sector coupling provides a cheaper and more efficient storage technology than the other competitors. In addition to this, the fact that the storage contribution does not simply sum up might suggest two considerations. On the one hand, the storage available in the base case is already enough to guarantee the necessary flexibility for the analysed system. On the other

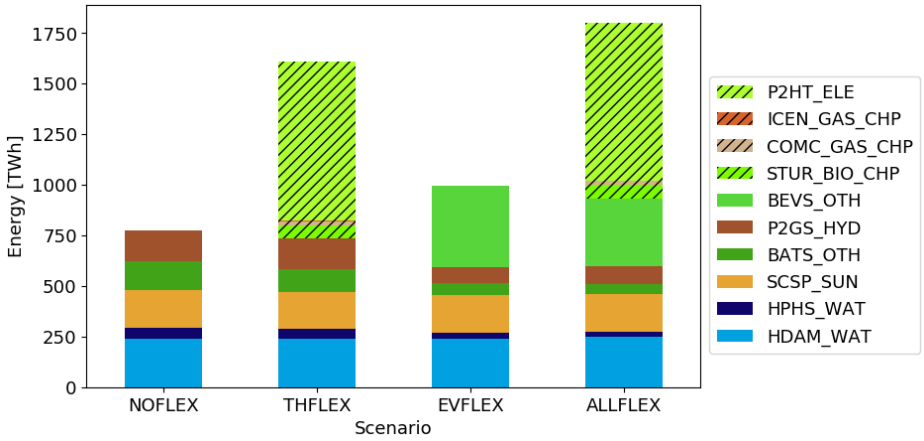

Figure 4.27. Shifted load per fuel and technology type in all scenarios. Hatched labels indicate TES storage from CHP and P2HT units.

hand, as it was also pointed out in the previous section, the limited NTCs is an important factor limiting the possibility to completely exploit the flexibility potential. The situation is different when analysing the introduction of TES. Indeed, here the contribution of the competing technology is almost constant. This can be explained by the fact that the thermal storage acts mainly on the thermal demand.

Storage shadow prices

After having presented an overview on the storage utilisation in the four scenarios, in this section a deeper analysis is performed, studying the trend of storage shadow price along the year. This quantity is important as it provides additional insights into the competition among different storage technologies. Indeed, the necessity of additional storage is highlighted by the presence of time steps when the storage shadow price equals the shed load price.

First, the storage shadow price is presented for the NOFLEX scenario, to investigate if the available storage capacity is enough to cover the flexibility needs. Figure 4.28 presents an overview of the storage shadow prices for the BATS and HDAM technologies for selected countries. The other technologies and countries present a uniform, low, storage shadow price. Thus, are not reported. The cases when the storage shadow price reaches the shed load price are visible for both BATS and HPHS in January, in northern countries such as Sweden, Estonia and Finland. Therefore, the necessity of additional storage might be due to a high heating demand, linked to low outside temperatures.

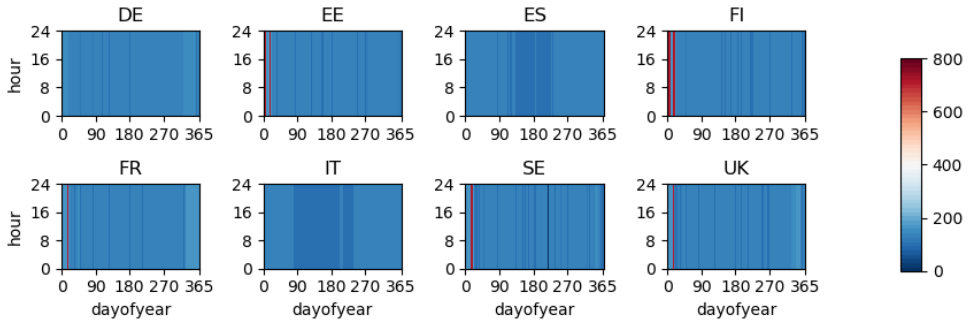

(a) BATS storage shadow price in the NOFLEX scenario for selected countries.

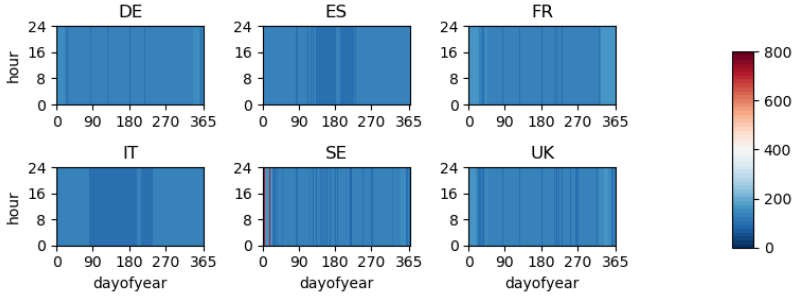

(b) HPHS storage shadow price in the NOFLEX scenario for selected countries.

Figure 4.28. Storage shadow price for BATS and HPHS storage technologies in the NOFLEX scenario for selected countries. The legend indicates shadow prices in €/MWh. Blue represents variable dispatch costs, red indicates shed load.

After having established that the NOFLEX scenario requires little additional storage capacity, it can be analysed which role the transport sector integration has in increasing the flexibility of the system. In Figure 4.29 the EVFLEX scenario storage shadow prices are reported for the BATS, being the technology with the highest shed load price events, and the BEVS technologies, as it is the new storage technology introduced. Looking at the results, it is visible that the transport sector only partially improves the conditions in Estonia, Finland and Sweden. This is highlighted also by Figure 4.29b. Here it can be seen that the BEVS storage shadow price is equal to the shed load price in the same periods as in the BATS case. Hence, the problems linked to the lack of storage capacity are not significantly improved by the introduction of V2G. This is a signal of the necessity of other types of storage solutions. In particular, these are represented by seasonal storage alternatives. Indeed, even if the presence of P2GS is considered, the precise analysis of its storage dynamics is out of the scope of this work.

The final step is towards a smart energy system is the integration of TES, reaching a complete sector coupling setup. Figure 4.30 reports the BEVS storage shadow price in the ALLFLEX scenario. For the sake of conciseness, the BATS plots is not reported, as these follow the same trend as BEVS. It is here visible how only the full sector coupling scenario manages to solve almost completely the storage adequacy issues noticed in the other scenarios. Nevertheless, a slight necessity of additional storage is still visible. This is again a signal of lack of seasonal storage alternatives.

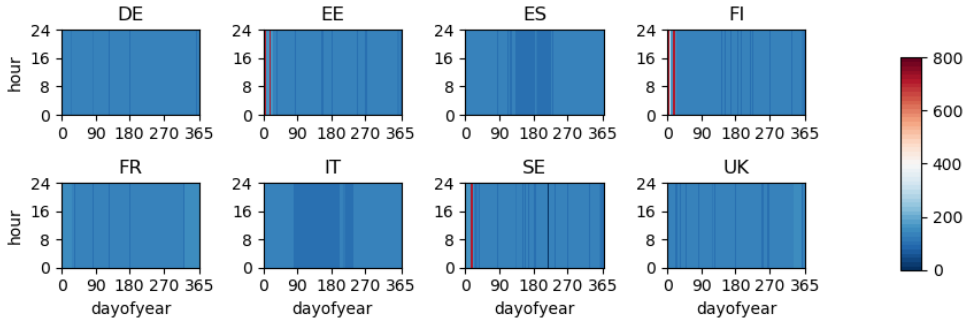

(a) BATS storage shadow price in the EVFLEX scenario for selected countries.

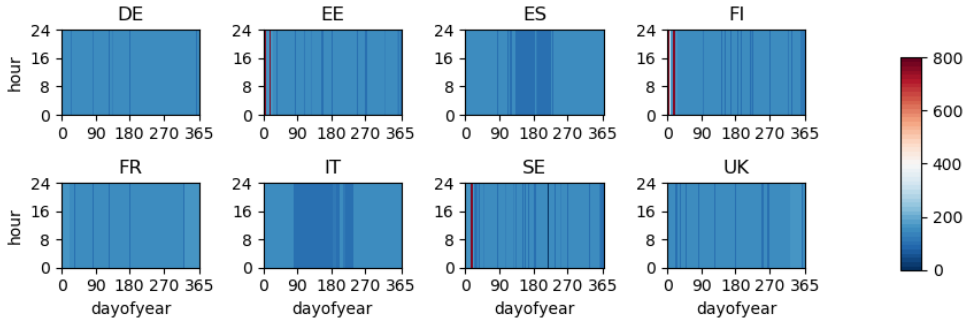

(b) BEVS storage shadow price in the EVFLEX scenario for selected countries.

Figure 4.29. Storage shadow price for BATS and BEVS storage technologies in the EVFLEX scenario for selected countries. The legend indicates shadow prices in €/MWh. Blue represents variable dispatch costs, red indicates shed load.

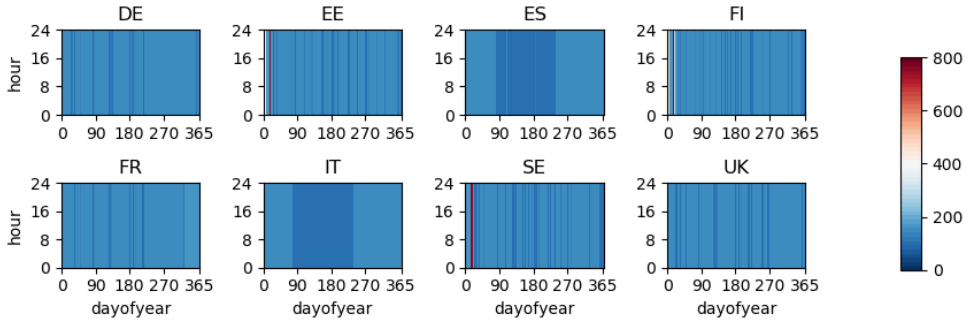

Figure 4.30. Storage shadow price for BEVS in the ALLFLEX scenario for selected countries. The legend indicates shadow prices in €/MWh. Blue represents variable dispatch costs, red indicates shed load.

Storage level dynamics

A final comparison is performed, analysing the storage level dynamics of the BEVS in Germany for both the EVFLEX and ALLFLEX scenarios. The results are reported in Figure 4.31. The first clear aspect is the *SOC* limitation given by the AF. The upper bound for the BEVS availability is given by the security margin, which in this work is set to 50%. This parameter is imposed to avoid that the utilisation of the V2G technology by the system operator causes problems in the users mobility patterns. As can be seen, it severely limits the possibility to exploit the overall BEVS storage capacity available. Therefore, a more precise modelling of the V2G technology in relation to the mobility demand could potentially unlock a significant storage capacity. In addition to this, the storage level is quite dynamic, with numerous charge and discharge events. In particular, with respect to the EVFLEX scenario, the smart energy system configuration simulated in the ALLFLEX scenario allows to exploit further the V2G technology. This is clear from the more frequent periods with BEVS *SOC* equal to zero, meaning that the storage capacity is completely utilised.

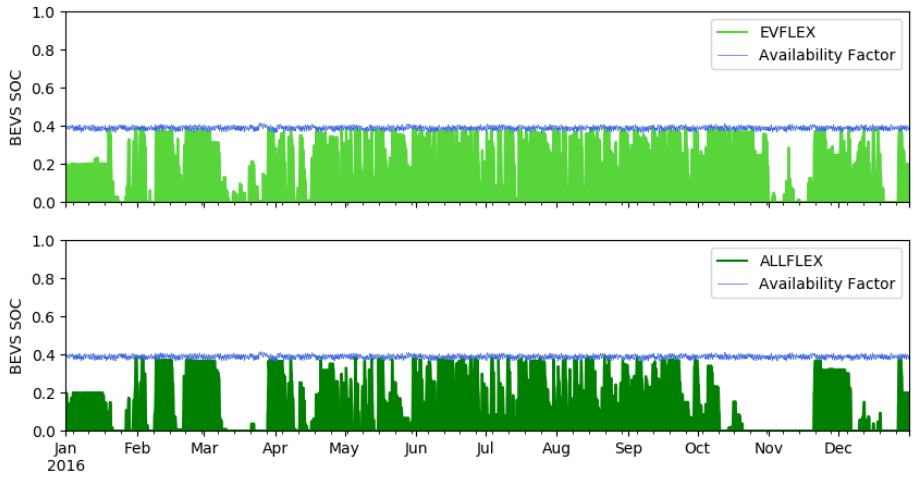

Figure 4.31. Overview of the BEVS storage level in Germany for the EVFLEX and ALLFLEX scenarios. The maximum storage level is determined by the availability factor, in blue, which is capped by the security margin, set to 0.5.

Chapter 5

Conclusions and future work

5.1 Conclusions

In this thesis work, the RAMP-Mobility original, open-source, stochastic model to simulate the EVs load profiles with high temporal detail for 28 European countries was successfully developed. The resulting profiles were then used as one of the inputs needed to assess the flexibility potential provided by sector coupling in a future energy system with high shares of VRES. This was simulated with the Dispa-SET optimal dispatch, in the context of the soft-linking with the long-term energy planning model JRC-EU-TIMES. Several conclusions can be drawn from this study.

First, the RAMP-Mobility model was validated with a satisfying degree of accuracy. This means that both the mobility and the charging demand profiles computed by the algorithm replicate effectively the real world data, under correct input conditions. The only discrepancies are ascribable to the lack of precise information about the conditions of the data sampling or of the measuring conditions. The result is relevant as it leads to the conclusion that the model can be applied to different scenarios, either representing a condition similar to the current situation, or predicting the evolution of the load profile under diverse assumptions.

Then, an analysis on the simulated database of European EVs load profiles was performed, highlighting that the different average mobility demand per car is the main factor differentiating the charging profiles. Furthermore, also the population composition plays an important role, in particular the share of Inactive users determines the difference between the base load and the peaks height. The different charging strategies implemented have been compared, proving to provide consistent results. In addition to this, a wide sensitivity analysis was conducted on both the mobility related arbitrary parameters and on the customizable features available in the charging process function. As regards arbitrary mobility parameters, the largest effect on the results is visible when varying the occasional use parameter. As for customizable features of the charging process, instead, the biggest impact is registered when introducing the logistic function to model the users' range anxiety. It is also worth noticing that overall the results are more sensible to the charging process customizable features rather than to the mobility arbitrary parameters. This is a relevant result, as it means that the goal of allowing each model user to define its own scenarios and assumptions was successfully achieved.

Moving to the results of the Dispa-SET simulations, four scenarios have been simulated, starting from a base case with no sector coupling option, and then gradually introducing the TES and V2G technologies. The first conclusion is that, as expected, the integration of heating and transport sector plays an important role in improving the performances of the energy system. Nevertheless, the results also indicate that some of the available storage capacity is not fully exploited. This is due mainly to the limited values of NTC, which proved to be insufficient for the simulated scenario. Therefore, considering higher interconnection capacities, it is reasonable that the benefits of sector coupling would be even higher. Furthermore, also the addition of seasonal storage to the model could improve the system performances, increasing the load shifting possibility to a wider time range. Indeed, even if the presence of P2GS is considered, the precise analysis of its storage dynamics is out of the scope of this work, and will be addressed in future research developments.

In addition to this, a deeper analysis was performed on the storage technologies and the flexibility needs. This demonstrated that the storage capacity available in the base case, without sector coupling, is already almost enough to provide the necessary flexibility for the simulated scenario. This is a peculiar result, which can be explained by the fact that the scenario considered in this work aims for an 80% reduction of greenhouse gases emissions with respect to the 1990 levels. Therefore, it can be inferred that the additional flexibility provided by sector coupling can be crucial from two perspectives. On the one hand, even if not strictly necessary for the technical feasibility of the system, it can provide more cost-effective storage solutions and allow a higher integration of VRES, thus accelerating and reducing the cost of the energy transition. On the other hand, it can be play an important role in pursuing even more ambitious goals with respect to the one analysed in this study, such as the zero net greenhouse gases emissions objective set in the European Green Deal.

5.2 Future work

There are different possible improvements that can be proposed as future development of the work described in this thesis. First, the RAMP-Mobility model strongly relies on the availability of country-specific data to be used as inputs for the algorithm. In particular, the possibility to rely on accurate mobility data for each of the simulated countries could potentially improve the results of the model. Nevertheless, it is important that the mobility data are collected with a uniform methodology across all the considered countries. It is also important to notice that the input data used in this work do not present extreme differences between each country. Hence, there is the possibility that the huge effort requested by obtaining precise data on the country level will not enhance the quality of the results significantly. In this regard, a possible approach could be to focus on one single country, evaluating if the quality of the results actually increases significantly. The same considerations apply also to the other input data necessary to the model, such as the time-related people behaviours. Second, the precise modelling of EV power consumption is a complex topic, since many variables are involved. For this reason, an additional possible improvement to the model lies in the introduction of an accurate model to obtain a more precise vehicle power consumption calculation with respect to the simplified quadratic function

used in this work. Third, the approach used in the Dispa-SET model manages to effectively consider the V2G technology. However, it potentially hinders the system from exploiting a relevant share of EVs' battery capacity for flexibility purposes, as highlighted by the analysis on the BEVS storage level dynamics. Hence, it can be proposed to adopt a more explicit representation of the transport sector in the model. Considering the share of battery capacity available to the TSO at each time step an endogenous variable might replicate more accurately the flexibility potential provided by the V2G technology. Lastly, the RAMP-Mobility could be easily adapted to other countries not initially included in this study. The only limit lies in the input data availability. In case several countries are simulated, the data should be collected with comparable methodology across the different countries.

Acronyms

AF	Availability factors
BASt	German Federal Highway Research Institute
BATS	Stationary batteries
BEVS	Battery-powered electric vehicles
CHP	Combined heat and power
CP	Electric Vehicle Charging Point
DH	District heating
DLC	Direct load control
EH	Electric heater
ENTSO-E	European Network of Transmission System Operators for Electricity
ESOM	Energy System Optimisation Model
EU	European Union
EV	Electric Vehicle
HDAM	Conventional hydro dam
HETUS	Harmonised European Time Use Surveys
HP	Heat pump
HPHS	Pumped hydro storage
HROR	Hydro run-of-river
JRC	Joint Research Centre
LF	Load Factor
LL	Lost load
MID	Mobilität in Deutschland
MILP	mixed-integer linear programming
MTS	Mid-term scheduling
NRMSE	Normalised Root-Mean-Squared Error
NTC	Net Transfer Capacity
NTS	National travel survey
P2HT	Power-to-Heat

P2L	Power to Liquid
PHEV	Plug-in Hybrid EV
PHOT	Solar photovoltaic
RES	Renewable energy sources
SCSP	Concentrated solar power
STUR	Steam turbine
TES	Thermal energy storage
TSO	Transmission System Operator
TYNDP	Ten-Year Network Development Plan
UCM	Unit-commitment and power dispatch model
UK	United Kingdom
V2G	Vehicle-to-grid
VRES	Variable renewable energy sources
P2GS	Power-to-gas storage

Nomenclature

ξ	Security margin.
$CHPPowerLossFactor_{chp}$	Power loss when generating heat [%]
$Committed_{i,u}$	Committed status of unit at hour h
$CostFixed_{u}$	Fixed costs [€/h]
$CostH2Slack_{p2h2,i}$	Cost of supplying hydrogen via other means [€/MWh]
$CostHeatSlack_{th,i}$	Cost of supplying heat via other means [€/MWh]
$CostLoadShedding_{i,n}$	Shedding costs [€/MWh]
$CostOfSpillage$	Cost of spillage from water reservoirs [€/MWh]
$CostRampDown_{i,u}$	Ramp-down costs [€/MW]
$CostRampUp_{i,u}$	Ramp-down costs [€/MW]
$CostRampUp_{i,u}$	Ramp-up costs [€/MW]
$CostShutDown_{i,u}$	Shut-down costs for one unit [€/u]
$CostStartUp_{i,u}$	Start-up costs for one unit [€/u]
$CostVariable_{i,u}$	Variable costs [€/MWh]
D	Electric power demand
$Demand_{DA,n,h}$	Hourly demand in each zone
$E_{min,i}$	Minimum energy in the battery to be guaranteed to the user.
$E_{sys,i}$	Energy available to the system for V2G.
$Flow_{i,l}$	Flow through lines [MW]
$Heat_{chp,i}$	Heat output by CHP plant [MW]
$HeatSlack_{th,i}$	Heat satisfied by other sources [MW]
$LineNode_{l,n}$	Line-zone incidence matrix

$LL_{2D,i,n}$	Deficit in reserve down [MW]
$LL_{2U,i,n}$	Deficit in reserve up [MW]
$LL_{3U,i,n}$	Deficit in reserve up - non spinning [MW]
$LL_{MaxPower,i,n}$	Deficit in terms of maximum power [MW]
$LL_{MinPower,i,n}$	Power exceeding the demand [MW]
$LL_{RampDown,u,i}$	Deficit in terms of ramping down [MW]
$LL_{RampUp,u,i}$	Deficit in terms of ramping up for each plant [MW]
$LoadShedding_{i,n}$	Maximum value of load shedding [MW]
$Location_{u,n}$	Location (one unit allocated in zone n)
P_{CP}^{nom}	Charging point nominal power
P_{el}^{PHOT}	Power produced from Solar photovoltaic
P_{el}^{WIN}	Power produced from Wind energy
$P_{ev,n,2050}^{TIMES}$	Yearly electric vehicles power demand in 2050 according to TIMES.
$P_{ev,n,i,2050}^{TIMES}$	Hourly electric vehicles power demand profile scaled up to 2050 total value.
$P_{n,2050}^{TIMES}$	Yearly power demand in 2050 according to TIMES.
$P_{n,i,2050}$	Hourly power demand in 2050 used in Dispa-SET.
$P_{n,i,2016}^{ENTSOE}$	Base power demand in 2016.
$Power_{i,u}$	Power output [MW]
$PowerConsumption_{p2h,i}$	Power consumption by P2H [MW]
$PriceTransmission_{i,l}$	Price of transmission between zones [€/MWh]
$Q_{p2h,n,i,2016}^{TIMES}$	Yearly electric heating power demand in 2016 according to TIMES.
$Q_{p2h,n,i,2050}^{TIMES}$	Yearly electric heating power demand in 2050 according to TIMES.
$ShedLoad_{i,n}$	Shed load [MW]
$Spillage_{s,i}$	Spillage from water reservoirs [MW]
$StorageInput_{s,h}$	Charging input for storage units [MW]

$StorageSlack_{th,i}$	Hydrogen satisfied by other sources [MW]
T_{amb}	Outdoor temperature
$TotalSystemCost$	Total power, heating and transportation system operational costs [€]
$VOLL$	Value of lost load [€/MWh]
$WaterSlack_s$	Unsatisfied water level at the end of the optimization period
$WaterValue$	Cost of water coming from unsatisfied water level
CP_{prob}	Probability of finding an available charging point at each parking event
COP_{nom}	Nominal efficiency for the P2HT technology group
$C_{battery,i}$	Total battery capacity.
$C_{battery}$	Size of the Electric Vehicle battery capacity
d_{min}	Minimum distance the mobility appliance drives after switch-on event
$D_{residual}$	Residual electric power demand
d_{tot}	Total daily distance travelled by the mobility appliance
P_{EV}	Power consumption of the Electric Vehicle at a given velocity
p_{max}	Maximum probability of the infrastructure availability piecewise function
p_{min}	Minimum probability of the infrastructure availability piecewise function
SOC	State of charge of the EV battery
SOC_{max}	Maximum State of charge at which the battery is charged
SOC_{min}	Minimum State of charge at which the user necessarily charges the battery
t_1	Time of the day when lower probability of the piecewise function starts
t_2	Time of the day when lower probability of the piecewise function ends
t_{func}	Minimum time the mobility appliance drives after switch-on event

t_{tot}	Total daily working time of the mobility appliance
$usage_{perc}$	Percentage of total travelled distance happening in a certain windows
v_{av}	Average travel velocity of the mobility appliance

Bibliography

[1] H. Lund, P. A. Østergaard, D. Connolly, and B. V. Mathiesen, "Smart energy and smart energy systems", *Energy*, vol. 137, pp. 556–565, 2017, ISSN: 0360-5442. DOI: https://doi.org/10.1016/j.energy.2017.05.123. [Online]. Available: http://www.sciencedirect.com/science/article/pii/S0360544217308812.

[2] B. Mathiesen, H. Lund, D. Connolly, H. Wenzel, P. Østergaard, B. Möller, S. Nielsen, I. Ridjan, P. Karnøe, K. Sperling, and F. Hvelplund, "Smart energy systems for coherent 100% renewable energy and transport solutions", *Applied Energy*, vol. 145, pp. 139–154, 2015, ISSN: 0306-2619. DOI: https://doi.org/10.1016/j.apenergy.2015.01.075. [Online]. Available: http://www.sciencedirect.com/science/article/pii/S0306261915001117.

[3] T. Brown, D. Schlachtberger, A. Kies, S. Schramm, and M. Greiner, "Synergies of sector coupling and transmission reinforcement in a cost-optimised, highly renewable European energy system", *Energy*, vol. 160, pp. 720–739, 2018, ISSN: 0360-5442. DOI: https://doi.org/10.1016/j.energy.2018.06.222. [Online]. Available: http://www.sciencedirect.com/science/article/pii/S036054421831288X.

[4] G. Pasaoglu, D. Fiorello, L. Zani, A. Martino, A. Zubaryeva, and C. Thiel, *Projections for electric vehicle load profiles in Europe based on travel survey data*, Scientific and Technical Research series, 2013. DOI: 10.2790/24108. [Online]. Available: https://setis.ec.europa.eu/publications/relevant-reports/projections-electric-vehicle-load-profiles-europe-based-travel-survey.

[5] D. Fischer, A. Harbrecht, A. Surmann, and R. McKenna, "Electric vehicles' impacts on residential electric local profiles, a stochastic modelling approach considering socio-economic, behavioural and spatial factors", *Applied Energy*, vol. 233-234, pp. 644–658, 2019, ISSN: 0306-2619. DOI: https://doi.org/10.1016/j.apenergy.2018.10.010. [Online]. Available: http://www.sciencedirect.com/science/article/pii/S0306261918315666.

[6] J. Brady and M. O'Mahony, "Modelling charging profiles of electric vehicles based on real-world electric vehicle charging data", *Sustainable Cities and Society*, vol. 26, pp. 203–216, 2016, ISSN: 2210-6707. DOI: https://doi.org/10.1016/j.scs.2016.06.014. [Online]. Available: http://www.sciencedirect.com/science/article/pii/S221067071630124X.

[7] J. Schäuble, T. Kaschub, A. Ensslen, P. Jochem, and W. Fichtner, "Generating electric vehicle load profiles from empirical data of three EV fleets in Southwest Germany", *Journal of Cleaner Production*, vol. 150, pp. 253–266, 2017, ISSN: 0959-6526. DOI: https://doi.org/10.1016/j.jclepro.2017.02.150. [Online]. Available: http://www.sciencedirect.com/science/article/pii/S0959652617303761.

[8] F. Lombardi, S. Balderrama, S. Quoilin, and E. Colombo, "Generating high-resolution multi-energy load profiles for remote areas with an open-source stochastic model", *Energy*, vol. 177, pp. 433–444, 2019, ISSN: 0360-5442. DOI: https://doi.org/10.1016/j.energy.2019.04.097. [Online]. Available: http://www.sciencedirect.com/science/article/pii/S0360544219307303.

[9] Eurostat, *Population by sex, age, citizenship and labour status (1 000)*, 2019. [Online]. Available: http://appsso.eurostat.ec.europa.eu/nui/show.do?lang=en&dataset=lfsa_pganws.

[10] Eurostat, *Students enrolled in tertiary education by education level, programme orientation, sex, type of institution and intensity of participation*, 2019. [Online]. Available: https://appsso.eurostat.ec.europa.eu/nui/show.do?dataset=educ_uoe_enrt01&lang=en.

[11] Eurostat, *Participation rate in the main activity (wide groups) by sex and time of the day*, 2019. [Online]. Available: https://appsso.eurostat.ec.europa.eu/nui/show.do?dataset=tus_00startime&lang=en.

[12] G. Pasaoglu, D. Fiorello, A. Martino, G. Scarcella, A. Alemanno, A. Zubaryeva, and C. Thiel, *Driving and parking patterns of European car drivers, a mobility survey*, Scientific and Technical Research series, 2012. DOI: 10.2790/7028. [Online]. Available: https://op.europa.eu/en/publication-detail/-/publication/2d5d968f-4f4c-4ee0-82e2-a7a136dfd187/language-en.

[13] A. Beltramo, A. Julea, N. Refa, Y. Drossinos, C. Thiel, and S. Quoilin, "Using electric vehicles as flexible resource in power systems: a case study in the Netherlands", in *2017 14th International Conference on the European Energy Market (EEM)*, 2017, pp. 1–6.

[14] W. Nijs, P. R. Castello, D. Tarvydas, I. Tsiropoulos, and A. Zucker, *Deployment Scenarios for Low Carbon Energy Technologies*, EUR 29496 EN, Luxembourg, 2018. DOI: 10.2760/249336.

[15] M. Pavičević, K. Kavvadias, T. Pukšec, and S. Quoilin, "Comparison of different model formulations for modelling future power systems with high shares of renewables – the dispa-set balkans model", *Applied Energy*, vol. 252, p. 113 425, 2019, ISSN: 0306-2619. DOI: https://doi.org/10.1016/j.apenergy.2019.113425. [Online]. Available: http://www.sciencedirect.com/science/article/pii/S0306261919310992.

[16] I. Staffell and S. Pfenninger, "Using bias-corrected reanalysis to simulate current and future wind power output", *Energy*, vol. 114, pp. 1224–1239, 2016, ISSN: 0360-5442. DOI: https://doi.org/10.1016/j.energy.2016.08.068. [Online]. Available: http://www.sciencedirect.com/science/article/pii/S0360544216311811.

[17] S. Pfenninger and I. Staffell, "Long-term patterns of European PV output using 30 years of validated hourly reanalysis and satellite data", *Energy*, vol. 114, pp. 1251–1265, 2016, ISSN: 0360-5442. DOI: https://doi.org/10.1016/j.energy.2016.08.060. [Online]. Available: http://www.sciencedirect.com/science/article/pii/S0360544216311744.

[18] A. Kies, L. von Bremen, and D. Heinemann, *Hydro energy inflow for power system studies*, 2017. DOI: 10.5281/zenodo.804244.

[19] D. Patteeuw, K. Bruninx, A. Arteconi, E. Delarue, W. D'haeseleer, and L. Helsen, "Integrated modeling of active demand response with electric heating systems coupled to thermal energy storage systems", *Applied Energy*, vol. 151, pp. 306–319, 2015, ISSN: 0306-2619. DOI: https://doi.org/10.1016/j.apenergy.2015.04.014. [Online]. Available: http://www.sciencedirect.com/science/article/pii/S0306261915004535.

[20] O. Ruhnau, L. Hirth, and A. Praktiknjo, "Time series of heat demand and heat pump efficiency for energy system modeling", *Sci Data*, vol. 6, no. 189, 2019, ISSN: 2052-4463. DOI: 10.1038/s41597-019-0199-y. [Online]. Available: https://doi.org/10.1038/s41597-019-0199-y.

[21] E. Hartvigsson and E. O. Ahlgren, "Comparison of load profiles in a mini-grid: Assessment of performance metrics using measured and interview-based data", *Energy for Sustainable Development*, vol. 43, pp. 186–195, 2018, ISSN: 0973-0826. DOI: https://doi.org/10.1016/j.esd.2018.01.009. [Online]. Available: http://www.sciencedirect.com/science/article/pii/S0973082617309675.

[22] Directorate-General for Mobility and Transport (European Commission), *EU transport in figures*, Statistical pocketbook 2019, Brussels, 2019. [Online]. Available: https://op.europa.eu/en/publication-detail/-/publication/f0f3e1b7-ee2b-11e9-a32c-01aa75ed71a1.

[23] S. Pfenninger, J. DeCarolis, L. Hirth, S. Quoilin, and I. Staffell, "The importance of open data and software: Is energy research lagging behind?", *Energy Policy*, vol. 101, pp. 211–215, 2017, ISSN: 0301-4215. DOI: https://doi.org/10.1016/j.enpol.2016.11.046. [Online]. Available: http://www.sciencedirect.com/science/article/pii/S0301421516306516.

[24] European Commission, *The European Green Deal*, Communication from the Commission to the European Parliament, the European Council, the Council, the European Economic and Social Committee and the Committee of the Regions, Brussels, 2019. [Online]. Available: https://eur-lex.europa.eu/legal-content/EN/ALL/?uri=CELEX:52019DC0640.

[25] P. D. Lund, J. Lindgren, J. Mikkola, and J. Salpakari, "Review of energy system flexibility measures to enable high levels of variable renewable electricity", *Renewable and Sustainable Energy Reviews*, vol. 45, pp. 785–807, 2015, ISSN: 1364-0321. DOI: https://doi.org/10.1016/j.rser.2015.01.057. [Online]. Available: http://www.sciencedirect.com/science/article/pii/S1364032115000672.

[26] M. Yilmaz and P. T. Krein, "Review of the impact of vehicle-to-grid technologies on distribution systems and utility interfaces", *IEEE Transactions on Power Electronics*, vol. 28, no. 12, pp. 5673–5689, 2013.

[27] D. Luca de Tena, "Large scale renewable power integration with electric vehicles: Long term analysis for Germany with a renewable based power supply", PhD thesis, Institut für Thermodynamik und Wärmetechnik der Universität Stuttgart, 2014.

[28] A. Harbrecht, R. McKenna, D. Fischer, and W. Fichtner, "Behavior-oriented modeling of electric vehicle load profiles: A stochastic simulation model considering different household characteristics, charging decisions and locations", Karlsruher Institut für Technologie (KIT), Tech. Rep., 2018, 241 pp. DOI: 10.5445/IR/1000082537.

[29] BASt, *Automatische zählstellen auf autobahnen und bundesstraßen*, Accessed: 2020-03-08. [Online]. Available: https://www.bast.de/BASt_2017/DE/Verkehrstechnik/Fachthemen/v2-verkehrszaehlung/zaehl_node.html.

[30] M. Pavičević, A. Mangipinto, W. Nijs, F. Lombardi, K. Kavvadias, J. P. [Navarro], E. Colombo, and S. Quoilin, "The potential of sector coupling in future european energy systems: Soft linking between the dispa-set and jrc-eu-times models", *Applied Energy*, vol. 267, p. 115 100, 2020, ISSN: 0306-2619. DOI: https://doi.org/10.1016/j.apenergy.2020.115100. [Online]. Available: http://www.sciencedirect.com/science/article/pii/S0306261920306127.

[31] Eurostat, *Passenger cars, by type of motor energy and size of engine*, 2019. [Online]. Available: https://appsso.eurostat.ec.europa.eu/nui/show.do?dataset=educ_uoe_enrt01&lang=en.

[32] M. Montel, *Python holidays*, 2020. [Online]. Available: https://github.com/dr-prodigy/python-holidays.

[33] Eurostat, *Harmonised European Time Use Surveys (HETUS)*, 2019. [Online]. Available: https://ec.europa.eu/eurostat/web/time-use-surveys.

[34] G. Pasaoglu, A. Zubaryeva, D. Fiorello, and C. Thiel, "Analysis of European mobility surveys and their potential to support studies on the impact of electric vehicles on energy and infrastructure needs in Europe", *Technological Forecasting and Social Change*, vol. 87, pp. 41–50, 2014, ISSN: 0040-1625. DOI: https://doi.org/10.1016/j.techfore.2013.09.002. [Online]. Available: http://www.sciencedirect.com/science/article/pii/S004016251300228X.

[35] Eurostat, *Passenger cars, by type of motor energy*, 2019. [Online]. Available: https://appsso.eurostat.ec.europa.eu/nui/show.do?dataset=road_eqs_carpda&lang=en.

[36] ——, *New registrations of passenger cars by type of motor energy and engine size*, 2019. [Online]. Available: https://appsso.eurostat.ec.europa.eu/nui/show.do?dataset=road_eqr_carpda&lang=en.

[37] A. Donati, P. Dilara, C. Thiel, A. Spadaro, D. Gkatzoflias, and Y. Drossinos, *Individual mobility: From conventional to electric cars*, Scientific and Technical Research series, 2015. DOI: 10.2790/405373. [Online]. Available: https://op.europa.eu/en/publication-detail/-/publication/5201da6f-7230-4f66-892e-ea5ac9291ab1/language-en.

[38] D. Fiorello and L. Zani, *EU survey on issues related to transport and mobility*, Scientific and Technical Research series, 2015. DOI: 10.2791/48322. [Online]. Available: https://op.europa.eu/en/publication-detail/-/publication/8965664b-77e8-11e5-86db-01aa75ed71a1/language-en.

[39] Renewables.ninja, *Weather (hourly data, 1980-2016)*. [Online]. Available: https://doi.org/10.1175/JCLI-D-16-0758.1.

[40] Department for Transport, *Electric vehicle smart charging*, Closed consultation report, 2019. [Online]. Available: https://www.gov.uk/government/consultations/electric-vehicle-smart-charging.

[41] J. García-Villalobos and I. Zamora and J. I. San Martín and F. J. Asensio and V. Aperribay, "Plug-in electric vehicles in electric distribution networks: A review of smart charging approaches", *Renewable and Sustainable Energy Reviews*, vol. 38, pp. 717–731, 2014, ISSN: 1364-0321. DOI: https://doi.org/10.1016/j.rser.2014.07.040. [Online]. Available: http://www.sciencedirect.com/science/article/pii/S1364032114004924.

[42] Y. Zheng, S. Niu, Y. Shang, Z. Shao, and L. Jian, "Integrating plug-in electric vehicles into power grids: A comprehensive review on power interaction mode, scheduling methodology and mathematical foundation", *Renewable and Sustainable Energy Reviews*, vol. 112, pp. 424–439, 2019, ISSN: 1364-0321. DOI: https://doi.org/10.1016/j.rser.2019.05.059. [Online]. Available: http://www.sciencedirect.com/science/article/pii/S136403211930382X.

[43] E. Wikner and T. Thiringer, "Extending battery lifetime by avoiding high SOC", *Applied Sciences*, vol. 8, p. 1825, 2018, ISSN: 1364-0321. DOI: doi:10.3390/app8101825. [Online]. Available: https://www.mdpi.com/2076-3417/8/10/1825.

[44] J. Gómez Vilchez, G. Harrison, L. Kelleher, A. Smyth, and C. Thiel, *Quantifying the factors influencing people's car type choices in Europe: Results of a stated preference survey*, Publications Office of the European Union, 2017. DOI: 10.2760/695017.

[45] Electric Vehicle Database, *Volkswagen e-Up*, Accessed: 2020-02-24. [Online]. Available: https://ev-database.uk/car/1189/Volkswagen-e-Up.

[46] ——, *Opel Ampera-e*, Accessed: 2020-02-24. [Online]. Available: https://ev-database.org/car/1051/Opel-Ampera-e.

[47] ——, *Tesla Model X Long Range*, Accessed: 2020-02-24. [Online]. Available: https://ev-database.org/car/1198/Tesla-Model-X-Long-Range.

[48] K. Kavvadias, I. H. Gonzalez, A. Zucker, and S. Quoilin, *Integrated modelling of future EU power and heat systems - the Dispa-SET 2.2 open-source model*, EUR 29085 EN, Luxembourg, 2018. DOI: 10.2760/860626.

[49] M. Pavičević, W. Nijs, K. Kavvadias, and S. Quoilin, "Modelling flexible power demand and supply in the eu power system: Soft-linking between jrc-eu-times and the open-source dispa-set model", Institute of Thermal Technology, 2019. [Online]. Available: https://lirias.kuleuven.be/retrieve/542431.

[50] S. Simoes, W. Nijs, P. Ruiz, A. Sgobbi, D. Radu, P. Bolat, C. Thiel, and S. Peteves, *The JRC-EU-TIMES model – Assessing the long-term role of the SET Plan energy technologies*, EUR 26292 EN, Luxembourg, 2013. DOI: 10.2790/97596.

[51] J.-P. Jimenez-Navarro, K. Kavvadias, F. Filippidou, M. Pavičević, and S. Quoilin, "Coupling the heating and power sectors: The role of centralised combined heat and power plants and district heat in a european decarbonised power system", *Applied Energy*, vol. 270, p. 115 134, 2020, ISSN: 0306-2619. DOI: https://doi.org/10.1016/j.apenergy.2020.115134. [Online]. Available: http://www.sciencedirect.com/science/article/pii/S0306261920306462.

[52] W. Nijs and P. R. Castello, *JRC-EU-TIMES Full model.* European Commission, Joint Research Centre (JRC), 2019.

[53] J. P. Jiménez Navarro, K. C. Kavvadias, S. Quoilin, and A. Zucker, "The joint effect of centralised cogeneration plants and thermal storage on the efficiency and cost of the power system", *Energy*, vol. 149, pp. 535–549, 2018, ISSN: 0360-5442. DOI: https://doi.org/10.1016/j.energy.2018.02.025. [Online]. Available: http://www.sciencedirect.com/science/article/pii/S0360544218302536.

[54] I. Staffell, D. Brett, N. Brandon, and A. Hawkes, "A review of domestic heat pumps", *Energy Environ. Sci.*, vol. 5, pp. 9291–9306, 11 2012. DOI: 10.1039/C2EE22653G. [Online]. Available: http://dx.doi.org/10.1039/C2EE22653G.

[55] W. Nijs, P. R. Castelló, and I. H. González, *Baseline scenario of the total energy system up to 2050 - JRC-EU-TIMES model outputs for the 14 MS and the EU - Deliverable 5.2: Business-as-usual reference scenarios*, Heat Roadmap Europe project, 2017.

[56] ENTSO-E, *Ten year network development plan*, Full Report, 2015. [Online]. Available: https://www.entsoe.eu/publications/tyndp/tyndp-2014/.

[57] e-Highway2050 project, *e-Highway2050 modular development plan of the pan-european transmission system 2050*, Project results, 2015. [Online]. Available: https://docs.entsoe.eu/baltic-conf/bites/www.e-highway2050.eu/e-highway2050/.

[58] J. Helmus, J. Spoelstra, N. Refa, M. Lees, and R. [den Hoed], "Assessment of public charging infrastructure push and pull rollout strategies: The case of the Netherlands", *Energy Policy*, vol. 121, pp. 35–47, 2018, ISSN: 0301-4215. DOI: https://doi.org/10.1016/j.enpol.2018.06.011. [Online]. Available: http://www.sciencedirect.com/science/article/pii/S0301421518303999.

[59] A. Hoekstra and N. Refa, "Characteristics of Dutch EV drivers", English, 30th International Electric Vehicle Symposium and Exhibition, EVS 2017, EVS 2017 ; Conference date: 09-10-2017 Through 11-10-2017, Jan. 2017. [Online]. Available: http://www.messe-stuttgart.de/en/evs30.